

Doctoral Dissertation

Gamunu L. Samarakoon S. P. A.

Post combustion CO₂ capture
using aqueous amine solvents:
Investigations on molecular
structure-activity relationships
for amine solvents



Telemark University College
Faculty of Technology

Gamunu L. Samarakoon S. P. A.

Post combustion CO₂ capture using
aqueous amine solvents: Investigations on
molecular structure-activity relationships
for amine solvents

PhD Thesis 3:2015

ISBN 978-82-7206-395-4

ISSN 1893-3068

Telemark University College

P.O. Box 203

NO-3901 Porsgrunn

Norway

Phone: +47 35 57 50 00

Fax: +47 35 57 50 01

<http://www.hit.no/>

© 2015 Gamunu L. Samarakoon S. P. A

Dedicated to my sister and my brother!

Preface

This thesis is submitted to the Telemark University College as a partial fulfilment of the requirements for the degree of philosophiae doctor (Ph.D.)

The work has been carried out at the Department of Process, Energy and Environmental Technology in Telemark University College, Norway; under the supervision of Professor Klaus Joachim Jens and Professor Dag Eimer.

This PhD work is a part of the main project named “Better and more intelligently formulated CO₂ absorbents” funded by the Research Council of Norway under the CLIMIT program, the national programme for research, development and demonstration of technology for CO₂ capture, transport and storage (CCS).

Porsgrunn, March 25, 2015

Gamunu Samarakoon

Acknowledgements

Let me present my gratitude to many who have helped me in different ways, with my work on this doctoral thesis.

First of all, I would like to thank my main supervisor Prof. Klaus J. Jens for his close supervising, great support and encouragement. I am also grateful to him for helping me to broaden my knowledge on organic chemistry. I would like to express my gratitude to Prof. Dag Eimer for his invaluable guidance provided and discussions during the project meetings. And I am thankful to Dr. John Arild Svendsen for his programs develop for some tasks in this research.

The NMR experimental work was carried out in co-operation with Dr. B. Arstad, Dr. A. Bouzga and Dr. Cristina Perinu at the SINTEF NMR facility in Oslo. I am also grateful to them. And let me extend my gratitude to Dr. C. Perinu, not only for the experimental work but also for her valuable suggestions and for sharing her knowledge with me when writing manuscripts. Raman spectroscopic experiment was carried out at Department of Chemistry in University of Oslo. I express appreciations to Prof. Claus J. Nielsen for giving the opportunity; and also Dr. Niels H. Andersen for helping in carrying out the experiment and processing data.

Financial support by the Research Council of Norway through the CLIMIT program is gratefully acknowledged.

Three master students; Van Khanh Tong, Vanessa Ferreira Garcia and Soheila Taghavi worked on various parts of this thesis work. I thank them for their hard work. I also thank former CO₂ laboratory manager in TUC, Per. M. Hansen for his support in the lab. I enjoy academic work at TUC and I am grateful to both the academic and administrative staff for making nice and friendly working environment in the institution.

And I would like to thank Prof. Rune Bakke from TUC and Dr. Sanja Gunawardena from University of Moratuwa (UoM), Sri Lanka, who gave me the inspiration to engage in research work. I appreciate very much Dr. P.G. Rathnasiri from UoM who was the pioneering person responsible for building the educational co-operation between TUC and UoM. This co-operation made my path to come to this beautiful country, Norway for my higher education.

I am thankful to my colleagues (former and present) and all my friends in and outside TUC for making everyday life simply better, here in Norway. Finally, I present my love and gratitude to my family; father, mother, sister and brother for their loving care.

Gamunu Samarakoon
Porsgrunn, March, 2015.

Abstract

The study in this dissertation focuses on chemical absorption of CO₂ using aqueous amine which is expected to be the technology of choice for early large scale deployment of post-combustion carbon capture (PCC). However the technology still faces challenges. Reduction in cost of this process, in terms of both capital and operational is required to make the process economically feasible. One possible approach for it, is the improvement of absorbents. Since this process is chemically driven, understanding fundamental chemistry of amine-CO₂ reactivity could assist the rational development of the absorbents.

With respect to primary and secondary amines, the amine carbamate formation reaction and the carbamate hydrolyses reaction are important reactions. The equilibrium constants governing these reactions can define the performance of amine solvents. Understanding the molecular structure-activity relationships for the CO₂-aqueous amine reactions aid prediction/estimation of their equilibrium constants. The influence of molecular structure on the free energy of activation of a reaction or the reaction may be treated as the sum of independent contributions of polar, resonance and steric effects of substituents in the molecule. We can separate these effects individually and assign numerical values to elements or substituent groups as empirical constants related to their effects on reaction rates and equilibria. The “Taft polar parameter” defines a quantitative scale which assigns a value to the polar nature of a substituent.

The study reported in this thesis aims to increase understanding of aqueous amine-CO₂ reactivity and estimate the equilibrium constants of carbamate formation and carbamate hydrolysis reactions by means of Taft polar parameter. According to the relations between Taft polar parameter and the equilibrium constants, relative reduced electron density on N atom leads to increased alkylamine carbamate formation and decreased alkylamine carbamate hydrolysis. Note that this study is limited to primary (1°) alkylamines. The relative electron density, present on the N nucleus, which is depending on molecular structure and medium effects influences the chemical reactions between amine and CO₂. Therefore, ¹⁵N NMR experiment data was also used to qualitatively analyse the structure-activity relationships of 1° alkylamines. The current study provides evidence that in addition to polar effects from substituents, water solvents and steric hindrance (in terms of electron delocalization) influence the reaction of the alkylamine toward CO₂. The results show that higher basicity and higher α -C substituent effect (steric hindrance) reduce carbamate formation.

Further, this dissertation includes modifying analytical methods for speciation in carbonated aqueous amine solutions which is required to determine the equilibrium constants of interested reactions. In this respect, a complementary wet chemical method (WCM) for determination of species distribution in carbonated aqueous amine solution was developed. The method employs analytical techniques readily available in any laboratory. The results obtained using WCM were compared to those obtained using ^{13}C NMR analysis for identical solutions for validation. They were in good agreement. The method was then used for speciation in carbonated primary alkylamine solutions; propyl-, butyl- and pentylamine.

Application of Raman spectroscopy as an analytical tool to determine the speciation of carbonated aqueous alkanolamine systems was attempted. It constitutes a simple 'short-cut' type approach to semi-quantitative speciation information employing measurement of selected Raman bands in conjunction with an internal standard (ClO_4^-), assisted by ^{13}C -NMR .

Contents

Preface	i
Acknowledgements	ii
Abstract.....	iii
Contents.....	v
List of Figures	viii
List of Tables.....	x
Nomenclature.....	xi

Background

1. Background	1
1.1. Climate change and CCS	1
1.2. Post-combustion CO ₂ capture	3
1.3. Chemical absorption of CO ₂ using aqueous amine solutions.....	4
1.4. Importance of equilibrium constants	8
1.5. Research objectives and scope	9
1.6. Main results	10
1.7. Outline of the PhD thesis.....	11
References	12

Part I: Wet chemical method for speciation of carbonated aqueous amine solutions

1. Overview.....	17
1.1. Carbamate stability	17
2. Literature review.....	20
3. Method Development	23

3.1.	Preparation of carbonated aqueous amine solution.....	23
3.2.	Carbamino quenching method.....	23
3.3.	Titration with a strong base	24
3.4.	pH measurement	25
3.5.	Density measurements.....	26
3.6.	¹³ C NMR experiment.....	26
4.	Chemistry of the method and mathematical procedure.....	27
5.	Method validation and discussion	31
5.1.	Discussion on pH measurement	34
6.	Speciation in HCO ₃ ⁻ loaded alkylamine solution.....	37
6.1.	Results and discussion	37
7.	Determination of ideal equilibrium constants from apparent equilibrium constants.....	40
8.	Conclusion, recommendations and further work	44
	References.....	45

Part II: Raman spectroscopy for speciation of carbonated aqueous amine solutions

1.	Overview.....	49
1.1.	Nuclear magnetic resonance (NMR) spectroscopy.....	49
1.2.	Fourier transform infrared spectroscopy (FT-IR) spectroscopy	50
2.	Raman spectroscopy.....	52
2.1.	Major components in a Raman spectrometer.....	54
3.	Literature review on Raman spectroscopy in CO ₂ capture field	56
4.	Method development: Raman spectrometer for speciation of carbonated aqueous amine solution	58
4.1.	Experiment method.....	58
4.2.	Characteristic Raman active bands.....	60
4.3.	Quantitative analysis: factor analysis approach.....	63

4.3.1. HCO ₃ ⁻ loaded alkanolamine solutions	65
5. Conclusions and Recommendations	70
References	72

Part III: Molecular structure-activity relationships

1. Overview	77
1.1. Carbamate related equilibrium constants	78
2. Previous studies on molecular structure–activity relationships	80
2.1. Quantitative structure-activity relationships for the base strength of amines	83
3. Molecular structure and activity	85
4. ¹⁵ N NMR spectroscopy	89
4.1. ¹⁵ N NMR experimental method	90
5. Correlations for carbamate related equilibrium constants	91
6. Conclusions and further work	100
Reference	101

Appendices

Appendix A: List of Chemicals	105
Appendix B: List of Publications	109

List of Figures

Background

Figure 1.1-1 : Overview of CO ₂ capture processes	3
Figure 1.3-1: Process flow diagram for CO ₂ recovery from flue gas by chemical absorption.	5

Part I: Wet chemical method for speciation of carbonated aqueous amine solutions

Figure 3.3-1: Titration curve for Dynamic Equivalence Titration (DET). Titration curve for a sample of carbonated amine solution titrated with 1.0 mol•dm ⁻³ NaOH.....	25
Figure 1.5-1: Comparison of concentrations determined by WCM to those obtained from the NMR experiment.....	33
Figure 6.1-1: K_{HYDa} vs. Loading (ratio of initial $[\text{NaHCO}_3]_{\text{init}} / [\text{amine}]_{\text{init}}$)	39
Figure 7-1 : $\log K_{HYDa}$ vs. ionic strength	43

Part II: Raman spectroscopy for speciation of carbonated aqueous amine solutions

Figure 2-1: Energy diagram for vibration energy of molecule transitions in Raman spectroscopy.	52
Figure 2.1-1: A block diagram of generic components making up a Raman Spectrometer.	55
Figure 4.2-1: Reference Raman spectra for CO ₃ ²⁻ (a) and HCO ₃ ⁻ (b). CO ₃ ²⁻	60
Figure 4.2-2: Reference Raman spectra of MEA	61
Figure 4.2-3: Reference Raman spectra for protonated MEA	62
Figure 4.2-4 : Reference Raman spectra for DEA	62
Figure 4.3.1-1: Raman spectra of MEA 20 wt % aqueous solution without loading (green) and with 0.5 loading (red).....	66
Figure 4.3.1-2: Raman spectra of DEA 20 wt % aqueous solution without loading (green) and with 0.5 loading (red).....	68
Figure 4.3.1-3: Raman spectra of MDEA 20 wt % aqueous solution without loading (green) and with 0.5 loading (red).....	68
Figure 4.3.1-4: Raman spectra of AMP 20 % w/w aqueous solution without loading (green) and with 0.5 loading (red).....	69

Part III: Molecular structure-activity relationships

Figure 2.1-1 : Taft's polar parameter ($\sum \sigma^*$) has been plotted against pK_a of non-aromatic amines.	84
Figure 3-1 : Amine- CO_2 interaction to form carbamate	85
Figure 3-2: Illustration for estimating cumulative polar substituents constant ($\sum \sigma^*$) of an amine molecule.	87
Figure 5-1: Polar substituent constants versus (a) carbamate forming equilibrium constants ($\text{Log } K_{\text{CMB}}$) and (b). carbamate hydrolyzing equilibrium constants ($\text{Log } K_{\text{HYD}}$).....	92
Figure 5-2: Dependence of basicity pK_a (at 25 °C) on the equilibrium constants (at 18 °C) of (a) carbamate forming equilibrium constants ($\text{Log } K_{\text{CMB}}$) and (b). carbamate hydrolyzing equilibrium constants ($\text{Log } K_{\text{HYD}}$).	94
Figure 5-3: ^{15}N NMR chemical shift values of aqueous primary alkyl amines versus a). carbamate forming equilibrium constants ($\text{Log } K_{\text{CMB}}$) and b). carbamate hydrolyzing equilibrium constants ($\text{Log } K_{\text{HYD}}$).	96
Figure 5-4 : Protonation constants of alkylamines at 25 °C against ^{15}N chemical shift values at 25 °C.....	97
Figure 5-5: Protonation constants at 25 °C against Polar substituent constants ($\sum \sigma^*$)	98

List of Tables

Part I: Wet chemical method for speciation of carbonated aqueous amine solutions

Table 4-1: Coefficients of temperature-dependent functions for dissociation constants of HCO_3^- and water.	29
Table 5-1: Speciation by wet chemical method and ^{13}C -NMR analysis for carbonated 2 % MEA solution at 25 °C.....	31
Table 6.1-1: Speciation using WCM for carbonated propyl-, butyl- and pentylamine solutions at 25 °C.	38
Table 7-1 : Apparent equilibrium constant values for a carbamate hydrolysis reaction ($K_{\text{HYD}a}$) at 25 °C with different ionic strengths.....	42

Part II: Raman spectroscopy for speciation of carbonated aqueous amine solutions

Table 4.2-1: Characteristic Raman bands for species	62
Table 4.3-1: Molar scattering intensity factors J_i	65
Table 1.4.3-2: Concentration determined from NMR measurement for MEA/ HCO_3^{1-} and DEA/ HCO_3^{1-} systems.....	67

Part III: Molecular structure-activity relationships

Table 3-1: σ^* for selected substituents are presented	86
Table 3-2: Collective polar substituent effects ($\sum \sigma^*$) of systematically selected primary alkylamines and alkanolamines.	88
Table 5-1: Chemical structure, polar substituent constants ($\sum \sigma^*$), equilibrium constants for carbamate formation and hydrolysis (K_{CBM} and K_{HYD}) at 18 °C and protonation constants at 25 °C. ^{15}N chemical shift values at 25 °C (expressed in ppm).....	91

Nomenclature

Symbols

Symbols	Description
a_i	Activities of component i
A_i	Integrated area
c_i	Concentration of the species [$\text{mol}\cdot\text{dm}^{-3}$]
E	Electromotive force
E^0	Standard state of unit activity
E_j	Liquid junction potential
F	Faraday constant
I	Ionic strength [$\text{mol}\cdot\text{dm}^{-3}$]
I_i	Relative integrated intensity
J_i	Molal intensity coefficient of species i
k	Reaction rate constant
K_a	Amine protonation constant
$K_{a\text{HCO}_3^-}$	Equilibrium dissociation constant of the bicarbonate ion [$\text{mol}\cdot\text{dm}^{-3}$]
K_c	Carbamate stability constant
K_{CBM}	Equilibrium constant of carbamate formation
K_{HYD}	Equilibrium constant of carbamate hydrolysis reaction
K_{HYDa}	Apparent equilibrium constant of carbamate hydrolysis reaction [$\text{mol}\cdot\text{dm}^{-3}$]
K_w	Water dissociation constant
m_i	Concentration [mol/kg]
R	Universal gas constant
γ_i	Activity coefficient of component i
σ^*	Polar substituent constants or Taft polar parameter

Abbreviations

AEEA	2-(2-aminoethyl-amino)ethanol
AMP	2-Amino-2-methyl-1-propanol
BBFO	Broadband fluorine observe
CCS	Carbon capture and storage
CLC	Chemical looping combustion
DEA	Diethanolamine
DET	Dynamic equivalence titration
DIPA	Diisopropanolamine
EMF	Electromotive force
ERC	Endpoint recognition criterion
GHG	Greenhouse gases
IEA	International energy agency
IPCC	Intergovernmental Panel on Climate Change
MDA	1,8-p-menthanediamine
MDEA	Methyldiethanolamine
MEA	Monoethanolamine
NIST	National Institute of Standards and Technology
NMR	Nuclear magnetic resonance
PCC	Post- combustion carbon capture
PE	2-piperdineethanol
PZ	Piperazine
rpm	Round per minute
UN	United Nations
WCM	Wet chemical method
FT-IR	Fourier transform infrared
RF	Radio frequency
ATR	Attenuated total reflectance
DCLS	Direct classical least squares
PLS1	Partial least squares, one principal component
AP	2-amino-1-propanol

1. Background

1.1. Climate change and CCS

Anthropogenic global warming has been recognized as intense environmental issue in the present time. The third assessment report from the UN's Intergovernmental Panel on Climate Change (IPCC) emphasised that if no action was taken the globally averaged surface temperature was projected to increase by between 1.4 and 5.8 °C during the period 1990 to 2100. Leading to greater impact on physical and biological systems as well as some social and economic systems.¹ There is already evidence of the effects of rising temperatures, such as sea level rise, increases and decreases in precipitation regionally, changes in the variability of climate, and changes in the frequency and intensity of some extreme climate phenomena.^{1b} Emissions of long-lived greenhouse gases (GHG) have a lasting effect on atmospheric composition, radiative forcing and climate. Among these GHGs, CO₂ is the largest contributor, contributing to 60 % of global warming effect, due to the amount present in the atmosphere. However, methane and chlorofluorocarbons have a much higher greenhouse effect per mass of gases.²

The demand for energy obviously increases with increased global population. The energy outlook released by IEA (2012) states that energy demand and CO₂ emissions will raise even higher while fossil fuels remain the dominant energy sources. Global energy demand is predicted to increase by over one third in the period to 2035. It further claims that energy related CO₂ emissions will rise from an estimated 31.2 Gt in 2011 to 37.0 Gt in 2035, pointing to a long-term average temperature increase of 3.6 °C.³ This temperature increase is higher than the set goal by IPCC. IPCC have set a goal ahead to reduce the emission by 50 % to 85 %, by 2050, in order to the global warming is to be confined to between 2 °C and 2.4 °C.

Therefore, global attention has been focused to reduce CO₂ emissions to mitigate climate change. The fifth assessment report of IPCC reiterated the importance of a global agreement to limit carbon emission. The temperature change caused by anthropogenic GHG emissions can likely be kept to less than 2 °C relative to pre-industrial levels, by reaching atmospheric concentrations level of about

450 ppm CO₂ equivalent by 2100. Decarbonizing (i.e. reducing the carbon intensity of) electricity generation is a key component of cost effective mitigation strategies in achieving low-stabilization levels (430 – 530 ppm CO₂eq). Low-carbon electricity supply (comprising renewable energy (RE), nuclear and carbon capture and storage (CCS)) must be increased from the current share of approximately 30 % to more than 80 % by 2050, and fossil fuel power generation without CCS has to be phased out almost entirely by 2100.⁴ The importance of implementing CCS should be highlighted, since it is an immediate facilitator for decarbonised energy in the future.

CCS is a “process consisting of the separation of CO₂ from industrial and energy-related sources, transport to a storage location and long-term isolation from the atmosphere”⁵. Separation of CO₂ can be approached through four basic systems (Figure 1.1-1). Capturing CO₂ from the exhaust gas is referred to as post-combustion capture. Pre-combustion capture involves converting fuel (mainly hydrocarbon) to hydrogen and carbon dioxide and then separating CO₂ before hydrogen rich fuel is sent to combustion. Using pure oxygen for the combustion results only in CO₂ and water in the flue gas, this technology is referred as oxyfuel. Chemical looping combustion (CLC) is a promising technology for separation of CO₂. Oxygen is transferred to the fuel via a metal oxide as an oxygen carrier. Thus, there is no direct contact between fuel and air.

CO₂ can be produced in industrial processes such as purification of natural gas and production of synthesis gas for the manufacture of ammonia. Pre-combustion technologies can be employed for CO₂ separation in such occasions. Cement and steel processes are also a source of CO₂ by combustion. Any of the technologies mentioned earlier can be used to capture CO₂ produced in industrial processes.

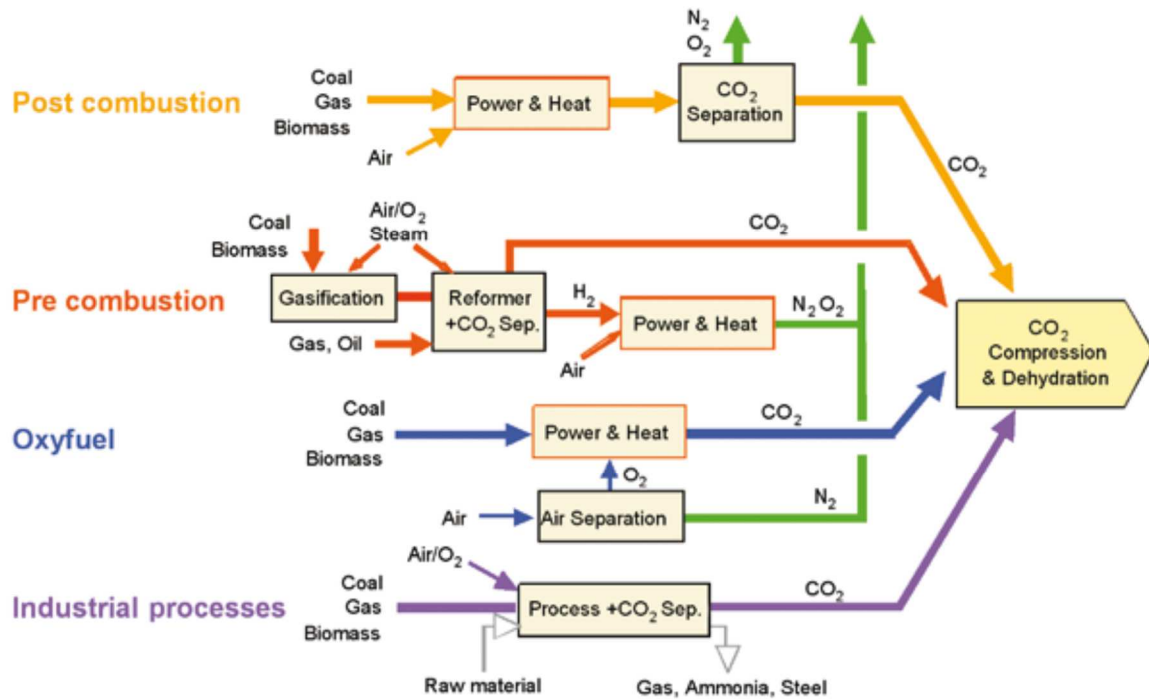


Figure 1.1-1 : Overview of CO₂ capture processes ⁵

1.2. Post-combustion CO₂ capture

Post-combustion capture can be implemented without major changes to existing combustion technologies. This is advantageous when retrofitting the technology to existing plants, in such cases it is superior to the other two approaches (pre-combustion and oxyfuel). Adsorption, absorption (physical or chemical), cryogenic separation and membrane separation are technologies which can be employed in post-combustion capture.⁶ Adsorption is the physical attachment of gas or liquid to a solid surface. The low adsorption capacity and low selectivity of most available adsorbents limits this application in large-scale gas treatment. Cryogenic separation is separation of CO₂ by condensation. The cost of refrigeration is the main challenge for this application. It is suitable for treating high CO₂ concentrated gas streams e.g. for oxyfuel process.⁶ The membrane separation is characterized by the relative rates of the species permeate. Low CO₂ selectivity of membranes is the main challenge which results in a multistage process to achieve the required target. The low partial pressure in flue gas streams is also a problem because this process is driven by the partial pressure difference.⁶⁻⁷ Physical absorption of CO₂ is not economically viable since it requires high CO₂ partial pressure. Chemical absorption is the most economical separation at lower CO₂ partial pressure. It has relatively high selectivity and affinity.

The study in this dissertation focuses on chemical absorption of CO₂ using aqueous amine which is expected to be the technology of choice for early large scale deployment of post-combustion carbon capture (PCC).⁸ Factors contributing to this as the technology of choice include its maturity, efficiency and flexibility in implementation in existing power plants when compared with available capture processes.

1.3. Chemical absorption of CO₂ using aqueous amine solutions

The technology of treating process gas with alkanolamines in absorption/stripping systems is decades old technology and has been used successfully. Credit should go to R. R. Bottoms, who was granted a patent covering this application in 1930.⁹ With the recognition of CO₂ as a greenhouse gas, the technology is being implemented in another important application, CO₂ removal from combustion gases. The amino group in the molecule makes necessary alkalinity available in the solution to affiliate acid gas while the hydroxyl group provides necessary solubility in water, reducing vapour pressure.

Chemical absorption processes in post-combustion capture makes use of the reversible nature of the chemical reaction of an aqueous alkaline solvent with an acid or sour gas. A weakly bonded intermediate compound is formed which is regenerated with the application of heat, producing the original solvent and a CO₂ stream.⁵ Figure 1.3-1 illustrates a typical arrangement of a process diagram for chemical absorption of CO₂ using aqueous amine.

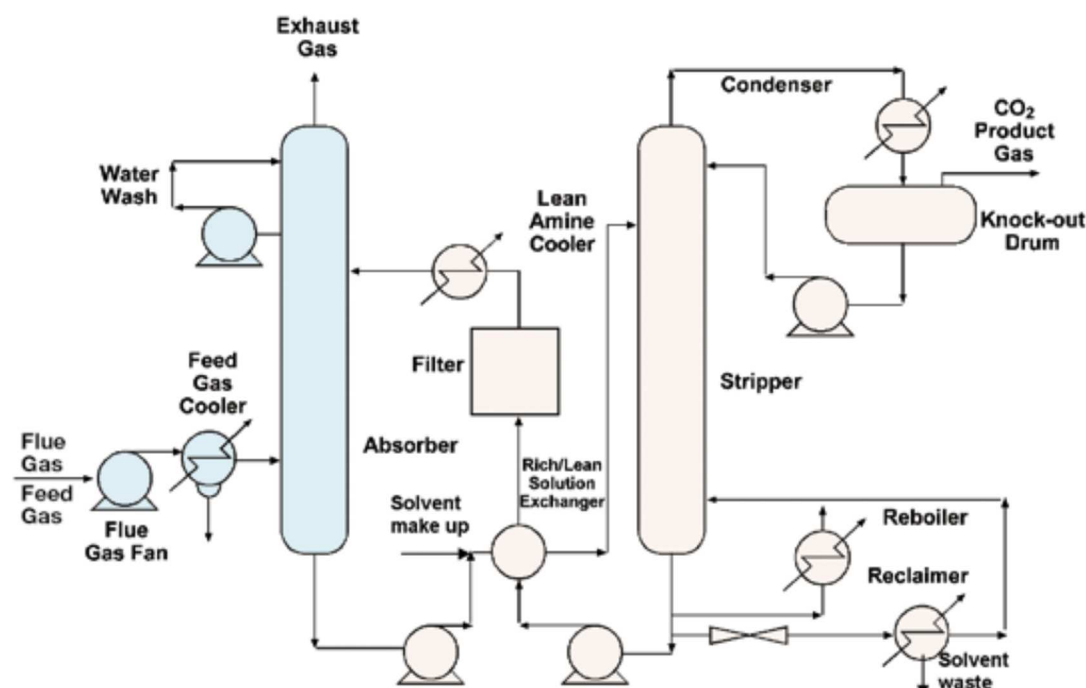
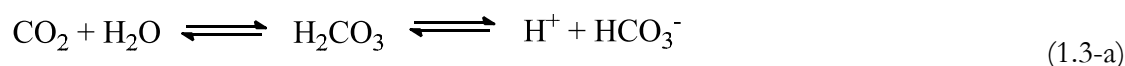


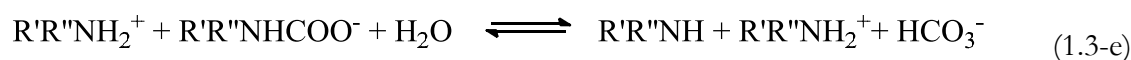
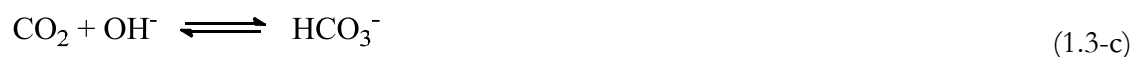
Figure 1.3-1: Process flow diagram for CO₂ recovery from flue gas by chemical absorption⁵.

In this process, the cooled flue gas is brought into contact counter currently with the solvent in the absorber. Cleaned gas with low CO₂ concentrations is released into the atmosphere at the top of the column. CO₂ is chemically bound with the solvent as it goes down. Absorber temperatures typically lie between 40 and 60°C. The solvent with rich CO₂ content leaves the column at the bottom and is then pumped to the top of a stripper via a heat exchanger. The regeneration of the chemical solvent is carried out in the stripper at elevated temperatures (100°C–140°C) so that chemical equilibrium in the liquid is reversed. However, the pressure is not very much higher than atmospheric pressure (though the lower pressure is favourable). Heat is supplied to the reboiler to maintain the regeneration conditions; providing the required desorption heat for removing the chemically bound CO₂ and for steam production which acts as a stripping gas. The gas phase consists of only steam and CO₂. The steam is recovered in a condenser and fed back to the stripper. Separated CO₂ leaves at the top of the stripper. The regenerated solvent (“lean” solvent) is pumped back to the absorber via the lean-rich heat exchanger where the temperature of the lean solvent is brought down and the temperature of the rich is increased. Though the process diagram of the absorption and desorption is principally the same as in Figure 1.3-1, there are some other variations in process flow diagram, basically to optimize the process, solution management and to reduce the desorption energy demand.¹⁰

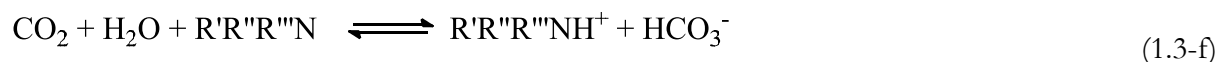
As mentioned earlier, amines are the most used alkaline solvents used in this process and the central topic of the present dissertation. They fall into different groups depending on the numbers of carbon atoms directly bonding to the nitrogen atom. These groups are primary, secondary, and tertiary amines. General reaction scheme involving in the system of CO₂ and primary and secondary amines can be presented as given in from 1.3-a to 1.3-e.¹¹



(R', R'' = organic radicals, for primary amine R'' = H)



Basically, carbamate formation reaction is the fastest reaction (1.3-d) which defines the CO₂ capacity of the aqueous amine solvent to be 0.5 mol CO₂ per mol of amine. Other reactions are less important under this circumstance. However, carbamate hydrolysis reaction (1.3-e) is important at high CO₂ partial pressure. The tertiary amines do not form carbamate and reactions (1.3-b) and (1.3-c) are important in such circumstances. Their reaction with CO₂ leads to formation of the bicarbonate ion as shown in reaction (1.3-f)



In addition to the tertiary amine, reaction (1.3-f) is also important for sterically hindered amines. A sterically hindered amine is defined structurally as a primary amine in which the amino group is attached to a tertiary carbon atom or a secondary amine in which the amino group is attached to a secondary or tertiary carbon atom.¹² Since they are also primary or secondary amines they have the

ability to form carbamate. However, the instability of carbamate ions that are formed in an aqueous system of sterically hindered amines have been claimed to be responsible for the high absorption capacity of such solution¹² over the other two carbamate forming amine types (primary and secondary).

Even though amine based processes are expected to be the most widely employed because of high affinity for CO₂ at low partial pressure of CO₂ in the flue gas stream, the technology faces some drawbacks, mainly the large amount of energy required for regeneration. Other drawbacks include solvent degradation, environmental issues and equipment corrosion. The solvent degradation, in the presence of flue gas impurities (e.g. O₂, SO_x and NO_x), leads to many problems including reduction in capacity, corrosion, release of pollutants from toxic degradation products, foaming etc.¹³ Reduction in cost in terms of both capital and operational is required to make the process economically feasible. One possible approach is the improvement of absorbents. High cyclic capacity, high reaction rate, chemical stability, ease of handling, low vapour pressure, low corrosiveness and low cost are the features of preferred absorbents for this process. Monoethanolamine (MEA) is so far the benchmark for this process. MEA, as a primary amine, has been used extensively since it has high reactivity, low cost and ease of handling. However, the maximum CO₂ absorption capacity is stoichiometrically limited to 0.5 mol CO₂/ mol MEA. Further, its high enthalpy of reaction with CO₂, leads to higher desorption energy consumption. Other disadvantages include the formation of a stable carbamate, the formation of degradation products with COS (carbonyl sulfide) or oxygen bearing gases, inability to remove mercaptans, vaporization losses because of high vapour pressure and its corrosiveness (more corrosive than many other alkanolamines).¹⁴

Other amines which have been typically used in the gas treating industry are diethanolamine (DEA), diisopropanolamine (DIPA) and methyldiethanolamine (MDEA). DEA and DIPA are secondary amines. Secondary amines are much less reactive COS and CS₂ than primary amines, and the reaction products are not particularly corrosive. Another advantage of DEA is that its' low vapour pressure minimises the solvent loss by vaporisation.⁹ MDEA is a tertiary amine. Its' low energy requirements, high capacity and chemical stability are very important for the application. However, its' low rate of reaction with CO₂ limits the application. Because of various properties and advantages of various amines, mixed amines have been proposed for considerable improvement in absorption and a great savings in energy requirements.^{9,15} Steric hindrance amines (e.g. 2-Amino-2-methyl-1-propanol (AMP) 1,8-p-menthane diamine (MDA) 2-piperdine ethanol(PE)) are also interesting because the reduced carbamate stability allows

thermodynamic CO₂ loading to exceed those attainable with conventional, stable-carbamate amines. Hydrolysis of carbamate (reaction 1.3-e) results in the formation of free amine and consequently could lead to a high reaction rate.¹² Piperazine (PZ) has a higher reaction rate with CO₂ to form carbamate. However it has several drawbacks, such as low solubility and higher volatility. Therefore PZ has been used as a promoter in amine blends.¹⁶

In addition to conventional alkanolamines, recent research has focused on diamine and amino acid salts as better absorbent for CO₂ capture. 2-(2-aminoethyl-amino)ethanol (AEEA) has been found to be a potentially good absorbent for capturing CO₂ from low pressure gases because of its higher absorption rate combined with higher absorption capacity compared to MEA.¹⁴ Amino acid salts (formed from inorganic base) have been promising due to their low volatility and resistance to oxygen degradation in the absorption process and with an absorption rate similar to MEA.¹⁷ Use of amino acid salts formed from the neutralization of amino acids with an amine has also been of recent research interest.¹⁸ This indicates that current research has been focusing on improvement of cost-effective and superior-performing amines.

1.4. Importance of equilibrium constants

Since this process is chemically driven, understanding fundamental chemistry of amine-CO₂ thermodynamic could assist the rational development of the absorbents. It mainly follows two pathways, either to form bicarbonate (1.3-b and c) in an acid-base reaction, or to form carbamate (1.3-d). The equilibrium constants governing the formation of these species therefore can determine the potential of a solvent and hence the performance of solvents.

The carbonate formation pathway is mainly governed by the protonation constant of the amine, in other words, on the base strength of the amine. The carbamate formation reaction (1.3-d) depends on how easily two electron pairs available a nitrogen atom to donate; and the stability of carbamate formed. Therefore, an equilibrium point of view, carbamate hydrolysis constant (1.3-e) is thus very important and strongly influences the speciation.¹²

Additionally, hydrolysis of carbamate amine (1.3-e) occurs at higher CO₂ partial pressure in the system with primary or secondary amines. Tertiary amines do not form carbamate and follow only the carbonate formation pathway (1.3-b,c) resulting in higher CO₂ loading in absorbent solution. Steric hindered amines form carbamate but it has reduced stable and hydrolysis as (1.3-e). The study of these reaction equilibria (1.3-b, 1.3-d, 1.3-e), together with speciation based predictive models, is beneficial to rationally evaluate the performance of amines.

The equilibrium constants of protonation for many amines (1.3-b) are available in current literature. However, despite the importance of equilibrium constants of other key reactions (1.3-d & e), reliable data is lacking in the current literature. Experimentally determination of such values typically requires time and resource consuming laboratory work and sometimes suffers from reproducibility of data. Theoretically, study of these equilibrium constants could be performed by computational molecular modelling. However, such modelling has been carried out in the gas phase and the free energy in solution was determined as a summation of free energy in gaseous phase and solvation energies of relevant species. Therefore these values depend on the solvation models chosen for the determination.¹⁹

1.5. Research objectives and scope

The present dissertation focuses on developing a strategy for the prediction of carbamate related equilibrium constants more relevant to real systems. Here, the prediction approach is based on the molecular structure of the amine. The change in the molecular structure of the reactant changes the reactivity of the molecule. Therefore, equilibrium constants of the above reactions can be influenced by changing substituents on the amine molecule and its structure. More precisely, reactivity of the amine with CO₂ is influenced by electronic density on the N atom (amino is the functional group in the amine molecule.), on which the substituents attached on the amine structure have an influence. Such structure- activity relationship can be built by correlating the equilibrium constants with empirical parameters that describe the characters of substituents.

In addition to such substituents parameters, the equilibrium constants of the particular reaction, involving the amine with different structure, must be known. This dissertation work mainly focuses on carbamate stability reaction (1.3-e) i.e determination of the carbamate hydrolysis constant (K_{HYD}). This equilibrium constant is considered to be the most ‘floating’ parameter in thermodynamic modelling and strongly influences the speciation in the models. Therefore, the scope of this work also included evaluating and modifying analytical methods for speciation in carbonated amine solution to determine K_{HYD} of amine with different structures. This comprised development of a wet chemical method using available technique in any laboratory. Since this is an early stage study, the determination of the equilibrium constants was limited to a temperature of 25 °C.

In situ speciation based on spectroscopy methods has received increased attention. Therefore, the possibility of Raman spectroscopy as an analytical tool to determine the speciation in carbonated alkanolamines was attempted.

^{13}C NMR experiment was used to validate the data obtained from the analytical methods mentioned above. Further, the ^{15}N NMR experiment gives information on electron density on the N atom in the amine structure. The scope was extended to investigate possible effects on the electron density on N, which influences the amine reaction with CO_2 .

1.6. Main results

- Based on the co-relations between amine molecular structure and reaction equilibrium constants constructed, one can estimate the unknown equilibrium constants of amines. Additionally, one can get information on what kind of substitutes should be in the molecule or how the structure should be, to achieve specific equilibria. This is a novel approach in CCS for the prediction of equilibrium constants based on molecular structure.
- Interpretation of ^{15}N -NMR data for insights into the relative reactivity of the nitrogen atom in an amine. The ^{15}N chemical shift values of aqueous primary alkylamines (before CO_2 loading) have been related to corresponding carbamate-related constants available in literature. This broadens the current understanding of CO_2 -aqueous amine reactivity.
- A new wet chemical method for determination of species distribution in carbonated aqueous amine solutions for CO_2 capture was developed. The method employs analytical techniques readily available in any laboratory.
- Application of Raman spectroscopy as an analytical tool to determine the speciation of carbonated aqueous alkanolamine systems was presented. This work constitutes a simple ‘short-cut’ type approach to semi-quantitative speciation information employing measurement of selected Raman bands in conjunction with an internal standard (ClO_4^-).

1.7. Outline of the PhD thesis

This thesis consists of three main parts. Part one presents the wet chemical method developed. It gives method development, validations and application. An approach to determine the ideal equilibrium constant from the apparent equilibrium constant is also included.

The second part presents possibility of using the Raman spectroscopy as an analytical tool for speciation in carbonated amine solution.

The final part presents relationships of equilibrium constants related to amine carbamate and molecular structure effects. The interpretation of ^{15}N NMR data to explain the trends on the equilibrium constants with the amine molecular structure is addressed.

References

1. (a) IPCC *Climate Change 2001: The scientific basis*; Cambridge, UK, 2001; (b) IPCC *Climate Change 2001: Impacts, adaptation, and vulnerability*; Cambridge, UK, 2001.
2. Yang, H.; Xu, Z.; Fan, M.; Gupta, R.; Slimane, R. B.; Bland, A. E.; Wright, I., Progress in carbon dioxide separation and capture: A review. *Journal of Environmental Sciences* **2008**, *20* (1), 14-27.
3. IEA World Energy Outlook 2012 Factsheet.
<http://www.worldenergyoutlook.org/media/weowebiste/2012/factsheets.pdf> (accessed 5th September 2014).
4. IPCC *Climate Change 2014: Mitigation of Climate Change*; Cambridge, UK, 2014.
5. IPCC *IPCC Special Report on Carbon Dioxide Capture and Storage*; the United States of America, New York, 2005.
6. Wang, M.; Lawal, A.; Stephenson, P.; Sidders, J.; Ramshaw, C., Post-combustion CO₂ capture with chemical absorption: A state-of-the-art review. *Chem. Eng. Res. Des.* **2011**, *89* (9), 1609-1624.
7. Favre, E., Membrane processes and postcombustion carbon dioxide capture: Challenges and prospects. *Chem. Eng. J. (Lausanne)* **2011**, *171* (3), 782-793.
8. Rochelle, G. T., Amine Scrubbing for CO₂ Capture. *Science* **2009**, *325* (5948), 1652-1654.
9. Kohl, A.; Nielsen, R., *Gas purification* 5th ed. Houston: Gulf Publishing Company **1997**.
10. Eimer, D., *Gas Treating: Absorption Theory and Practice*. John Wiley & Sons: 2014.
11. McCann, N.; Phan, D.; Wang, X.; Conway, W.; Burns, R.; Attalla, M.; Puxty, G.; Maeder, M., Kinetics and Mechanism of Carbamate Formation from CO₂(aq), Carbonate Species, and Monoethanolamine in Aqueous Solution. *The Journal of Physical Chemistry A* **2009**, *113* (17), 5022-5029.
12. Sartori, G.; Savage, D. W., Sterically hindered amines for carbon dioxide removal from gases. *Industrial & Engineering Chemistry Fundamentals* **1983**, *22* (2), 239-249.
13. Strazisar, B. R.; Anderson, R. R.; White, C. M., Degradation Pathways for Monoethanolamine in a CO₂ Capture Facility. *Energy Fuels* **2003**, *17* (4), 1034-1039.
14. Ma'mun, S.; Svendsen, H. F.; Hoff, K. A.; Juliussen, O., Selection of new absorbents for carbon dioxide capture. *Energy Conversion and Management* **2007**, *48* (1), 251-258.
15. Chakravarty, T.; Phukan, U. K.; Weiland, R. H., Reaction of acid gases with mixtures of amines. *Chem. Eng. Prog.* **1985**, *81* (4), 32-36.

-
16. Freeman, S. A.; Dugas, R.; Van Wagener, D. H.; Nguyen, T.; Rochelle, G. T., Carbon dioxide capture with concentrated, aqueous piperazine. *International Journal of Greenhouse Gas Control* **2010**, *4* (2), 119-124.
 17. Holst, J. v.; Versteeg, G. F.; Brillman, D. W. F.; Hogendoorn, J. A., Kinetic study of with various amino acid salts in aqueous solution. *Chem. Eng. Sci.* **2009**, *64* (1), 59-68.
 18. Ciftja, A. F.; Hartono, A.; Svendsen, H. F., Selection of Amine Amino Acids Salt Systems for CO₂ Capture. *Energy Procedia* **2013**, *37* (0), 1597-1604.
 19. Gupta, M.; da Silva, E. F.; Svendsen, H. F., Computational Study of Equilibrium Constants for Amines and Amino Acids for CO₂ Capture Solvents. *Energy Procedia* **2013**, *37* (0), 1720-1727.

Part I

Wet chemical method for speciation of carbonated aqueous amine solutions

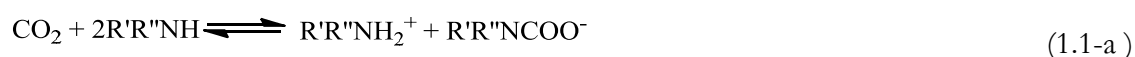
1. Overview

Chemical absorption of CO₂ into an amine-based solvent typically comprises several parallel reaction pathways leading to the formation of many different species.¹ Analysis of the liquid phase species distribution is mandatory for thermodynamic model optimization to ensure that such models account the liquid phase composition correctly. Furthermore, the chemical structure of an amine has a strong impact on the amine's capacity to capture CO₂. Determination of reaction equilibrium constants in different amine systems provides molecular structure-property information on reactivity of a specific amine towards CO₂. The speciation in different amine-CO₂ systems is required to determine the equilibrium constant of important reactions.

Despite the importance, detailed and direct information on the liquid phase speciation in these multi-equilibrium reaction systems is still challenging and so is the experimental determination of equilibrium constants.² Therefore, the present dissertation comprises development of a wet chemical method (WCM) for speciation. This work mainly focuses on the species distribution in carbonated aqueous amine solution to determine the equilibrium constant of carbamate hydrolysis reaction. The method employs analytical techniques readily available in any laboratory.

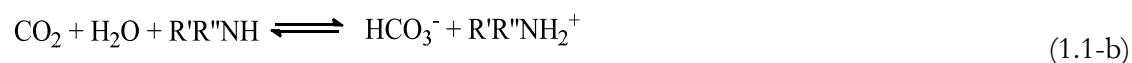
1.1. Carbamate stability

Sterically unhindered primary and secondary amines react directly with CO₂ to form carbamate as shown in reaction (1.1-a). R' and R'' are any organic radicals and one of them is replaced by H for the primary amines. This reaction pathway features faster kinetics towards formation of carbamate.



The carbamate formation, as given in above reaction (1.1-a), depends both on the stability of the carbamate and the base strength of the amine.²⁻³ CO₂ reacts with amine and forms amine carbamic acid which further reacts with the amine and forms the carbamate ion. Thus, the basicity of the amine is important for this carbamic acid- amine base reaction as well.

Any type of amine follows reaction (1.1-b). The tertiary amines (R'R''R'''N) follow only reaction (1.1-b) and hence have higher capacity than the primary and secondary amines.



Understanding the carbamate stability reaction (1.1- c) i.e. equilibrium between bicarbonate and carbamate is important since the thermodynamic behavior of the CO₂-amine system is dominated by the value of the carbamate stability constant.⁴ Further, the instability of the carbamate ions that are formed in an aqueous system of sterically hindered amines have been claimed to be responsible for the high absorption capacity of such solutions.⁴ However, at high CO₂ partial pressure, the carbamates of primary and secondary amines may also hydrolyse to generate free amines which can react further with additional CO₂ to give loading over the stoichiometric ratio of reaction (1.1-a).⁴

5



How the carbamate stability constant governs the thermodynamic behavior was explained by Sartori and Savage by deriving an expression for equilibrium vapor pressure of CO₂.⁴ Equations representing amine balance, CO₂ balance, the requirements of electrical neutrality together with amine protonation constant, K_a (1.1-1) and the amine carbamate stability constant K_c (1.1-2) were solved simultaneously to a build simple thermodynamic model to show the influence of K_c value in the model.

$$K_a = \frac{[\text{R}'\text{R}''\text{NH}][\text{H}^+]}{[\text{R}'\text{R}''\text{NH}_2^+]} \quad (1.1-1)$$

$$K_c = \frac{[\text{R}'\text{R}''\text{NCOO}^-]}{[\text{R}'\text{R}''\text{NH}][\text{HCO}_3^-]} \quad (1.1-2)$$

It can be shown that the carbamate formation equilibrium constant, by direct reaction involving CO₂ and amine (1.1-a), can be expressed as a product of the equilibrium constant of bicarbonate formation by CO₂ and H₂O, the protonation constant of amine and the inverse of K_c.²

Furthermore, at high CO₂ partial pressure, the carbamates of primary and secondary amines may also hydrolyse to generate free amines which can further react with additional CO₂ to give loading over the stoichiometric ratio of reaction (1.1-a).⁴⁻⁵

Since the carbamate stability constant is so important for characterization of specific amines, the present work targets the speciation in carbonated aqueous amine solution to determine the equilibrium constant of eq.(1.1-c), K_{HYD} (HYD : hydrolysis); equation(1.1-3) It is the inverse of the ideal carbamate stability constant. γ represents activity coefficient of species.

$$K_{HYD} = \frac{[R_2NH] \cdot \gamma_{R_2NH} [HCO_3^-] \cdot \gamma_{HCO_3^-}}{[R_2NCOO^-] \cdot \gamma_{R_2NCOO^-}} \quad (1.1-3)$$

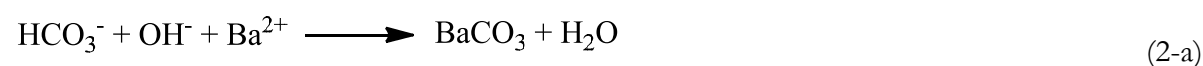
2. Literature review

Studies on carbamate stability go back to the early 1920s. In the period of 1925-1957⁶, C. Faurholt and coworkers reported the equilibrium constant of the carbamate hydrolysis reaction (K_{HYD}) for several amines.

In their studies, the carbamate solutions were prepared by dissolving carbon dioxide in solutions of a pure amine, thus all the carbon dioxide was converted to carbamate. The solutions of carbonate were prepared by mixing equivalent amounts of solutions of ammonium chloride and sodium carbonate, ($\text{AmHCl} + \text{Na}_2\text{CO}_3 = (\text{AmH})_2\text{CO}_3 + 2\text{NaCl}$). Using these solutions, the equilibrium solutions of carbonate-carbamate were made.^{6b, 6c} NaCl formed in this reaction was assumed to be insignificant. The carbamino quenching method was employed for the analysis of equilibrium solutions. In this method, BaCl_2 was used to precipitate the carbonate fractions, leaving the carbamate in the solution. The speciation was done by solving the following equations; equilibrium equations for the dissociation of protonated amine, bicarbonate and water characterized by thermodynamic constants, mass balances for amine and carbon and the requirement of electrical neutrality. Dissociation constants for protonated amines are thus required for the analysis. The activity coefficient (f) for a monovalent ion was calculated from the expression of Bjerrum, $-\log f = 0.3 \sqrt[3]{C_{\text{ion}}}$.

Chan and Danckwert (1981) used a similar method to calculate the apparent K_{HYD} values related to monoethanolamine (MEA) and diethanolamine (DEA).⁷ In their method, the carbonated solutions were prepared allowing the solutions containing amine (MEA or DEA) and NaHCO_3 to come to equilibrium at a specified temperature. The carbamino quenching method (as in the study by Faurholt and coworkers) has been used for the analysis but alkaline BaCl_2 solution was kept at 0°C . An excess amount of the alkaline BaCl_2 solution at 0°C was added to the equilibrated solution to precipitate the carbonate fraction and then it was filtered out. Rapid lowering of the temperature (0°C) and subsequent filtration of the precipitate was employed to prevent hydrolysis of the carbamate. Therefore, only HCO_3^- could be precipitated and separated. The filtrate was then titrated with HCl. The reactions involved are as follows:

At the carbamino quenching stage, alkaline BaCl_2 reacts with HCO_3^- as shown in reaction (2-a).



At the titration stage, the acid (H^+) reacts with the amine (2-b) and OH^- remained after the carbamino quenching stage (2-c). Further, carbamate undergoes acid hydrolysis (2-d).



The moles of H^+ consumed for the titration and the initial concentrations of amine, $NaHCO_3$ and OH^- which were used to make the $BaCl_2$ solution alkaline, were known. Stoichiometric balances for the H^+ (consumed for the titration) and OH^- and mass balances for amine and $NaHCO_3$ give a system of four equations. By solving this system of equations simultaneously, concentrations of amine, HCO_3^- and carbamate at the equilibrium can be calculated and so was the apparent K_{HYD} . The experiments were run at different initial concentrations of the amines and carbonate solutions so that apparent K_{HYD} were calculated at different ionic strengths. However, in this method, the initial concentration of $NaHCO_3$ has to be known, which is generally at the equilibrium of $NaHCO_3/CO_3$. Moreover, this method does not give a complete speciation.

The temperature dependence on the carbamate stability constant for MEA and DEA was studied by Haji-Sulaiman and Aroua.⁸ The carbonated aqueous amine solutions were prepared by adding powdered solid $NaHCO_3$ to amine solution (MEA or DEA) and allowing it come to equilibrium. The procedure was repeated for several molar ratios of initial concentrations of $NaHCO_3$ and the amine solution (MEA or DEA). The ionic strength of the solution was changed by adding $NaClO_4$ in order to determine the apparent equilibrium constants at varying ionic strengths at a specific temperature. After the equilibration, samples of the equilibrated solutions were titrated with $NaOH$ employing dynamic equivalence-point titration. This titration gives the total concentration of bicarbonate protonated amine at equilibrium. Together with this titration value, three equilibrium equations characterized by thermodynamic constants (dissociation of protonated amine, bicarbonate and water in the equilibrated solutions), two mass balances (for amine and carbon) equations and electrical neutrality balance in the solution gives a system of seven equations. By solving this system of equations simultaneously, a complete speciation can be carried

out and hence the apparent equilibrium constant at different ionic strengths can be determined. The apparent equilibrium constants were plotted against the square root of the ionic strengths to determine the ideal equilibrium constants by extrapolating the curve to zero ionic strength. Dissociation constants of protonated amine, bicarbonate and water were taken from the literature. This method is fast and consistent, but protonation constants for all the amines are not easily available.

3. Method Development

In the present work, a wet chemical method for speciation of carbonated amine solutions was developed. The method employs the carbamino quenching technique, a strong base titration and pH measurement. The method was developed using Monoethanolamine (MEA). The speciation for identical solutions was done by using ^{13}C NMR spectroscopic analysis to compare the results.

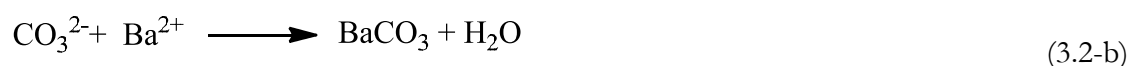
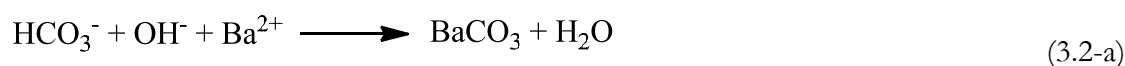
3.1. Preparation of carbonated aqueous amine solution

In a typical sample preparation run, the carbonated aqueous amine solution was prepared by dissolution of a predetermined amount of NaHCO_3 into an aqueous amine solution according to the literature.^{7,8b} The ratio of initial concentrations $[\text{NaHCO}_3]_{\text{init}} / [\text{amine}]_{\text{init}}$ was varied 0.5, 0.75 and 1.0. The system was allowed to equilibrate for 24 hours in a thermostated closed cell (Grant LTD6G) at $24 \pm 1^\circ\text{C}$. Three parallel equilibrium experiments were run for MEA. After equilibration, the samples were analysed with two parallels using the wet chemical method proposed here.

All chemicals were of analytical grade or better quality and used as received (Details of the chemicals is given in Appendix A). Deionised (Milli-Q water, resistivity = $18.2 \text{ M}\Omega\cdot\text{cm}$ at 25°C) and degassed water was used to prepare the aqueous amine solution (2 wt % of MEA or $0.321 \pm 0.004 \text{ mol}\cdot\text{dm}^{-3}$). The concentrations were checked by titration with $1.0 \text{ mol}\cdot\text{dm}^{-3}$ HCl.

3.2. Carbamino quenching method

The concentrations of carbonate fractions (HCO_3^- and CO_3^{2-}) in the carbonated solutions can be determined by the carbamino quenching method, where alkaline BaCl_2 is used to precipitate the carbonate fractions, leaving the carbamate in solution (3.2-a and b).



To apply this technique for the current procedure, an aliquot of the carbonated amine solution (≈ 1.5 g) was transferred and mixed with an excess of alkaline BaCl_2 at 0°C . Precipitated BaCO_3 was then filtered quickly off while the flask was rinsed thoroughly with distilled water, to make sure all the precipitate transferred to the next step; (i.e. carbonate titration). Here, it is assumed that low temperature and rapid filtration prevent hydrolysis of the carbamate.⁷ The next step was the carbonate titration. The BaCO_3 precipitate slurry, in ca. 100 cm^3 of distilled water was titrated with $0.1\text{ mol}\cdot\text{dm}^{-3}$ HCl to a predefined endpoint at $\text{pH} = 2$ so that all the BaCO_3 was dissolved. The solution was heated to remove all dissolved CO_2 and cooled down to ambient temperature followed by back titration with $0.1\text{ mol}\cdot\text{dm}^{-3}$ NaOH solution to determine excess HCl . The results were corrected for the blank value of the procedure. The titrations were carried out with a PC controlled potentiometric titrator (Metrohm 905 Titrando).

3.3. Titration with a strong base

20 ml of the samples from the carbonated amine solution were titrated with $1.0\text{ mol}\cdot\text{dm}^{-3}$ NaOH employing the Dynamic equivalence Titration (DET) technique⁹ using the PC controlled Metrohm 905 Titrando titrator. A typical DET titration curve for a titration of a sample of carbonated amine solution with $1.0\text{ mol}\cdot\text{dm}^{-3}$ NaOH is shown in Figure 3.3 1. The first derivative of the titration curve is determined and the highest change in the derivative is corresponding to the end point. NaOH reacts with HCO_3^- and RNH_3^+ as shown in (3.3- a and b) and this analysis gives the total concentration of HCO_3^- and RNH_3^+ .



A strong base, such as NaOH , could hydrolysis the carbamate and form extra HCO_3^- in the sample during the titration. Consequently, it could lead to error in the analysis. However, the carbamate hydrolysis reaction with NaOH at room temperature is very slow and can be neglected. Further, addition of strong base does not change the reaction equilibrium during the shorter titration period.⁹

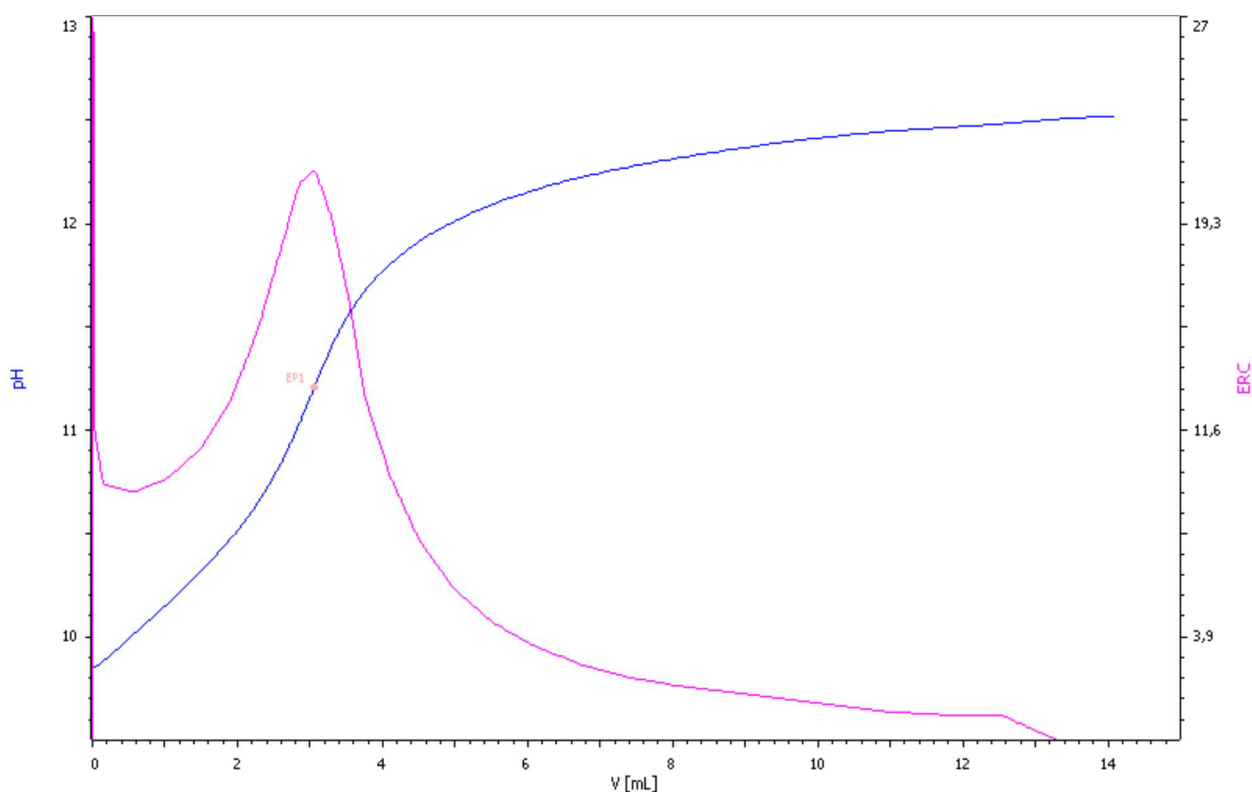


Figure 3.3-1: Titration curve for Dynamic Equivalence Titration (DET). Titration curve for a sample of carbonated amine solution titrated with $1.0 \text{ mol}\cdot\text{dm}^{-3}$ NaOH. ERC: Endpoint Recognition Criterion.

3.4. pH measurement

The pH measurement was carried out using a combination pH glass electrode (Metrohm iEcotrode Plus with Ag/AgCl cartridge Internal reference electrode) connected to the same (above) titrator. The resolution of the pH meter is 0.001 pH. NIST (National Institute of Standards and Technology) traceable buffer solutions at pH 4.00 / 7.00 / 9.00 at 25 °C (single use sachets; purchased from Metrohm) were used for three point calibration of the glass electrode. The sample was stirred with a magnetic stirrer rod during the measurement. The intensity of stirring was limited ≈ 200 rpm, and it was assumed to be low enough not to influence the electrode potential.

There are two studies which showed that the measured pH value could be used as a measurement for the ionic activities of H^+ with a minimum error. One study, by Critchfield and Johnson¹⁰, on the effect of natural salt (calcium chloride ionic concentration 0 – 5 M) on the pH of acid solution (0.1 M hydrochloric acid), reported that the measured pH value using a glass electrode (Leeds & Northrup line-operated pH meter equipped with glass and calomel electrodes) and the calculated acidity, using Hammett acidity function, were essentially the same quantities. The maximum

deviation between the two quantities was reported to be 0.1 units. In the other study¹¹, Pitzer's Equations for the single-ion activity coefficient was used to determine the pH of aqueous solution of potassium hydrogen phthalate (ranging from 0.01 to 0.1 mol • kg⁻¹), in mixtures with KCl and NaCl at 298.15 K and high ionic strength. The concentration of KCl was reported to vary 0.01 to 2 mol • kg⁻¹, and the concentration of NaCl was 1 mol • kg⁻¹. Calculated pH values were compared with measured pH values (using a combination glass electrode) and the difference was found to be less than 1 %.

3.5. Density measurements

All the solutions were prepared with concentrations based in mol per kg solution, and later the concentration unit was converted to molar (mol•dm⁻³) basis. Therefore, densities of carbonated aqueous amine solutions were measured using an Anton Paar densimeter; model DMA 4500 employing oscillating U-tube technique (oscillation of a known volume is influenced by mass of the fluid filled in the known volume). The densimeter was calibrated using degassed distilled water and air.

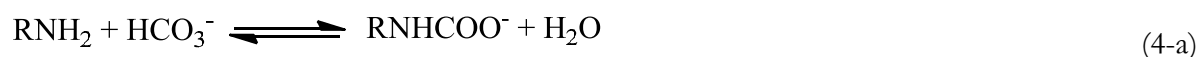
3.6. ¹³C NMR experiment

The ¹³C-NMR experiments were performed at 9.4 T (tesla) on a Bruker Avance III 400 MHz spectrometer using a BBFO Plus double resonance probehead at 298.15 K, and the spectra were processed using MestreNova software v 7.1.1. The method used has been fully described previously¹². The experimental work was carried out in cooperation with B. Arstad, A. Bouzga and C. Perinu at the SINTEF NMR facility in Oslo.

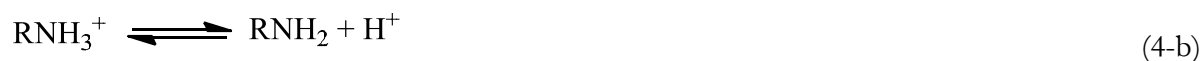
4. Chemistry of the method and mathematical procedure

When an aqueous solution of amine is allowed to react with bicarbonate, the following equilibria are established; From (4-a) to (4-d)

Formation of carbamate,



Dissociation of protonated amine,



Dissociation of bicarbonate,



Dissociation of water,



Considering the above equilibria, $[\text{OH}^-]$, $[\text{H}^+]$, $[\text{HCO}_3^-]$, $[\text{CO}_3^{2-}]$, $[\text{RNHCOO}^-]$, $[\text{RNH}_3^+]$ and $[\text{RNH}_2]$ are the potential species in the system at equilibrium.

In the carbamino quenching method (described in section 3.2), the total concentration P of $[\text{HCO}_3^-]$ and $[\text{CO}_3^{2-}]$ is determined as expressed in equation (4-1).

$$P = [\text{HCO}_3^-] + [\text{CO}_3^{2-}] \quad (4-1)$$

A sample of carbonated solution titrated with strong base (as described 3.3) gives the total concentration B of $[\text{HCO}_3^-]$ and $[\text{RNH}_3^+]$ as expressed in (4-2).

$$B = [\text{HCO}_3^-] + [\text{RNH}_3^+] \quad (4-2)$$

The equilibrium dissociation constant of the bicarbonate ion ($K_{\text{aHCO}_3^-}$) is as given in equation (4-3).

$$K_{\text{aHCO}_3^-} = \frac{[\text{CO}_3^{2-}]\gamma_{\text{CO}_3^{2-}}[\text{H}^+]\gamma_{\text{H}^+}}{[\text{HCO}_3^-]\gamma_{\text{HCO}_3^-}} \quad (4-3)$$

The pH determined by an electrode measures the activity of H^+ as given by equation 4-4.¹³

$$\text{pH} = -\log_{10}([\text{H}^+]\gamma_{\text{H}^+}) \quad (4-4)$$

By equations 4-3 and 4-4 together, the ratio of $[\text{CO}_3^{2-}]/[\text{HCO}_3^-]$ can be determined with known values for $K_{\text{aHCO}_3^-}$ and measured pH. A similar approach was taken in a NMR study for speciation in MEA– CO_2 systems¹⁴, to calibrate concentration ratio between MEA and MEAH^+ with pH of the solution. In the context of NMR analysis, molecular and protonated forms of the amine appears with a common signal; leading to that only the sum of their concentration can be quantified by NMR. The neutral and the protonated amines were determined according to the dissociation constant of the amine and to the pH measured. However, the activity correction was not considered in that study.

The value for the bicarbonate dissociation constant ($K_{\text{aHCO}_3^-}$,) is reported in the literature as a function of temperature (4-5).¹⁵

$$\ln K = A_1/T + A_2 \ln T + A_3 T + A_4 \quad (4-5)$$

The coefficient values of the temperature dependent functions are as given in Table 4-1.

Table 4-1: Coefficients of temperature-dependent functions for dissociation constants of HCO_3^- and water. Taken from Edwards et al.¹⁵

Equilibrium constant	A_1	A_2	A_3	A_4	Range of validity T (K)
$K_{\text{aHCO}_3^-}$	-12431.70	-35.4819	0	220.067	273-498
K_w	-1344.90	-22.4773	0	140.932	273-498

γ_i is the activity coefficient of the relevant component i . An extended form of the Debye-Huckel law as shown in equation (4-6) was used to calculate the activity coefficient.

$$\log_{10} \gamma_i = \frac{-Az_i^2\sqrt{I}}{1+b_i\sqrt{I}} \quad (4-6)$$

The parameter A depends on temperature and the value is equal to 0.511¹⁶ at 25 °C. b is dependent on the size of the involved ions, but usually considered constant. The value for b is taken to be 1.2 as suggested by Pitzer.¹⁷ z_i is the charge of ion i and the ionic strength I is given as equation (4-7).

$$I = \frac{1}{2} \sum_i c_i z_i^2 \quad (4-7)$$

The mass balances for amine and NaHCO_3 can be introduced as given in equations (4-8) and (4-9). The species with subscript *init* represent initial concentrations of the relevant species, while the species without subscripts represent those at equilibrium.

$$[\text{HCO}_3^-] + [\text{CO}_3^{2-}] + [\text{RNHCOO}^-] = [\text{HCO}_3^-]_{\text{init}} \quad (4-8)$$

$$[\text{RNH}_2] + [\text{RNH}_3^+] + [\text{RNHCOO}^-] = [\text{RNH}_2]_{\text{init}} \quad (4-9)$$

By solving equations (4-1) to (4-4) and (4-6) to (4-9) simultaneously for given values of P , B , pH , $K_{\text{aHCO}_3^-}$, $[\text{HCO}_3^-]_{\text{init}}$ and $[\text{RNH}_2]_{\text{init}}$, the concentration of species $[\text{HCO}_3^-]$, $[\text{CO}_3^{2-}]$, $[\text{RNHCOO}^-]$, $[\text{RNH}_3^+]$ and $[\text{RNH}_2]$ can be determined.

Further, using the water dissociation constant K_w as the expression given in equation (4-10), the value of $[\text{OH}^-]$ is known assuming the activity of water $a_{\text{H}_2\text{O}}$ equals to 1. The value for water dissociation constant, K_w is found in the literature as a function of temperature as expressed in equation (4-5).¹⁵

$$K_w = \frac{[\text{H}_3\text{O}^+]\gamma_{\text{H}_3\text{O}^+}[\text{OH}^-]\gamma_{\text{OH}^-}}{a_{\text{H}_2\text{O}}} \quad (4-10)$$

The system of above algebraic linear and nonlinear equations was solved by an in-house Fortran77 program, DNONLIN which was developed for these kinds of chemical systems by John A. Svendsen (Statoil Research Centre, Porsgrunn). The system of equations was solved by the subroutine DNEQNF or DNEQNJ located in the commercial IMSL Library. Double precision floating-point format was used to obtain maximum accuracy. An analytical Jacobian matrix to be used by subroutine DNEQNJ was derived. However, a numerical Jacobian matrix, which is automatically calculated by DNEQNF, also works well.

Based on the speciation, apparent equilibrium constants for carbamate hydrolysis were calculated at 25 °C and at different loading (ratio of initial $[\text{NaHCO}_3]_{\text{init}}/[\text{amine}]_{\text{init}}$). The apparent equilibrium constant (K_{HYDa}) for carbamate hydrolysis reaction (1.1-c) is as given in equation (4-11).

$$K_{\text{HYDa}} = \frac{[\text{RNH}_2][\text{HCO}_3^-]}{[\text{RNHCOO}^-]} \quad (4-11)$$

5. Method validation and discussion

Concentrations of species in carbonated MEA solution determined using the proposed wet chemical method (WCM) are compared to results from NMR based speciation on identical solutions (Table 5-1). In Table 5-1, the concentrations obtained from the WCM method are the average of three parallel equilibrium runs and the calculated apparent equilibrium constants (K_{HYDa}) at three different loadings are based on the average values; whereas the data obtained by NMR measurements are the average of two parallel equilibrium runs. Uncertainty of K_{HYDa} was determined, according to equation (5-1). The uncertainty of specific species' concentration (Δ [species]) was taken as the standard deviation of three parallel runs.

$$\Delta K_{HYDa}^2 = \left(\frac{\partial K_{HYDa}}{\partial [RNH_2]} \right)^2 \cdot (\Delta [RNH_2])^2 + \left(\frac{\partial K_{HYDa}}{\partial [HCO_3^-]} \right)^2 \cdot (\Delta [HCO_3^-])^2 + \left(\frac{\partial K_{HYDa}}{\partial [RNHCOO^-]} \right)^2 \cdot (\Delta [RNHCOO^-])^2 \quad (5-1)$$

$$\Delta K_{HYDa}^2 = \left(\frac{[HCO_3^-]}{[RNHCOO^-]} \right)^2 \cdot (\Delta [RNH_2])^2 + \left(\frac{[RNH_2]}{[RNHCOO^-]} \right)^2 \cdot (\Delta [HCO_3^-])^2 + \left(\frac{-[RNH_2][HCO_3^-]}{[RNHCOO^-]^2} \right)^2 \cdot (\Delta [RNHCOO^-])^2 \quad (5-2)$$

Table 5-1: Speciation by wet chemical method and ^{13}C -NMR analysis for carbonated 2 % MEA solution at 25 °C. Loading = the ratio of initial $[NaHCO_3]_{init} / [amine]_{init}$. P is the total concentration of $[HCO_3^-]$ and $[CO_3^{2-}]$ and B is the total concentration of $[HCO_3^-]$ and $[RNH_3^+]$.

Loading	0.50		0.75		1.00	
	WCM	NMR	WCM	NMR	WCM	NMR
Chemical analysis						
P ($mol \cdot dm^{-3}$)	0.059 ± 0.003		0.087 ± 0.005		0.149 ± 0.007	
B ($mol \cdot dm^{-3}$)	0.063 ± 0.003		0.105 ± 0.002		0.144 ± 0.003	
pH	10.32 ± 0.01		10.02 ± 0.01		9.78 ± 0.01	
Speciation ($mol \cdot dm^{-3}$)						
$[HCO_3^-]$	0.015 ± 0.001	0.016	0.032 ± 0.003	0.033	0.074 ± 0.005	0.068
$[CO_3^{2-}]$	0.044 ± 0.004	0.046	0.047 ± 0.010	0.053	0.075 ± 0.005	0.065
$[RNHCOO^-]$	0.103 ± 0.002	0.109	0.161 ± 0.011	0.152	0.172 ± 0.007	0.193
$[RNH_2]$	0.184 ± 0.011	0.169	0.100 ± 0.001	0.108	0.077 ± 0.008	0.058
$[RNH_3^+]$	0.038 ± 0.007	0.042	0.063 ± 0.006	0.053	0.070 ± 0.003	0.061
K_{HYDa} ($mol \cdot dm^{-3}$)	0.027 ± 0.003	0.025	0.020 ± 0.002	0.023	0.033 ± 0.004	0.021
Ionic strength ($mol \cdot dm^{-3}$)	0.248		0.342		0.447	

Variation in species' concentrations determined using both methods at different loadings are shown in Figure 5-1. At lower loading (0.5 and 0.75), the species concentrations obtained by both methods are the same (within the standard deviation of WCM), except free $[\text{RNH}_2]$ in the case of 0.5 and $[\text{RNH}_2]$ and $[\text{RNH}_3^+]$ in the case of the 0.75 loading. The deviation from the NMR results are 2 % for $[\text{RNH}_2]$ in the case of 0.5 loading and 6 -7 % for $[\text{RNH}_2]$ and $[\text{RNH}_3^+]$ in the case of 0.75 loading. However, in both cases, total concentration of $[\text{RNH}_2]$ and $[\text{RNH}_3^+]$ obtained from both methods were comparable. (i.e. 0.222 by WCM and 0.211 by NMR - in the case of 0.5 loading, 0.163 from WCM, and 0.161 from NMR in the case of 0.75 loading). This comparison is reasonable since fast exchanging proton species, such as $[\text{RNH}_2]/[\text{RNH}_3^+]$ appears as a common signal in NMR spectra. At loading 1.0, the species concentrations by NMR were outside the error margin of WCM, except $[\text{HCO}_3^-]$. Deviations are less than 10 % for all the species except $[\text{RNH}_2]$. $[\text{HCO}_3^-]$ and $[\text{CO}_3^{2-}]$ also appears as a common signal in the NMR. The WCM measured the total of $[\text{HCO}_3^-]$ and $[\text{CO}_3^{2-}]$ together (P in equation 4-1) as well. It allows the assessment of both concentrations together. The sum of these concentrations determined by the WCM shows around 6 % deviation as compared to NMR analysis.

The comparison of the results shows that the current method is suitable for speciation within the ionic strength range of the current study. According to the equilibrium reaction system, the concentrations of CO_3^{2-} and RNH_3^+ should be theoretically equal. From loading 0.5 to 1.0, the concentration $[\text{CO}_3^{2-}]$ and $[\text{RNH}_3^+]$, determined by the current WCM, were comparable in each loading. This indicates that the current method is quite precise within these loadings, even though some species concentrations determined by the WCM deviated from NMR based values.

Chan and Danckwerts (1981)⁷ have reported a similar study to the current work and published K_{HYD_a} values at different ionic strengths (from 0.531 to 0.686 mol•dm⁻³ at 25 °C). Within this ionic strength reported K_{HYD_a} increases with increasing ionic strength. In our work, we have found K_{HYD_a} to be 0.033 ± 0.004 mol•dm⁻³ at an ionic strength of 0.447 mol•dm⁻³. It is less than the lowest K_{HYD_a} value (0.0342 mol•dm⁻³) reported at the lowest ionic strength (0.531 mol•dm⁻³) by Chan and Danckwerts.⁷ It shows that our values are in a comparable order of magnitude.

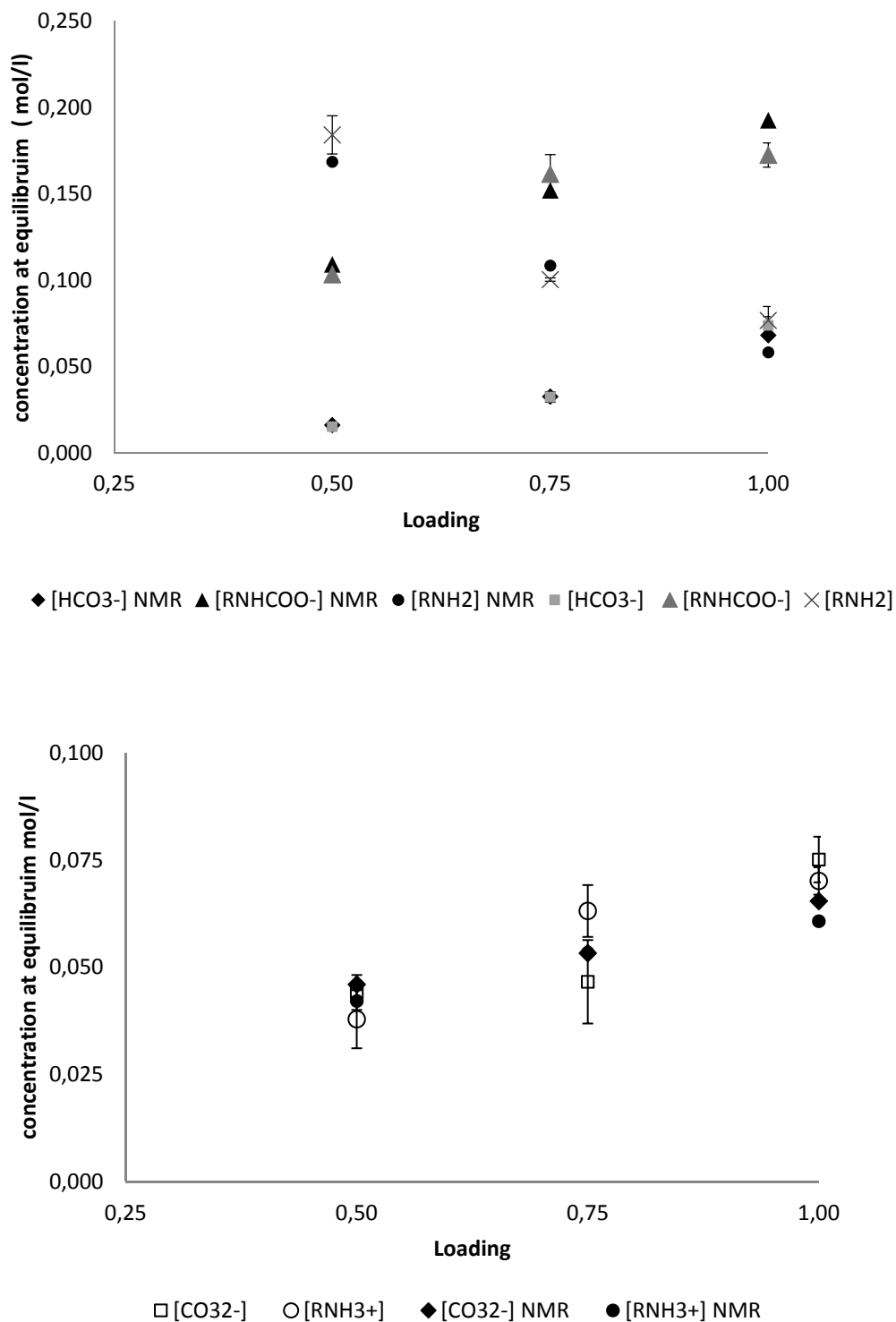


Figure 5-1: Comparison of concentrations determined by WCM to those obtained from the NMR experiment. Loading = ratio of initial $[\text{NaHCO}_3]_{\text{init}} / [\text{amine}]_{\text{init}}$.

The ionic strength of the solution increases as the loading increases. The deviation between the results by NMR analysis and WCM increases as ion strength increases and is expected to be due to the use of the Debye-Huckel approximation in species determination for the WCM. This illustrates

that the applicable range of WCM might be limited to application range of the applied Debye-Huckel approximation. The deviations for $[\text{RNH}_2]$ and $[\text{RNH}_3^+]$ are higher compared to the other species. It may imply that these two compounds are more sensitive to activity interaction.

However, failure to prepare exact initial concentration for identical solutions for both method can also contribute to differences between the result from NMR and WCM analysis. Moreover, the NMR speciations come from the average of two parallel equilibrium runs, instead of three as for WCM value. Further, accurate determination of pH is important for this analysis. There are some potential errors when the measured pH is taken to be $-\log a_{\text{H}^+}$.^{13, 18}

5.1. Discussion on pH measurement

Possible errors which may arise when using measured pH as proton activities (a_{H^+}) are important to discuss.

A potentiometric meter measures the millivolt potential difference established between two electrodes in a solution. The two electrodes are the reference electrode and the working electrode. pH approximation is based on the measured potential difference in a solution related to the potential measured in a standard buffer solution. It is expressed as given equation (5.1-1).¹³

$$pH(x) = pH(s) + \frac{E(s) - E(x)}{(RT/F) \ln 10} \quad (5.1-1)$$

$pH(x)$ represents pH of the solution to be measured and $pH(s)$ is the pH of the standard solution. R denotes the universal gas constant. T is the absolute temperature and F is the Faraday constant. The electromotive force (E. M. F.) measured by any electrode circuit is given by equation 5.1-2.¹⁹ E represents the E.M.F.

$$E = E^0 - \frac{2.303 RT}{F} \log a_{\text{H}} a_{\text{Cl}} + E_j \quad (5.1-2)$$

E_j is the algebraic sum of the liquid junction potentials. The liquid junction potential arises between two electrolyte solutions of different compositions. The compositions of the solution in the electrode and the sample solution to be measured, or pH standard solution, are different. Therefore, there exists liquid junction between the filling solution and the test sample or pH standard. Across such junctions there arises a potential difference. E^0 is the standard state of unit

activity. a_H and a_{Cl} are activities of hydrogen and chlorine. The natural logarithm value of 10 ($\ln 10$) equals to 2.303. If this equation (5.1-2) is reformulated to measure pH (i.e. negative logarithmic value of H^+ activities) it can be expressed as given in (5.1-3).

$$\log a_H = \frac{F(E-E^0-E_j)}{2.303RT} + \log a_{Cl} \quad (5.1-3)$$

A difference of two pH measurements (pH_1 and pH_2) using the same reference electrode can be expressed as shown in (5.1-4). When the same reference electrode is used, E^0 and $\log a_{Cl}$ will be the same at these two pH measurements and they are cancelled out in equation (5.1-4). Furthermore, if the liquid junction potential (E_j) is constant or the difference of E_j at the two measurements ($E_{j1}-E_{j2}$) is negligible, it makes it possible to determine the pH of the unknown solution using a solution with known or assigned pH.¹⁹

$$\frac{F(E_1-E_2)}{2.303RT} = (pH)_1 - (pH)_2 + \frac{F(E_{j1}-E_{j2})}{2.303RT} \quad (5.1-4)$$

If the liquid junction potential is the same; E_j , E^0 and $\log a_{Cl}$ are determined by calibration of the cell with a reference/standard solution of known pH(s). Then, the pH scale can be built to measure pH(x) in a solution as given in (5.1-1). However, in practice the liquid junction potential E_j does not remain constant in the sample solution and the calibration solutions (standards) due to the difference in ionic strength and ionic mobility. Therefore, the difference of liquid junction potential between these solutions cannot be negligible. Thus, it leads to error in measuring pH. A high concentration of filling solution, comprising cations and anions of almost equal mobility, is filled in the reference electrode to maintain a low and approximately constant liquid junction potential on substitution of test solution for standard solution.¹³ It is possible only when using mono pair electrodes (a separate pH measuring and reference electrode).

pH glass electrode can give inaccurate response from hydrogen-ion response function when sodium ion present in the alkaline solution and may give inaccurate measurement.¹³ This could be another possible error arising in pH measurement. However, the modern pH glass formulations have been developed to minimize this effect, increasing the selectivity of the electrode to respond to H^+ .

Stirring during the measurement is important to obtain a homogenous solution and faster pH electrode response. However, it produces a streaming potential E_s which is proportional to the pressure drop in the vortex and inversely proportional to conductivity.²⁰ Thus it is important to maintain the proper stirring rate to make the solution homogeneous and not to influence the electron potential.

6. Speciation in HCO_3^- loaded alkylamine solution

The analytical method developed above was subsequently applied to study the carbamate hydrolysis reaction (6-a) for primary alkylamines at increasing carbon chain length e.g. propyl-, butyl- and pentylamine. The main purpose was to apply the developed method for the speciation in carbonated solutions. This speciation analyses provided information on the effect of carbon chain length on the carbamate hydrolysis constant of primary alkylamines.



The aqueous amine solutions and equilibrated samples were prepared as described in previous solution 3.1 (preparation of carbonated aqueous MEA). The concentration of the aqueous amine solutions were $0.190 \text{ mol}\cdot\text{dm}^{-3}$.

6.1. Results and discussion

Speciation in carbonated primary alkylamine solution using the wet chemical method (WCM) is presented in Table 6.1-1. The values are the average of two parallel equilibrated carbonated amine solutions. Based on the speciation (Table 6.1-1), apparent equilibrium constants for carbamate hydrolysis reaction (6-a) were calculated at 25°C and at different loading (ratio of initial $[\text{NaHCO}_3]_{\text{init}}/[\text{amine}]_{\text{init}}$). The apparent equilibrium constant (K_{HYDa}) for carbamate hydrolysis reaction (6-a) is as given in equation (6.1-1).

$$K_{HYDa} = \frac{[\text{RNH}_2][\text{HCO}_3^-]}{[\text{RNHCOO}^-]} \quad (6.1-1)$$

Uncertainty of K_{HYDa} was determined, according to equation (6.1-2). The uncertainty of specific species' concentration (Δ [species]) was taken as the standard deviation of two parallel runs.

$$\Delta K_{HYDa}^2 = \left(\frac{\partial K_{HYDa}}{\partial [\text{RNH}_2]}\right)^2 \cdot (\Delta [\text{RNH}_2])^2 + \left(\frac{\partial K_{HYDa}}{\partial [\text{HCO}_3^-]}\right)^2 \cdot (\Delta [\text{HCO}_3^-])^2 + \left(\frac{\partial K_{HYDa}}{\partial [\text{RNHCOO}^-]}\right)^2 \cdot (\Delta [\text{RNHCOO}^-])^2 \quad (6.1-2)$$

$$\Delta K_{HYDa}^2 = \left(\frac{[HCO_3^-]}{[RNHCOO^-]} \right)^2 \cdot (\Delta[RNH_2])^2 + \left(\frac{[RNH_2]}{[RNHCOO^-]} \right)^2 \cdot (\Delta[HCO_3^-])^2 + \left(\frac{-[RNH_2][HCO_3^-]}{[RNHCOO^-]^2} \right)^2 \cdot (\Delta[RNHCOO^-])^2 \quad (6.1-4)$$

Table 6.1-1: Speciation using WCM for carbonated propyl-, butyl- and pentylamine solutions at 25 °C. Loading = the initial $[NaHCO_3]_{init} / [amine]_{init}$ ratio. P is the total concentration of $[HCO_3^-]$ and $[CO_3^{2-}]$ and B is the total concentration of $[HCO_3^-]$ and $[RNH_3^+]$.

	Propylamine			Butylamine			Pentylamine		
Loading	0.50	0.75	1.00	0.50	0.75	1.00	0.50	0.75	1.00
Chemical analysis									
P (mol•dm ⁻³)	0.065	0.095	0.131	0.073	0.099	0.146	0.075	0.099	0.147
B (mol•dm ⁻³)	0.050	0.072	0.116	0.058	0.082	0.113	0.047	0.057	0.100
pH	11.05	10.75	10.28	11.09	10.74	10.30	10.98	10.64	10.3
Speciation (mol•dm ⁻³)									
$[HCO_3^-]$	0.004	0.01	0.032	0.004	0.011	0.034	0.005	0.013	0.034
$[CO_3^{2-}]$	0.061	0.085	0.099	0.069	0.088	0.112	0.069	0.086	0.113
$[RNHCOO^-]$	0.034	0.054	0.065	0.027	0.047	0.050	0.026	0.049	0.050
$[RNH_2]$	0.122	0.08	0.049	0.114	0.075	0.064	0.123	0.098	0.067
$[RNH_3^+]$	0.046	0.063	0.084	0.054	0.072	0.079	0.042	0.044	0.067
K_{HYDa} (mol•dm ⁻³)	0.015	0.015	0.024	0.017	0.017	0.042	0.026	0.026	0.045
	±0.002	±0.002	±0.001	±0.003	±0.004	±0.008	±0.005	±0.004	±0.010
Ionic strength (mol•dm ⁻³)	0.214	0.307	0.387	0.232	0.314	0.404	0.226	0.300	0.400

The ideal equilibrium constant (K_{HYD} at 18 °C) of n-propylamine^{6c} and n-butylamine^{6g} were reported to be 0.013 and 0.016 respectively. It appears that K_{HYD} increases, as the length of the molecular chain increases from C3 to C4. The apparent equilibrium constant (K_{HYDa}) determined by this wet chemical method follows a similar trend from C3 to C5. K_{HYDa} increases as the length of the molecular chain increases at all the loadings (Figure 6.1-1). It may indicate that the longer the molecular chain, the lower the stability of carbamate. However, considering the uncertainties of the results, there is no significant difference in K_{HYDa} between propyl- and butylamine at lower loading and between butyl- and pentylamine at higher loading. Therefore, ideal equilibrium data should be obtained to arrive at a comprehensive conclusion.

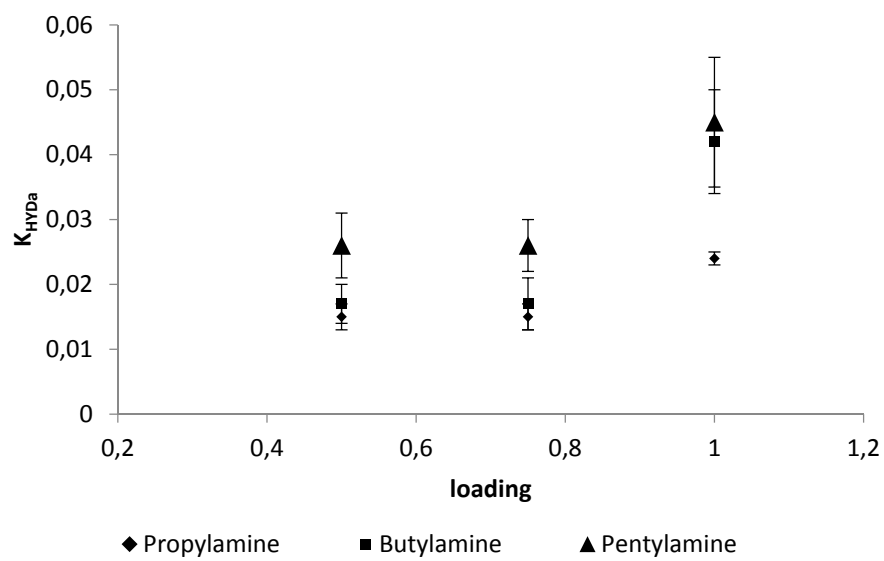


Figure 6.1-1: K_{HYDa} vs. Loading = ratio of initial $[\text{NaHCO}_3]_{\text{init}} / [\text{amine}]_{\text{init}}$.

7. Determination of ideal equilibrium constants from apparent equilibrium constants

In this section, an approach to determine the ideal carbamate hydrolysis constant at a specified temperature from the apparent constants at the same temperature is discussed using literature data.⁷ The ideal equilibrium constant is necessary to compare the performance of amines based on their thermodynamic equilibrium. Further, the ideal equilibrium constant can be related to Gibbs free energy of the reaction via the algebraic expression given in (7-1).

$$\Delta G^\theta = RT \ln K_{eq} \quad (7-1)$$

Carbamate hydrolysis reaction for any primary amine is given in (7-a).



The equilibrium constant of the carbamate hydrolysis reaction is expressed in equation (7-2).

$$K_{HYD} = \frac{[\text{RNH}_2] \cdot \gamma_{\text{RNH}_2} [\text{HCO}_3^-] \cdot \gamma_{\text{HCO}_3^-}}{[\text{RNHCOO}^-] \cdot \gamma_{\text{RNHCOO}^-}} \quad (7-2)$$

γ_i is the activity coefficient of relevant component i .

Equation (7-2) is rewritten as,

$$K_{HYD} = \frac{[\text{R}_2\text{NH}][\text{HCO}_3^-]}{[\text{R}_2\text{NCOO}^-]} \cdot \frac{\gamma_{\text{RNH}_2} \cdot \gamma_{\text{HCO}_3^-}}{\gamma_{\text{RNHCOO}^-}} \quad (7-3)$$

Apparent equilibrium constant for the carbamate hydrolysis reaction is expressed in eq (7-4)

$$K_{HYD\alpha} = \frac{[\text{R}_2\text{NH}][\text{HCO}_3^-]}{[\text{R}_2\text{NCOO}^-]} \quad (7-4)$$

Thus, equation (7-3) can be reformulated as given in eq. (7-5)

$$K_{HYD} = K_{HYDa} \cdot \frac{\gamma_{RNH_2} \gamma_{HCO_3^-}}{\gamma_{RNHCOO^-}} \quad (7-5)$$

γ_i is the activity coefficient of the relevant component i . The extended Debye-Hukel law (7-6) defines the activity coefficient of moderately dilute ionic solutions.

$$\log_{10} \gamma_i = \frac{-Az_i^2 \sqrt{I}}{1+b_i \sqrt{I}} \quad (7-6)$$

The parameter A (the Debye-Huckel limiting slope) depends on temperature. b is dependent on the size of the involved ions, but it is usually considered constant. z_i is charge of ion i . I is ionic strength as expressed as eq.(7-6).

$$I = \frac{1}{2} \sum_i c_i z_i^2 \quad (7-6)$$

c_i is concentration of the ion i . The logarithm of equation (7-5) can be expressed as in eq (7-8).

$$\log K_{HYD} = \log K_{HYDa} + \log \left(\frac{\gamma_{RNH_2} \gamma_{HCO_3^-}}{\gamma_{RNHCOO^-}} \right) \quad (7-8)$$

By substituting the expression (7-6) of activity coefficients in eq (7-8), we will get the equation (7-9)

$$\log K_{HYD} = \log K_{HYDa} + 0 + \frac{-A(1)\sqrt{I}}{1+b_i\sqrt{I}} - \frac{-A(1)\sqrt{I}}{1+b_i\sqrt{I}} \quad (7-9)$$

According to equation (7-9), the activity coefficient terms are cancelled out since b_i is assumed to be constant, and then the ideal equilibrium constant becomes nearly equal to the apparent equilibrium constant (7-10).

$$\log K_{HYD} \cong \log K_{HYDa} \quad (7-10)$$

However, deviations from the Debye-Huckel equation occur as ionic strength increases. Such deviations can be adjusted by introducing a term linear in ionic strength to the expression for the activity coefficient²¹ (e.g. $d_i I$) as given in 7-11. d_i is an adjustable parameter.

$$\log_{10} \gamma_i = \frac{-Az_i^2 \sqrt{I}}{1+b_i \sqrt{I}} + d_i I \quad (7-11)$$

Hence, a linear term can be added to the equation (7-10).

$$\log K_{HYD} = \log K_{HYDa} + dI \quad (7-12)$$

d is introduced as a common adjustable parameter for all d_i . Rearranging (7-12) for a plot of $\log K_{HYDa}$ against I should be linear with slope equal to $-d$ and intercept equal to $\log K_{HYD}$ (equation 7-13).

$$\log K_{HYDa} = \log K_{HYD} - dI \quad (7-13)$$

The above concept is demonstrated using apparent equilibrium constant values for the carbamate hydrolysis (K_{HYDa}) reaction at 25 °C and different ionic strengths taken from a previous study.⁷ The data is presented in Table 7-1.

Table 7-1: Apparent equilibrium constant values for a carbamate hydrolysis reaction (K_{HYDa}) at 25 °C with different ionic strengths (Chan and Danckwerts 1981⁷).

Ionic strength (mol•dm ⁻³)	K_{HYDa} (mol•dm ⁻³)	$\log K_{HYDa}$
0.531	0.0342	-1.46597
0.593	0.0360	-1.44370
0.624	0.0378	-1.42251
0.686	0.0390	-1.40894

Figure 7-1 shows the plot of $\log K_{HYDa}$ vs. I . The data points are fitted to linear trend line. The intercept of the line gives the value for $\log K_{HYD}$. The intercept equals to -1.666. Therefore, the ideal equilibrium constant of carbamate hydrolyses at 25 °C is 0.021 mol/dm³. This result is

comparable with a recent study on carbamate stability of amines based on the ^1H NMR spectroscopic method.²² The Ideal K_{HYD} for MEA was reported to be $0.017 \text{ mol}\cdot\text{dm}^{-3}$ at 298 K. The study²² was performed at lower initial concentrations so that it was fair enough to use the extended form of Debye- Huckel equation for activity coefficient correction.

This shows that if the apparent equilibrium constants at specific temperature are determined within a range of ionic strength which doesn't deviate excessively from the Debye-Huckel equation, the above concept can be applied to determine the ideal equilibrium constants. The developed wet chemical method in the previous section can be employed to determine the apparent equilibrium constants at different ionic strengths.

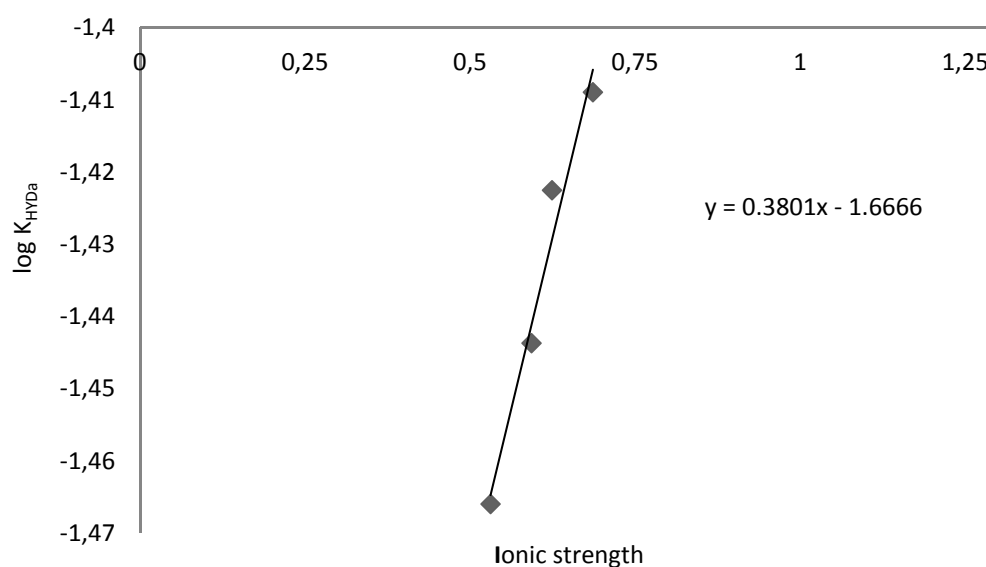


Figure 7-1 : $\log K_{HYDa}$ vs. ionic strength

8. Conclusion, recommendations and further work

Conclusion

- In order to find the carbamate stability constant, a new method for speciation determination in aqueous amine solutions for CO₂ capture was developed. This analytical method uses readily available laboratory techniques.
- The results of the WCM method were confirmed by speciation obtained by quantitative ¹³C NMR experiments.
- The apparent equilibrium constant (K_{HYD_a}) appears to increase as the carbon chain of primary alkylamine increases from C3 to C5.

Recommendations

- The extended Debye-Huckel law accurately corrects the activity coefficients of very dilute ionic solutions. Therefore, one should be cautious when choosing the concentrations of the samples. Lower ionic strength in samples will reduce the error since it makes the approximation for the activity coefficients more reasonable.
- Mono pair pH electrodes, instead of a combination electrode could minimize the error that arises during pH measurement.

Further work

- The method is still to be applied for speciation in CO₂ loaded aqueous amine solutions.
- Further in this study, the current method can be recommended to determine the K_{HYD_a} at varying ionic strengths, in order to find out ideal K_{HYD} as explained in section 7 in this Part I. However, the applicable range for activity coefficient correction should be considered when deciding the range of ionic strength.

References

1. McCann, N.; Phan, D.; Wang, X.; Conway, W.; Burns, R.; Attalla, M.; Puxty, G.; Maeder, M., Kinetics and Mechanism of Carbamate Formation from CO₂(aq), Carbonate Species, and Monoethanolamine in Aqueous Solution. *The Journal of Physical Chemistry A* **2009**, *113* (17), 5022-5029.
2. da Silva, E. F.; Svendsen, H. F., Study of the Carbamate Stability of Amines Using ab Initio Methods and Free-Energy Perturbations. *Ind. Eng. Chem. Res.* **2005**, *45* (8), 2497-2504.
3. da Silva, E. F., Theoretical study of the equilibrium constants for solvents for CO₂ capture. *Energy Procedia* **2011**, *4* (0), 164-170.
4. Sartori, G.; Savage, D. W., Sterically hindered amines for carbon dioxide removal from gases. *Industrial & Engineering Chemistry Fundamentals* **1983**, *22* (2), 239-249.
5. Astarita, G.; Savage, D. W.; Bisio, A., *Gas treating with chemical solvents*. Wiley: New York, 1983.
6. (a) Faurholt, C., Etudes sur les solutions aqueuses de carbamates et de carbonates. *J. Chim. Phys.* **1925**, *22*, 1; (b) Lund, V.; Faurholt, C., Carbamates. III. The carbamates of ethylamine and diethylamine. . *Dansk Tidsskrift for Farmaci* **1948**, *22*, 109-23; (c) Olsen, J.; Vejlbj, K.; Faurholt, C., Studies on Carbamates, VII. The Carbamates of *n*-Propylamine and *iso*-Propylamine. *Acta Chem. Scand.* **1952**, *6*, 398-403; (d) Jensen, A.; Jensen, M. B.; Faurholt, C., Studies on Carbamates, VII. The Carbamates of Benzylamine, Piperidine and Aniline. *Acta Chem. Scand.* **1952**, *6*, 1073-1085; (e) Jensen, M. B.; Jørgensen, E.; Faurholt, C., Reaction between Carbon Dioxide and Amino Alcohol, I. Monoethanolamine and Diethanolamine. *Acta Chem. Scand.* **1954**, *8*, 1137-1140; (f) Jensen, A.; Jensen, M. B.; Faurholt, C., Studies on Carbamate, X. The Carbamates of Di-*n*-propylamine and Di-*iso*-Propylamine. *Acta Chem. Scand.* **1954**, *8*, 1129-1136; (g) Jensen, M. B., Studies on Carbamates, XII. The Carbamates of the Butylamines. *Acta Chem. Scand.* **1957**, *11*, 499 - 505.
7. Chan, H. M.; Danckwerts, P. V., Equilibrium of MEA and DEA with bicarbonate and carbamate. *Chem. Eng. Sci.* **1981**, *36*, 229-230.
8. (a) Aroua, M. K.; Amor, A. B.; Haji-Sulaiman, M. Z., Temperature Dependency of the Equilibrium Constant for the Formation of Carbamate From Diethanolamine. *J. Chem. Eng. Data* **1997**, *42* (4), 692-696; (b) Aroua, M. K.; Benamor, A.; Haji-Sulaiman, M. Z., Equilibrium Constant for Carbamate Formation from Monoethanolamine and Its Relationship with Temperature. *J. Chem. Eng. Data* **1999**, *44* (5), 887-891.

9. Haji-Sulaiman, M. Z.; Aroua, M. K.; Pervez, M. I., Equilibrium concentration profiles of species in CO₂—alkanolamine—water systems. *Gas Separation & Purification* **1996**, *10* (1), 13-18.
10. Critchfield, F. E.; Johnson, J. B., Effect of Neutral Salts on pH of Acid Solutions. *Anal. Chem.* **1959**, *31* (4), 570-572.
11. Chan, C.-Y.; Eng, Y.-W.; Eu, K.-S., Pitzer Single-Ion Activity Coefficients and pH for Aqueous Solutions of Potassium Hydrogen Phthalate in Mixtures with KCl and with NaCl at 298.15 K. *J. Chem. Eng. Data* **1995**, *40* (3), 685-691.
12. Perinu, C.; Arstad, B.; Bouzga, A. M.; Svendsen, J. A.; Jens, K. J., NMR-Based Carbamate Decomposition Constants of Linear Primary Alkanolamines for CO₂ Capture. *Ind. Eng. Chem. Res.* **2014**, *53* (38), 14571-14578.
13. Covington, A. K.; Bates, R.; Durst, R., *Definition of pH scales, standard reference values, measurement of pH and related terminology*. Blackwell: 1985.
14. Fan, G.-j.; Wee, A. G. H.; Idem, R.; Tontiwachwuthikul, P., NMR Studies of Amine Species in MEA—CO₂—H₂O System: Modification of the Model of Vapor—Liquid Equilibrium (VLE). *Ind. Eng. Chem. Res.* **2009**, *48* (5), 2717-2720.
15. Edwards, T. J.; Maurer, G.; Newman, J.; Prausnitz, J. M., Vapor-liquid equilibria in multicomponent aqueous solutions of volatile weak electrolytes. *AIChE J.* **1978**, *24* (6), 966-976.
16. Lewis, G. N.; Randall, M.; Pitzer, K. S.; Brewer, L., *Theories of Electrolyte Solution In Thermodynamics* McGraw-Hill: New York, 1961; pp 332-348.
17. Pitzer, K. S., Thermodynamics of electrolytes. I. Theoretical basis and general equations. *The Journal of Physical Chemistry* **1973**, *77* (2), 268-277.
18. Bates, R. G., *Determination of pH; theory and practice*. Wiley: New York, 1973.
19. Bates, R. G., Definitions of pH Scales. *Chem. Rev. (Washington, DC, U. S.)* **1948**, *42* (1), 1-61.
20. Sisterson, D. L.; Wurfel, B. E., Methods for reliable pH measurements of precipitation samples. *Int. J. Environ. Anal. Chem.* **1984**, *18* (3), 143-165.
21. Wright, M. R., *An introduction to aqueous electrolyte solutions*. Wiley: Chichester, 2007.
22. Fernandes, D.; Conway, W.; Burns, R.; Lawrance, G.; Maeder, M.; Puxty, G., Investigations of primary and secondary amine carbamate stability by ¹H NMR spectroscopy for post combustion capture of carbon dioxide. *The Journal of Chemical Thermodynamics* **2012**, *54* (0), 183-191.

Part II

Raman spectroscopy for speciation of carbonated aqueous amine solutions

1. Overview

Speciation of carbonated solutions is required for the determination of equilibrium constants which are vital for the rational development of better absorbents for CO₂ capture. Speciation based on spectroscopic methods has received increased attention. Such spectroscopic methods are NMR (Nuclear magnetic resonance) spectroscopy, FT-IR (Fourier transform infrared) spectroscopy and Raman spectroscopy. In this section, the applicability of Raman spectroscopy as an analytical tool to determine speciation in carbonated aqueous alkanolamine solutions is studied. The section begins with brief introductions to NMR and FT-IR spectroscopic methods as applicable to the CO₂ capture field.

1.1. Nuclear magnetic resonance (NMR) spectroscopy

NMR is a non-invasive analytical technique which allows the study of atoms that have nuclei with a magnetic moment (i.e. a spin quantum number of the nucleus different from zero, such as ¹H, ¹³C, ¹⁵N NMR). Nuclei with spin have an angular momentum which create a magnetic field. These Nuclei with magnetic moments have random orientations. When a stronger magnetic field is applied over these nuclei, they align either with the field or against it. Nuclei at lower energy state align with the external magnetic field, while nuclei at higher energy align against it. However, there are more nuclei at lower energy spin state (ground state) than at higher energy spin state (excited state). While still in the external magnetic field, the nuclei at lower energy states can absorb RF (radio frequency) energy needed to align these against the external magnetic field. And then it is said to be “in resonance”. The NMR spectrometer detects the absorption of RF energy. A subsequent RF signal can only be determined if enough nuclei have ‘relaxed’ back from the excited into the ground state. The final observed NMR signal is composed of a predetermined number of RF pulses (scans). The NMR signal strength is proportional to the absorbed RF energy. For quantitative measurement of a specific nucleus, all nuclei of this type have to be in the equilibrated ground state before a new measurement can commence. The time for this relaxation process to go to completion is different for different nuclei and determines the total spectrum acquisition time at a given number of scans.

Essentially, the nuclei are surrounded by electrons that partially shield them from the external magnetic field. Shielded electron charges can also induce a magnetic field that opposes the externally applied field, making the external field weaker. The shielding around a specific nucleus is distinguishing character defined by chemical environment of it. Therefore, the same atomic nucleus at different positions in the same molecules or in different molecules requires different absorption energies. Thus, this phenomenon allows the detection of the different atomic species and; their quantification, since the peak areas are directly proportional to the number of nuclei contributing to the NMR signals. The variation in absorption frequency of NMR signal is measured by chemical shift. The chemical shift value is expressed relative to a signal from reference compound which is added to the sample.

NMR spectroscopy has been used for the speciation of CO₂ loaded aqueous amine solutions.¹ The speciation of CO₂ loaded aqueous alkanolamine solutions is commonly performed by ¹³C NMR experiments because information related to the carbon containing species can be gained. However, ¹³C NMR shows relatively poor sensitivity due to relatively weak carbon molar receptivity², and relatively slow relaxation of ¹³C spins back to thermal equilibrium. These combined effects often lead to long spectrum acquisition times.

Moreover, “inter- and intra-molecular exchanging species may lead to modulations of the NMR signals”.¹ Depending on how fast such exchange rates are in the NMR time scale, the different NMR signals may coalesce and appear at an average chemical shift. This average chemical shift value also depends on the relative amount of each species contributing to the NMR signal. In the context of ¹³C NMR determination of CO₂ loaded aqueous amine solutions, species with intermolecular proton exchange will appear with a common peak e.g. for the case of bicarbonate and carbonate. Quantification will only give the sum of the respective concentrations. In such cases, indirect methods are employed to quantify each species separately.³ Similarly, it is not possible to distinguish between molecular and protonated forms of amines.

1.2. Fourier transform infrared spectroscopy (FT-IR) spectroscopy

Fourier transform infrared spectroscopy (FT-IR) spectroscopy combined with an attenuated total reflectance (ATR) probe head is a recent method for alkanolamine-CO₂-H₂O system speciation.⁴

When infrared photons (weave length about 8×10^{-5} cm to 1×10^{-1}) are absorbed by a molecule, the energy of the molecule will increase depending on the energy of the photon. This energy may induce a transition of the molecules from one vibration or rotational energy state to another. But it does not cause electronic transitions. To absorb IR radiation, a molecule must undergo a net change in dipole moment as it vibrates or rotates. Only in such cases can the field associated with radiation interact with the molecule and cause changes in the amplitude of one of its motion.⁵ An IR spectrometer emits a specific IR radiation range and measures the IR frequencies absorbed by a chemical compound. Fourier Transformation (FT) converts the time domain amplitude function into the frequency domain so that the characteristic frequencies can be easily viewed. The attenuated total reflectance probe (ATR-IR) enables IR measurement of samples in highly absorbing media, such as aqueous solutions. The probe head allows the IR beam to interact only with molecules at the surface of the sample.⁶

FT-IR spectroscopy is an option for quantification of species which cannot be measured directly by NMR (i.e. species with inter- and intra-molecular exchanging nuclei). Since the acquisition times are considerably shorter than for ^{13}C NMR, FT-IR is used as an in-situ measurement method. However, compared to NMR based methods, vibration spectroscopic techniques require calibration models for quantitative analysis. Another advantage of using FT-IR is that the peak corresponding to the antisymmetric stretching of CO_2 is located at 2340 cm^{-1} where no other peak is observed.^{4a} Quantification of molecular CO_2 is thus readily possible. However, the broad O-H IR absorption feature of water still remains an obstacle in certain spectral ranges. It may result in blanketing of absorption peaks by other species.⁷

Therefore, in the context of the CO_2 amine system, Raman spectroscopy seems to be a promising technique for speciation analysis in carbonated alkanolamine solutions. It shows less sensitivity to water content in the sample when compared to IR spectroscopy. Furthermore, fiber optical cables are readily available for connection of the spectrometer to the measurement probe head and the method requires shorter acquisition times than for ^{13}C -NMR measurement.

2. Raman spectroscopy

This phenomenon, bearing his name, was discovered in 1928 by C. V. Raman. When monochromatic light of energy $h\nu_0$ (h – Planck’s constant, ν_0 –frequency of the beam) goes thorough matter, photons collide with the molecules and can excite to a virtual state of their vibration energy. In such an encounter, energy transfers between incident light and irradiated molecules (Figure 2-1)

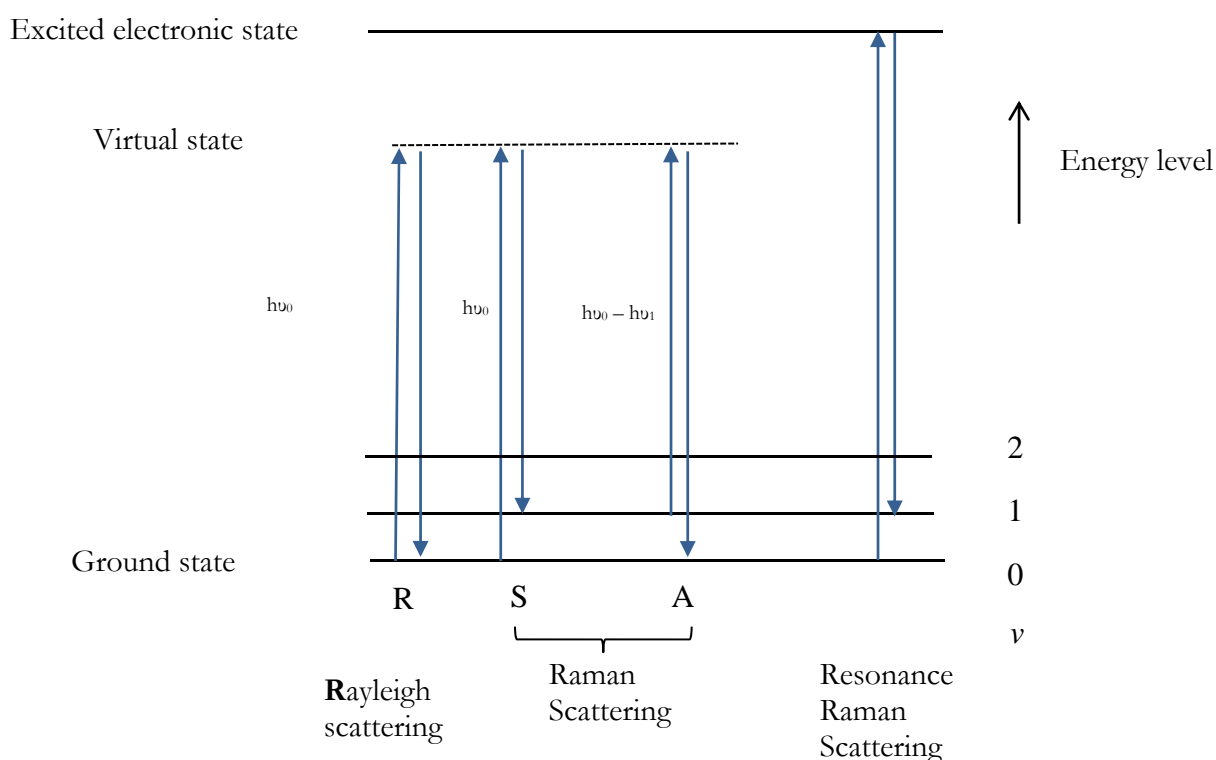


Figure 2-1: Energy diagram for vibration energy of molecule transitions in Raman spectroscopy ν_0 indicate laser frequency, while ν is the vibrational quantum number. The virtual state is a short-lived distortion of the electron distribution by the electric field of the incident light. R- Rayleigh scattering, S- Stokes Raman shift, A- Anti-stokes. Adapted from McCreery, 2009.⁸

As shown in Figure 2-1, after energy transformation from incident light to the molecule, the molecule can be considered excited to a virtual state of vibration energy. When the molecule is transferred back to the ground state from the virtual state, and emits the same energy as the

excitation photon, it is called Rayleigh scattering (R in Figure 2-1). Rayleigh scattering is strong and has the same frequency as the incident beam. When the molecule is transferred back to the new vibration mode of the molecule at the ground state and emits lower energy than the excitation photon it is called Stokes Raman scattering (S in Figure 2-1). The Stokes Raman scattering has lower frequency than the incident beam. Also, the molecule can already be in a vibrationally excited state when it interacts with the incident light. It can be excited to a higher virtual state, and then drop back down to the ground state emitting more energy than the excitation photon. It is referred to as anti-Stokes Raman scattering (A in Figure 2-1) and gets higher frequency than the incident light. Unfortunately, most of the photons undergo Rayleigh scattering. Raman scattering is very low. Among them anti-Stokes scattering is even lower than Stokes Raman scattering. Therefore, Stokes Raman scattering is used in Raman Spectroscopy and the resultant vibrational frequency is measured as a shift from the incident beam frequency. When the wavelength of the incident beam falls in the sample's electronic absorption band (referred to as resonance Raman spectroscopy, RRS) it greatly increases sensitivity and improves detection limits.

Raman and FT-IR both are vibration spectroscopies which analyse the vibrational energy levels of a molecule. IR instruments measure the loss of intensity (energy absorbed by the vibrational energy transition of the molecule) relative to the sources across a wavelength range.⁹ The dipole moment of a molecule should be changed during the vibration for an IR active vibration whereas for a Raman active vibration, the polarizability should be changed during the vibration.¹⁰ When a molecule is placed in an electric field (laser beam), it suffers some distortion since the positively charged nuclei are attracted toward the negative pole, and electrons towards the positive pole. This charge separation causes an induced electric dipole moment in the molecule and the molecule is said to be polarized. A change in polarizability is reflected by how easily the molecule can be distorted (i.e. a change in size, shape or orientation of the electron cloud as a three dimensional surface) during a normal vibration. For quantitative analysis, the Raman spectroscopic method requires calibration models. The calibration models are built with a set of standard samples and their concentrations are related to peak height or an integrated area at specific wavenumber. The calibration models will then be applied to unknown spectrum to obtain the species concentration of unknown samples.

2.1. Major components in a Raman spectrometer

The major components in a typical Raman spectrometer are presented below along with a brief description.

Excitation source: it is generally a continuous wave (CW) laser. There are different kinds of laser sources; CW gas laser, Neodymium- YAG solid state lasers (YAG -yttrium Aluminum garnet) and Diode lasers.¹⁰ The laser frequency should be stable to ensure errorless results. Additionally, the Raman signal intensity is proportional to the fourth power of the inverse of the incident wavelength.⁹ The shorter the laser wavelength, the higher the number of Raman photons available for detection. However, fluorescence is a common obstacle and its severity tends to increase with shorter wavelengths. By using a longer wavelength laser, many fluorescence problems can be avoided. The selection of a laser wavelength therefore results in trade-offs between maximizing Raman signal and minimizing fluorescence. Higher laser power is preferred to reduce acquisition time (signal strength) proportionally. However, it can damage the sample, for instance, by local sample heating.

Sampling apparatus: sampling apparatus includes devices for sample illumination and collection Raman scattered beam. Mainly there are three type of methods can be found; use of optics (e.g. lenses and mirror), fiber optics and optical microscopes. The main purpose is to focus the laser beam onto the sample and collect the scattered beam efficiently. 90° and 180° (back scattering) scattering geometries are the commonly used optical configurations.

Wavelength-selection devices: This is a necessity for optical filtering. An arrangement should be made to remove stray beams and Rayleigh scattered beams from scattered beams, otherwise it will saturate the detector. Traditionally, double- or triple grating monochromators are used. Recently holographic interference filters (notch filters), and holographic gratings have been used.⁵

Detection and processing system: The low intensity of Raman signals make the detection and processing of signal more crucial. There are several detection techniques ¹⁰ e.g. photo counting, Photodiode Array, and Charge- Coupled Device (CCD). CCD is increasing in Raman spectroscopy. It is a silicon-based semiconductor arranged as an array of photosensitive elements, each one of which generates photoelectrons and stores them as a small charge. Charges are stored on each individual pixel as a function of the number of photons striking that pixel. Charges are read by a single analogue –to-digital converter.

A block diagram of the generic components in a Raman spectrometer is shown in (Figure 2-2).¹¹The above components are assembled in the spectrometer in a way that the instrument provides good sensitivity, high resolution and large spectra coverage simultaneously.

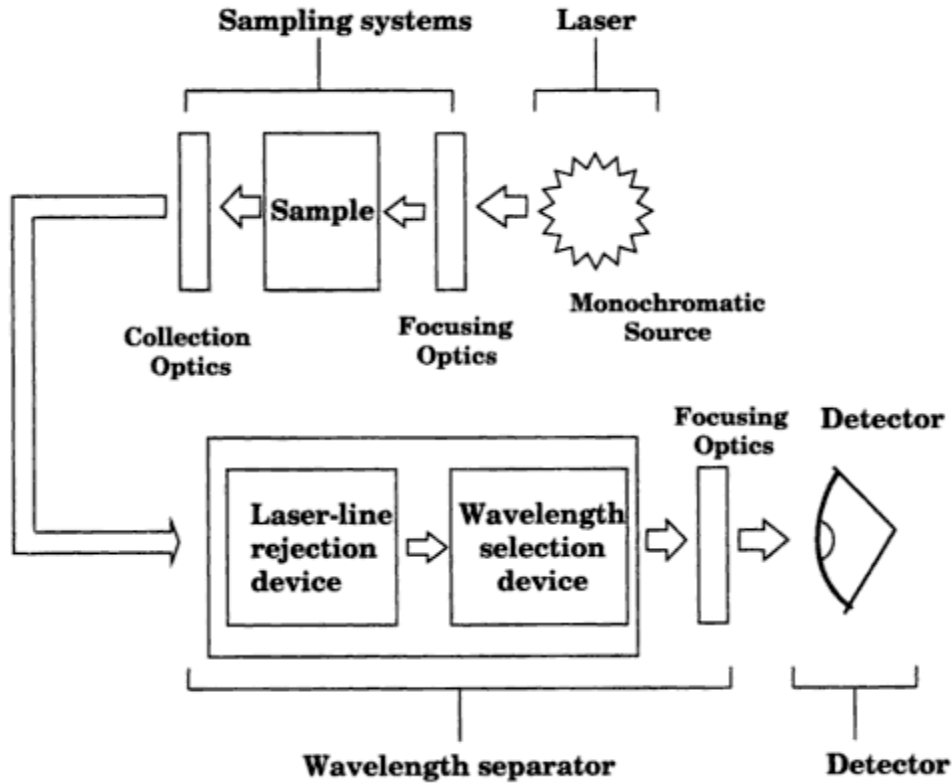


Figure 2-2: A block diagram of generic components making up a Raman Spectrometer.¹¹

3. Literature review on Raman spectroscopy in CO₂ capture field

The study of Raman spectroscopy to characterize CO₂-amine systems has recently received interest.¹² In one such study, Raman spectral measurement has been used for the characterization of speciation in CO₂ loaded alkonolamines aqueous solutions.^{12a} Concentration of free amine, protonated amine, bicarbonate and carbonate anions are determined for MDEA aqueous solution, CO₂ loaded at 40 °C. On the basis of pure component spectra of amines, protonated amines, bicarbonate (HCO₃⁻) and carbonates (CO₃²⁻), quantitative analysis for MDEA is achieved using the DCLS (direct classical least squares) algorithm. It has showed that Raman spectroscopy can particularly be used for quantitative analysis in tertiary amines. Since tertiary amines do not produce carbamate, the pure component spectra of amine carbamate are not necessary to calibrated. For primary and secondary amines, such an approach (DCLS) did not work since pure component spectra were not available for carbamate species. However, the spectral measurement could be used for fitting thermodynamic models using non-linear least-squares regression to determine the equilibrium constants related to carbamate. The accuracy of the thermodynamic model obviously affects the accuracy of this approach.

In another study, Raman spectra measurement has been used to measure the CO₂ loading (mole CO₂ to mole amine ratio).^{12b} A reliable calibration up to solvent loading of 0.5 mole CO₂/mole amine has been achieved for the primary amine MEA (30 wt %). Multivariate linear regression PLS1 (partial least squares, one principal component) has been used. 68 calibration samples and 12 test samples were used with spectral ranges between 300 and 1700 cm⁻¹. Further, the Raman spectra of 30 wt % MEA solutions at 25 °C, 40 °C, and 60 °C and different CO₂ loadings were recorded. It was discovered that temperature dependency of Raman spectroscopy can be neglected in this temperature range. Therefore, it may be to use the same set of calibration spectra at one temperature to analyse samples at another temperature.

Raman spectroscopy has been used to determine speciation in CO₂ aqueous ammonia systems.¹³ Jilvero et al.^{13c} used partial least-squares regression modeling. You Jeong et al.^{13a} and Zhao et al.^{13b} have followed the factor analysis method suggested by Wen and Brooker¹⁴ to calculate the concentration of aqueous ammonium carbonate solution from Raman spectra in the region between 965 and 1099.5 cm⁻¹. In the factor analysis method, frequency shifts for interested

species have been identified and the relative intensity I_i of the shifted band directly related to the concentration of a particular species through the expression (3-1).

$$I_i = J_i m_i \quad (3-1)$$

Where J_i called as the molal intensity coefficient of species i . It is the molal intensity of species i for the specified peak normalized to an internal intensity standard of 1.0 mol/kg of perchlorate ion (ClO_4^-), and m_i is the concentration (in mol/kg) of species i . The relative integrated intensity I_i is directly proportional to the band area. The Raman intensity depends not only on the concentration of chosen species but also on many other factors; such as effect of variation in refractive index and back ground scattering, the intensity of the source, sample container properties, scattering geometry, and instrument sensitivity. The use of an internal intensity standard is assumed to eliminate such factors other than effect of the concentration of species. Determination of the molar scattering intensity coefficient of species has been done by numbers of pure solution of chosen species having different concentrations, with ClO_4^- as the internal standard (since ClO_4^- is inert in this system).^{13b} However, it is not possible to obtain the corresponding pure solution for NH_2COO^- , since it dissociates in water. In such cases, molar scattering intensity coefficients of HCO_3^- and CO_3^{2-} determined at an earlier stage were used to determine the corresponding concentrations. Thereafter, the concentration of NH_2COO^- can be calculated using the law of carbon conservation, neglecting concentrations of CO_2 and H_2CO_3 at very low.

The principle component analysis / multivariate linear regression analysis seems to work well in practice for CO_2 -aqueous amine system, however, a drawback is the large number of calibration samples that has to be prepared and measured. In such situations, use of a factor analysis approach is advantageous. Even though it has worked well for CO_2 -aqueous ammonium systems^{13a, 13b}, no attempt for such an approach could be found for CO_2 -aqueous amine systems in present literature. Unable to obtain pure solution of amine carbamate to determine the molar scattering intensity coefficient makes such an approach difficult. In this work, a simple 'short-cut' type approach to semi-quantitative speciation information was introduced.

4. Method development: Raman spectrometer for speciation of carbonated aqueous amine solution

This section explains the experimental part to demonstrate that Raman Spectrometer could be used for speciation in carbonated aqueous amine solutions. The demonstration includes the identification of characteristic Raman bands for the interested species in the carbonated aqueous amine solution and a simple ‘short-cut’ type approach to semi-quantitative speciation information. The quantitative analysis was based on the factor analysis method. The same samples, which were analysed using Raman spectroscopy, were analysed with ^{13}C -NMR to compare the results and for calibration purposes (alkanolamine carbamate).

Monoethanolamine (MEA), Diethanolamine (DEA), Methyldiethanolamine (MDEA) and 2-Amino-2-methyl-1-propanol (AMP) were used for the experiment.

4.1. Experiment method

As in the previous part (Part I, wet chemical method for speciation), carbamate stability reaction was selected due to its importance in thermodynamic equilibria. In addition, preparation of the carbonated sample is quite easy. The same sample preparation was followed as in the wet chemical method section.

Sample preparation: Deionised (Milli –Q water, resistivity =18.2 M Ω .cm at 25 °C) water was used to prepare the aqueous alkanolamine solution (20 wt %: 3.28 mol•dm $^{-3}$ of MEA, 1.97 mol•dm $^{-3}$ of DEA 1.78 mol•dm $^{-3}$ of MDEA and 2.22 mol•dm $^{-3}$ of AMP) which was degassed before use. In a typical sample preparation run, the carbonated aqueous alkanolamine solution was prepared by dissolution of a predetermined NaHCO $_3$ powder into an aqueous alkanolamine (MEA, DEA, MDEA or AMP) solution. The amount of the NaHCO $_3$ was varied so that three different concentration levels (initial HCO $_3^-$ to alkanolamine concentration ratio: 0.5, 0.75, 1) of carbonated aqueous systems were analyzed for MEA and DEA. MDEA and AMP were analyzed only at 0.5 loading. The system was allowed to react and equilibrate for 24 hours in a thermostated closed cell (Grant LTD 6G) at 23 \pm 2 °C. After equilibration, the samples were transferred to NMR tubes

(Wilmad LabGlas, 500MHz quality) after addition of a known amount of the internal standard NaClO_4 ($\approx 0.10 \text{ mol}\cdot\text{dm}^{-3}$).

Raman spectroscopy: The Raman scans were performed with a Jobyn Yvon Horiba T64000 instrument working in backscattering single grating mode. The scattered light was collected through a confocal microscope with an Olympus 10x objective while the samples were kept in rotating NMR -tubes. The 400mW 532nm illumination was generated by a frequency doubled Millennia Pro 12sJS Nd:YVO₄ laser. To keep the “signal to noise” level low, 3 scans of 120 seconds were collected for each Raman spectral range. An extended range protocol was employed to cover the ranges from 700 to 1700 cm^{-1} (three overlapping spectra) and from 2600 to 3700 cm^{-1} (five overlapping spectra). A grating with 1800 rules pr. mm and a slit width of 100 microns ensured a spectral resolution ranging from 2 cm^{-1} at 1000 cm^{-1} to 1.6 cm^{-1} in the neighborhood of 3000 cm^{-1} . After removal of spikes and spectrograph artifacts, the overlapping spectra were merged. Fluorescence effects were subtracted by fitting with moderate degree polynomial functions. The wavenumber scale was calibrated against the Raman spectrum of a 50/50% (v/v) mixture of toluene and acetonitrile. No attempts were made to control polarization. However, the optical setup between each experiment was kept unchanged, to prevent such effects interfering. All the scans were done at room temperature ($20 \pm 1 \text{ }^\circ\text{C}$).

¹³C-NMR based speciation: The same samples which were analysed using Raman spectroscopy were analysed with ¹³C-NMR to compare the results and for calibration purposes (alkanolamine carbamate).

The ¹⁵N NMR experimental work was carried out in cooperation with B. Arstad, A. Bouzga and C. Perinu at the SINTEF NMR facility in Oslo, employing a Bruker Avance III spectrometer. The experiments were performed at 9.4 T on a Bruker Avance III 400 MHz spectrometer using a BBFO Plus double resonance probehead at room temperature and the spectra data was processed using MestreNova software v 7.1.1. A capillary containing a solution of $\text{CH}_3\text{CN} / \text{D}_2\text{O}$ was inserted in the ¹³C-NMR tube as a reference standard and ‘lock’ solvent respectively (i.e. field-frequency stabilization). After the measurements of the longitudinal relaxation time T_1 of the ¹³C nuclei of all the species in solution, including the standard in the capillary, the following ¹³C-NMR parameters were adjusted: recycle delay was 120 s, pulse angle=90° and number of scans was 480. To obtain quantitative results, the area under the spectral peaks were integrated and scaled to the area of the reference standard peak. The effective concentration of the reference standard in the capillary was calibrated as a function of the solutions under study. Since the fast exchanging protons species are

represented by a common signal in the ^{13}C -NMR spectra, calibration experiments to distinguish between HCO_3^- and CO_3^{2-} and between alkanolamine and its protonated form, were performed.

4.2. Characteristic Raman active bands

Identification of characteristic active bands relevant to interested species is required for the factor analysis approach. One species may have several active bands, but it is important to determine highly active bands for quantification. Identification was based on previous studies found in the present literature in addition to our work.

Raman spectroscopy has been used to obtain quantitative and structural information about CO_2 , CO_3^{2-} , and HCO_3^- dissolved in water (the species involved in the CO_2 - H_2O equilibria).¹⁵ Two prominent Raman active bands for CO_2 were observed at 1286 and 1390 cm^{-1} . For CO_3^{2-} an intense, polarized band at 1064 cm^{-1} was reported in the same study. In addition to a band at 1065 cm^{-1} , two more active bands at 1436 cm^{-1} and 1380 cm^{-1} were reported.¹⁴ Only the polarized band of carbonate at 1065 cm^{-1} was reported to be sufficiently intense for a quantitative measurement. The characteristic bands of HCO_3^- were reported at 1017, 1302, 1360 and 1630 cm^{-1} .¹⁵ All of these bands were detected in a later study.¹⁴ However, only the polarized band at 1017 cm^{-1} was suggested to be suitable for quantitative measurement.¹⁴⁻¹⁵ Figure 4.2-1 shows spectra for CO_3^{2-} and HCO_3^- , including the internal ClO_4^- standard (935 cm^{-1}) from our study. The characteristic CO_3^{2-} band at 1067 cm^{-1} and the characteristic HCO_3^- bands at 1017 and 1360 cm^{-1} were observed.

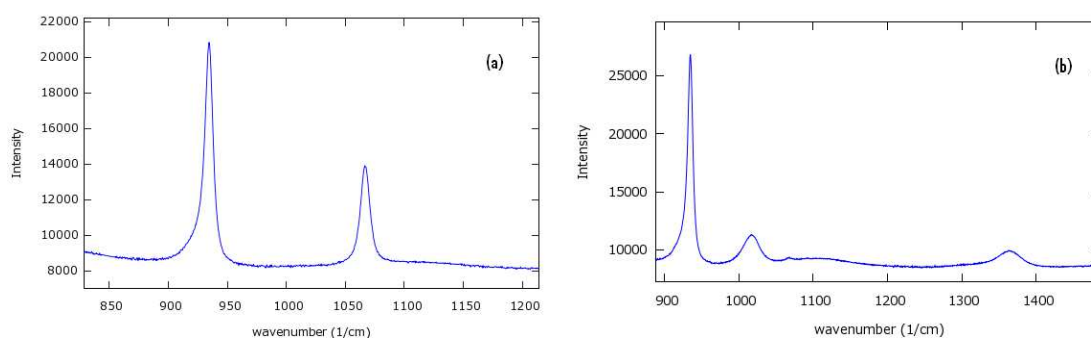


Figure 4.2-1: Reference Raman spectra for CO_3^{2-} (a) and HCO_3^- (b). CO_3^{2-} concentration is 0.185 $\text{mol}\cdot\text{dm}^{-3}$ and HCO_3^- concentration is 0.216 $\text{mol}\cdot\text{dm}^{-3}$. ClO_4^- concentration (internal standard) is 0.117 $\text{mol}\cdot\text{dm}^{-3}$.

For MEA and DEA solutions loaded with CO₂, the carbamate band was clearly identified at 1162 cm⁻¹ and 1160 cm⁻¹ respectively.^{12a} The intensity of these bands was found to have increased from 0 CO₂ mole/ alcohol amine moles to 0.5 CO₂ mole/ alkonolamine moles and then decreased.

The characteristic Raman bands for free alkanolamine have been assigned at 400, 1200, 1350 and 1600 cm⁻¹.^{12b} In our work, two of these were detected at 1350 and 1600 cm⁻¹ in spectra for MEA (Figure 4.2-2) which are not visible in the spectra of protonated MEA (Figure 4.2-3). The band at 1350 cm⁻¹ was found to be much easier for the quantitative measurement. Figure 4.2-4 shows corresponding bands in the DEA Raman spectrum near 1200 cm⁻¹. These two bands have the potential for quantification of free MEA (1350 cm⁻¹) and DEA (1200 cm⁻¹). However, these bands become weak at lower concentration leading to an under estimation of the quantification. As similarly for ammonia (3310 cm⁻¹)¹⁴, a band at 3313 cm⁻¹ in the MEA spectrum (Figure 4.2-2), which is not visible in the spectrum of the protonated form (Figure 4.2-3), can be observed. Therefore the 3313 cm⁻¹ band is characteristic for the free alkanolamine. However, the band is overlapping somewhat with a water band (broad Raman scattering in the region between 3000 and 3600 cm⁻¹ has been assigned to water.¹⁴). A proper curve model in this spectral range could enable quantification of free alkanolamines. In addition to the band at 3313 cm⁻¹, more bands were observed at 2890, 2930-2960 and 3381 cm⁻¹. Previous work¹⁶ on protonated alkanolamines has reported that characteristic bands at 2952, 2940 and 2884 cm⁻¹ for MEA shifted to 3005, 2971 and 2898 cm⁻¹ on protonation. A similar result is demonstrated in Figure 4.2-2 showing that protonated MEA leads to a Raman shift at 2900 and 2980 cm⁻¹ with a shoulder.

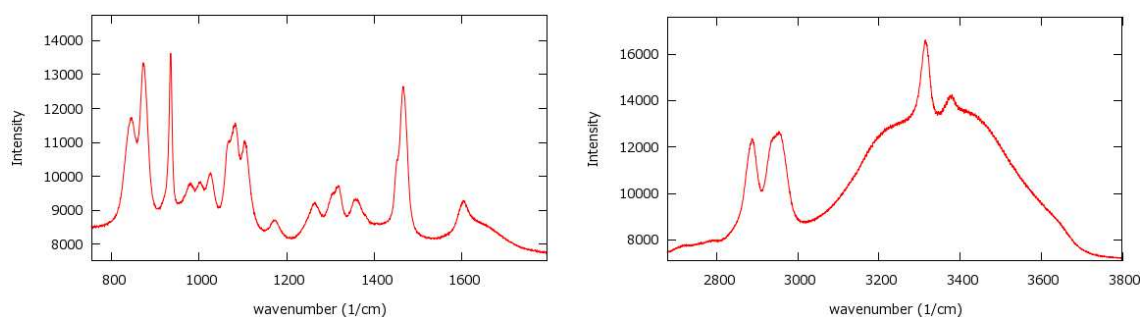


Figure 4.2-2: Reference Raman spectra of MEA

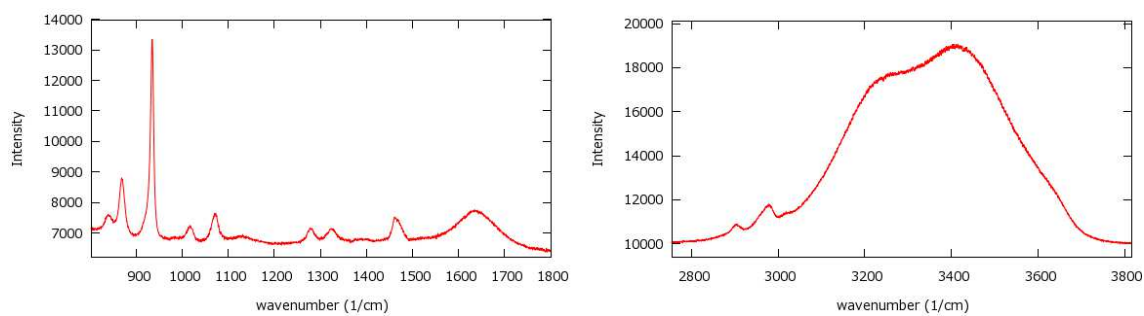


Figure 4.2-3: Reference Raman spectra for protonated MEA

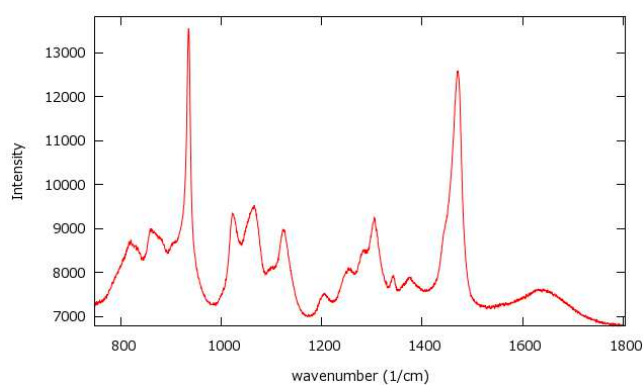


Figure 4.2-4: Reference Raman spectra for DEA

Table 4.2-1 summarizes the characteristic bands of chosen species that were used for analysis.

Table 4.2-1: Characteristic Raman bands for species

Species	characteristic band
CO_3^{2-}	1067 cm^{-1}
HCO_3^-	1017 cm^{-1}
Alkanolamine carbamate	1162 cm^{-1}
MEA	1350 cm^{-1}
DEA	1200 cm^{-1}

4.3. Quantitative analysis: factor analysis approach

Having identified the characteristic bands of interested species, concentration was calculated based on the factor analysis method suggested by Wen and Brooker.¹⁴ For a given Raman band j , of a given species i , the relative scattering intensity I_{ij} is directly related to the concentration of the interested species through the expression (4.3-1).

$$I_{ij} = J_{ij}C_i \quad (4.3-1)$$

I_{ij} is the relative scattering intensity. J_{ij} is the molar scattering intensity factor for each Raman band of each substance and is characteristic of the selected band at given measurement conditions and medium. c_i is the concentration of the species. Once the relative scattering intensity is known, the concentration of the substance can be calculated. Since many instrument and sample factors influence this linear relationship, an internal standard is added to each sample assuming its Raman band to be independent of the other molecules in the solution. Thus, the molar scattering intensity factors (J_i) can be calculated relative to the internal standard (in this case perchlorate ion, ClO_4^-) according to equation (4.3-2). The integrated area (\mathcal{A}) under the relevant band is calculated since it is proportional to the band intensity. \mathcal{A}_i is the integrated area under the selected characteristic band associated with the species i . $\mathcal{A}_{\text{ClO}_4^-}$ is the integrated area under the band at 935 cm^{-1} which is the characteristic band of ClO_4^- . The concentration C_i is measured in $\text{mol}\cdot\text{dm}^{-3}$, assuming the volume does not change (it is valid because the present work was restricted to a constant temperature)

$$\frac{\mathcal{A}_i}{\mathcal{A}_{\text{ClO}_4^-}} = J_i \frac{C_i}{C_{\text{ClO}_4^-}} \quad (4.3-2)$$

For the present work, the molar scattering intensity factor J_i of HCO_3^- , CO_3^{2-} and the alkanolamines can be determined by knowing the concentration C_i of them. Therefore, pure solutions of each substance at different concentrations were prepared containing Sodium perchlorate (NaClO_4) as an internal standard and scanned with Raman spectroscopy. Relevant integrated areas (\mathcal{A}_i and $\mathcal{A}_{\text{ClO}_4^-}$) were calculated from the spectra and the concentrations C_i and $C_{\text{ClO}_4^-}$ were known. Then J_i can be determined. This was repeated for three different concentration levels. After determination of J_i , the equation (4.3-2) could be used to determine the unknown concentration of interested species.

First, the molar scattering intensity factor of CO_3^{2-} was determined, since HCO_3^- dissociates in aqueous solution. Then, the concentrations of CO_3^{2-} in the calibration samples of HCO_3^- was calculated using equation (4.3-2). Then the conservation of carbon mass balance gives the concentration of HCO_3^- . The aqueous solutions of MEA and DEA were prepared on weight basis. The density measurement was done to convert to volume base. The concentrations were checked by titration with $1.0 \text{ mol}\cdot\text{dm}^{-3}$ HCl.

Having identified the relevant Raman active bands, the spectral envelopes were fitted to an area-normalized Gauss-Lorentzian peak function (4.3-3) along with a polynomial baseline. Numerical evaluation of the corresponding parameters was performed using the Gnuplot program. The accuracy of this method is dependent on sufficient resolution to clearly distinguish the bands to be analyzed.

$$y = 2a_0 \left[\frac{a_3 \sqrt{\ln 2}}{a_2 \sqrt{\ln \pi}} \exp \left(-4 \ln 2 \left(\frac{x-a_1}{a_2} \right)^2 \right) + \frac{1-a_3}{\pi a_2 \left[1+4 \left(\frac{x-a_1}{a_2} \right)^2 \right]} \right] \quad (4.3-3)$$

a_0 = area under the peak

a_1 = center of the peak, in this case frequency of characteristic band selected

a_2 = width of the peak

a_3 = shape [0;1] if $a_3=0$ peak of the shape is Lorentzian and $a_3=1$ it is Gaussian shape

Table 4.3-1 presents the determined molar scattering intensity factors J_i for each species with standard deviations. The values for HCO_3^- and CO_3^{2-} were calculated to be 0.1973 and 0.2901 respectively. Similar results were reported in a previous study^{13b} which found 0.188 and 0.302 for these species respectively. However, the values depend on the measurement conditions and medium.

Figure 4.3.1-1 and Figure 4.3.1-2 show a clearly distinguishable band at 1160 cm^{-1} in the carbonated aqueous amine solution. The band was not visible in the MDEA Raman spectrum with 0.5 loading (Figure 4.3.1-). Since MDEA is a tertiary alkanolamine, no carbamate can be formed. The molar scattering intensity factors for carbamate are relevant for this band. The reference concentrations for the calculations were taken from ^{13}C -NMR measurements on the carbonated solutions analyzed by Raman at different concentration levels. The calculated values for the MEA-

and DEA-carbamate are 0.0632 and 0.04 respectively. The calculation of molar scattering intensity factors for MEA and DEA are based on the 1350 and 1200 cm^{-1} band respectively. However these bands were weak in the scattering envelop which increases the error margin. It was found that the bands were not visible in samples with low alkanolamine concentration. Thus more work is needed to reduce the error margin.

Table 4.3-1: Molar scattering intensity factors J_i

Component	J_i	Standard deviation
CO_3^{2-}	0.2901	0.0062
HCO_3^{2-}	0.1973	0.0250
$\text{OHC}_2\text{H}_4\text{NHCOO}^-$	0.0632	0.0070
$(\text{HOC}_2\text{H}_4)_2\text{NCOO}^-$	0.0400	0.0060
$\text{HOC}_2\text{H}_4\text{NH}_2$ at 1350 cm^{-1}	0.0040	0.0012
$(\text{HOC}_2\text{H}_4)_2\text{NH}$ at 1200 cm^{-1}	0.0130	0.0014

4.3.1. HCO_3^- loaded alkanolamine solutions

Three different concentration levels (HCO_3^- to alkanolamine loading ratio: 0.5, 0.75, 1.0) of carbonated aqueous systems were analyzed with the Raman spectroscopy for MEA and DEA. MDEA and AMP were analyzed only at 0.5 loading. The spectra of MEA solution with/without 0.5 loading are given in Figure 4.3.1-1. The characteristic bands of CO_3^{2-} and MEA-carbamate are clearly visible at 1067 cm^{-1} and 1162 cm^{-1} respectively. A similar result was observed for the other two loadings.

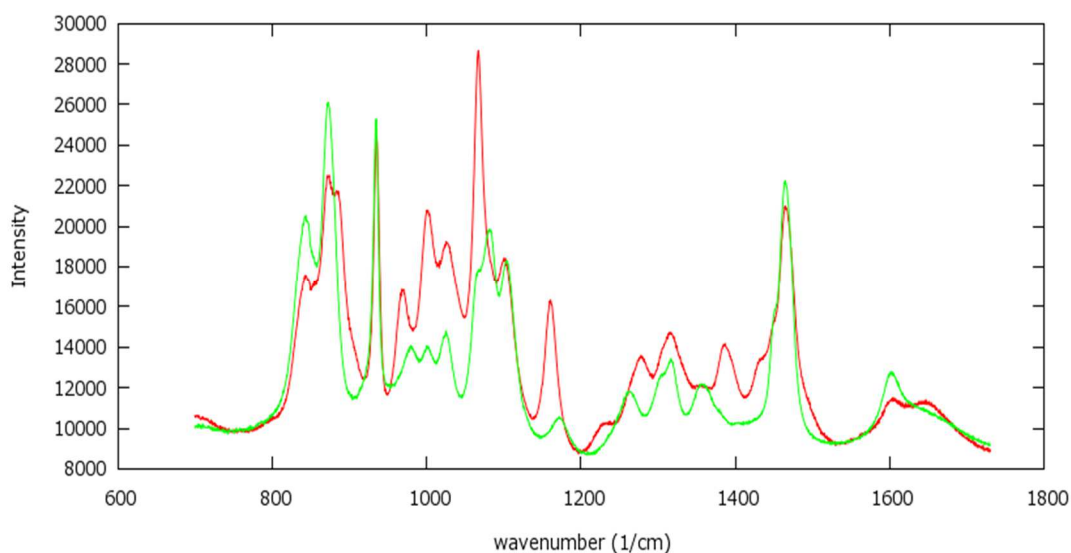


Figure 4.3.1-1: Raman spectra of MEA 20 wt % aqueous solution without loading (green) and with 0.5 loading (red). $0.10 \pm 0.015 \text{ mol}\cdot\text{dm}^{-3}$ of NaClO_4 was added to each solution. (Loading = ratio of initial HCO_3^- concentration to initial alkanolamine concentration)

The calculated concentrations of CO_3^{2-} based on Raman spectra analysis were 0.285, 0.382 and $0.536 \text{ mol}\cdot\text{dm}^{-3}$ at 0.5, 0.75 and 1.00 loadings respectively. ^{13}C -NMR measurements were run for each of the prepared samples. The results are summarized in Table 4.3.1-1. The CO_3^{2-} quantification based on Raman measurements are in the same order of magnitude as the ^{13}C -NMR quantifications. The CO_3^{2-} Raman band is particularly strong. It might be a reason for overestimated values. Another reason might be overlapping bands, in combination with the method of data deconvolution.

Furthermore, neither the characteristic HCO_3^- band (1017 cm^{-1}) nor the 1350 cm^{-1} alkanolamine band was truly visible at all three loadings. The reason may be that the HCO_3^- band is masked by the alkanolamine spectrum due to low concentration of the former. According to ^{13}C -NMR results, the HCO_3^- concentration is rather low. However, even though the alkanolamine concentration is quite high, the band at 1350 cm^{-1} is very weak and below the detection level. Thus the $1.521 \text{ mol}\cdot\text{dm}^{-3}$ of free MEA was under estimated by more than 50 %. Hence, use of the stronger bands in the high frequency range ($2800\text{-}4000 \text{ cm}^{-1}$) may be suitable enough for quantification of free- and protonated alkanolamine.

Table 4.3.1-1: Concentration determined from NMR measurement for MEA/HCO₃¹⁻ and DEA/HCO₃¹⁻ systems

HCO ₃ ¹⁻ loading*	Amine	CO ₃ ²⁻ <i>mole/l</i>	HCO ₃ ²⁻ <i>mole/l</i>	RNHCOO ⁻ <i>mole/l</i>	Amine <i>mole/l</i>
0.50	MEA	0.243	0.018	1.340	1.521
	DEA	0.219	0.108	0.595	0.953
0.75	MEA	0.360	0.044	1.880	0.793
	DEA	0.312	0.208	0.787	0.602
1.00	MEA	0.520	0.234	2.475	0.187
	DEA	0.396	0.412	0.911	0.344

* Loading = initial HCO₃⁻ to alkanolamine concentrations ratio

Similar results as for MEA were observed for the DEA solutions at the three different loadings. Again, clearly visible characteristic bands for CO₃²⁻ and carbamate were noticed. The Raman and ¹³C-NMR results are quite compatible with respect to the CO₃²⁻ concentration. The calculated 'Raman' concentrations were 0.273, 0.372 and 0.306 mol•dm⁻³ for the respective loadings at 0.5, 0.75 and 1.00. Figure 4.3.1-2 shows the Raman spectra of the DEA sample with and without 0.5 loading. The characteristic HCO₃⁻ Raman band at 1017 cm⁻¹ is probably masked by other bands near 1017 cm⁻¹ which are seen in the unloaded DEA solution spectra. Interestingly, a 0.412 mol•dm⁻³ of HCO₃⁻ concentration was not detected in the loaded DEA solution, while a 0.216 mol•dm⁻³ of HCO₃⁻ was clearly visible in the pure solution (Figure 4.2-1, b). This demonstrates clearly the masking of the 1017 cm⁻¹ band. In comparison with MEA, a quite distinct band at 1200 cm⁻¹ is visible for free DEA. However, it is barely visible at 0.75 and 1.00 loading and gave a concentration of 0.584 mol•dm⁻³ of DEA at the 0.5 loading.

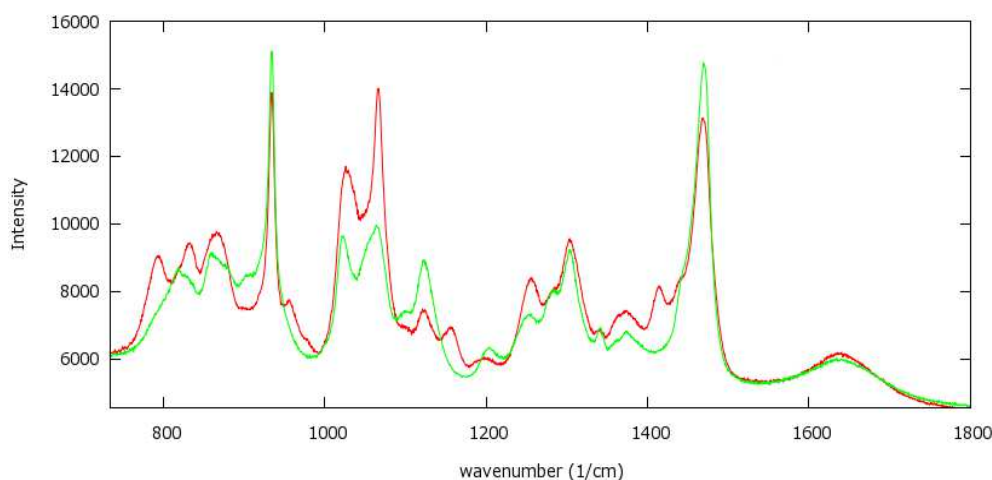


Figure 4.3.1-2: Raman spectra of DEA 20 wt % aqueous solution without loading (green) and with 0.5 loading (red). $0.10 \pm 0.015 \text{ mol}\cdot\text{dm}^{-3}$ of NaClO_4 was added to each solution. (Loading = ratio of initial HCO_3^- concentration to initial alkanolamine concentration)

The Raman spectra for MDEA solution with and without 0.5 loading were recorded (Figure 4.3.1-3). Since MDEA is a tertiary amine, carbamate was not formed. Therefore, the corresponding band at 1162 cm^{-1} is not noticed. A sharp band is recorded at 1067 cm^{-1} corresponding to CO_3^{2-} .

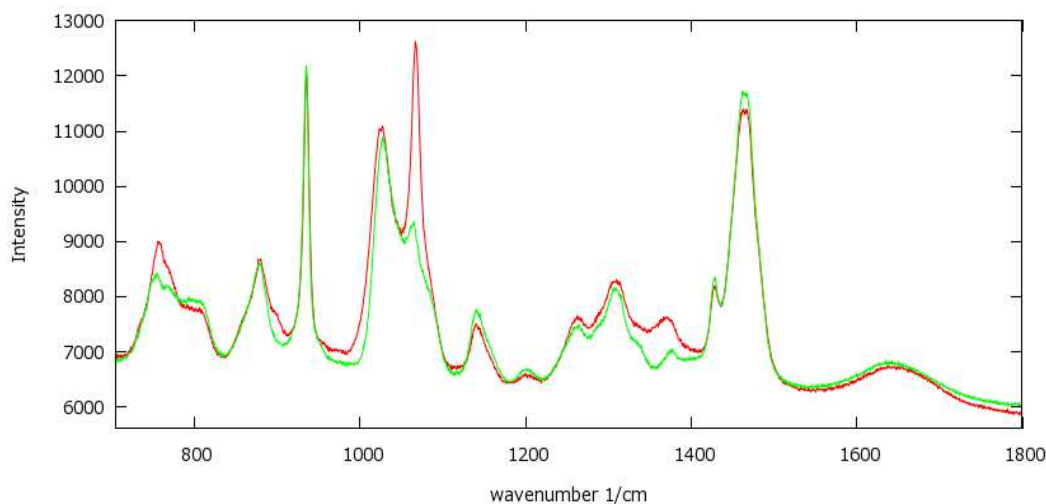


Figure 4.3.1-3: Raman spectra of MDEA 20 wt % aqueous solution without loading (green) and with 0.5 loading (red). $0.10 \pm 0.015 \text{ mol}\cdot\text{dm}^{-3}$ of NaClO_4 was added to each solution. (Loading = ratio of initial HCO_3^- concentration to initial alkanolamine concentration)

Figure 4.3.1-4 shows the AMP Raman spectra with/without 0.5 loading. AMP is a sterically hindered alkanolamine which is believed not to form carbamate. Hence no corresponding band at

1162 cm^{-1} is detected. The characteristic bands for CO_3^{2-} and free alkanolamine are visible. However the band of ClO_4^- internal standard is overlapping with the AMP spectrum precluding use of the internal standard for quantification.

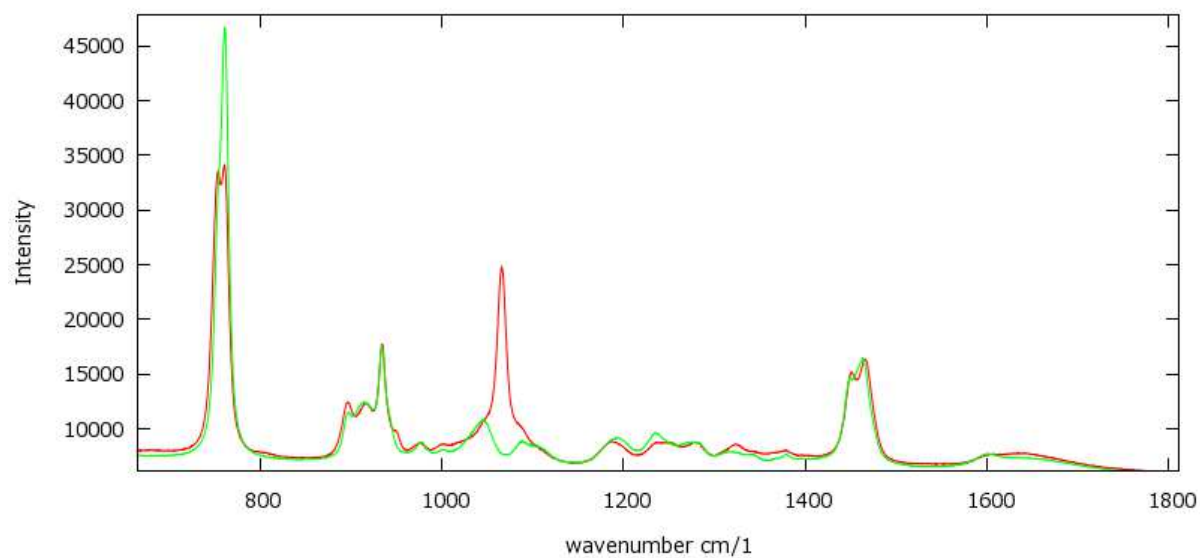


Figure 4.3.1-4: Raman spectra of AMP 20 % w/w aqueous solution without loading (green) and with 0.5 loading (red). $0.10 \pm 0.015 \text{ mol} \cdot \text{dm}^{-3}$ of NaClO_4 was added to each solution. (Loading = initial HCO_3^- to alkanolamine concentrations ratio)

5. Conclusions and Recommendations

Conclusions:

- This experimental work demonstrated that the Raman spectroscopic method is able to pick out selected characteristic Raman bands which allows quick, semi-quantitative insight into carbonated alkanolamine solutions.
- The molar scattering intensity factors for HCO_3^- , CO_3^{2-} and MEA- and DEA-carbamate were found to be 0.1973, 0.2901, 0.0632 and 0.0400 respectively.
- Potential bands for quantification of free- and protonated alkanolamine are identified in the spectral region of 2800 - 3800 cm^{-1} .
- The well-known internal ClO_4^- standard (with characteristic band at 935 cm^{-1}) cannot be used for AMP, because this characteristic band of ClO_4^- is blanketed with the AMP spectrum.

Recommendations:

- Better software for data deconvolution may give accurate integration results in a shorter time.
- Since the corresponding CO_3^{2-} band was always visible quite clearly, this Raman spectroscopic approach could be recommended to determine HCO_3^- and CO_3^{2-} concentrations separately, where the concentration of these two species is determined as a sum. For example, NMR based analysis and wet chemical method described in the previous part. The wet chemical method described in the previous part measures HCO_3^- and CO_3^{2-} concentrations together. Later, pH measurement and dissociation constant of HCO_3^- (corrected to ionic activities) were employed for determination of HCO_3^- and CO_3^{2-} concentrations separately. It has some issues such as proper model to correct the activities as ionic strength increases and errors related to pH measurement.

- The characteristic band of ClO_4^- peaks at 935 and is influenced by other bands in the spectra of AMP. It suggests that this method has to be verified before it is used for other amines.
- Principle components analysis (multivariate regression methods) rather than factor analysis might be better where the concentration of HCO_3^- is found at an undetectable level or corresponding band is overlapped. For such a multivariate regression method, the carbonated aqueous amine solutions can be prepared as done in this study, since it is not possible to prepare pure solutions of carbamate. The wet chemical method described in the previous Part (I) could be employed to determine carbamate concentration in the calibration samples and test samples.

References

1. Perinu, C.; Arstad, B.; Jens, K.-J., NMR spectroscopy applied to amine–CO₂–H₂O systems relevant for post-combustion CO₂ capture: A review. *International Journal of Greenhouse Gas Control* **2014**, *20*, 230-243.
2. Harris, R. K.; Becker, E. D.; Cabral de Menezes, S. M.; Goodfellow, R.; Granger, P., NMR nomenclature. Nuclear spin properties and conventions for chemical shifts (IUPAC Recommendations 2001). *Pure Appl. Chem.* **2001**, *73* (11), 1795-1818.
3. Mani, F.; Peruzzini, M.; Stoppioni, P., CO₂ absorption by aqueous NH₃ solutions: speciation of ammonium carbamate, bicarbonate and carbonate by a ¹³C NMR study. *Green Chem.* **2006**, *8* (11), 995-1000.
4. (a) Diab, F.; Provost, E.; Laloué, N.; Alix, P.; Souchon, V.; Delpoux, O.; Fürst, W., Quantitative analysis of the liquid phase by FT-IR spectroscopy in the system CO₂/diethanolamine (DEA)/H₂O. *Fluid Phase Equilib.* **2012**, *325* (0), 90-99; (b) Archane, A.; Fürst, W.; Provost, E., Influence of Poly(ethylene oxide) 400 (PEG400) on the Absorption of CO₂ in Diethanolamine (DEA)/H₂O Systems. *J. Chem. Eng. Data* **2011**, *56* (5), 1852-1856; (c) Jackson, P.; Robinson, K.; Puxty, G.; Attalla, M., In situ Fourier Transform-Infrared (FT-IR) analysis of carbon dioxide absorption and desorption in amine solutions. *Energy Procedia* **2009**, *1* (1), 985-994.
5. Skoog, D. A.; Crouch, S. R.; Holler, F. J., *Principles of instrumental analysis*. Thomson: Belmont, Calif., 2007
6. Smith, B. C., *Fundamentals of Fourier transform infrared spectroscopy*. CRC Press: Boca Raton, Fla., 2011.
7. Geers, L. F. G.; van de Runstraat, A.; Joh, R.; Schneider, R. d.; Goetheer, E. L. V., Development of an Online Monitoring Method of a CO₂ Capture Process. *Ind. Eng. Chem. Res.* **2011**, *50* (15), 9175-9180.
8. McCreery, R. L., *Raman spectroscopy for chemical analysis*. John Wiley & Sons: New York, 2000.
9. Bakeev, K. A., *Process analytical technology: spectroscopic tools and implementation strategies for the chemical and pharmaceutical industries*. Wiley: Chichester, 2010.
10. Ferraro, J. R.; Nakamoto, K.; Brown, C. W., *Introductory Raman spectroscopy*. Academic Press: Amsterdam, 2003.
11. Lewis, I. R.; Edwards, H., *Handbook of Raman spectroscopy: from the research laboratory to the process line*. CRC Press: 2001.
12. (a) Souchon, V.; Aleixo, M. d. O.; Delpoux, O.; Sagnard, C.; Mougín, P.; Wender, A.; Raynal, L., In situ determination of species distribution in alkanolamine- H₂O - CO₂ systems by

Raman spectroscopy. *Energy Procedia* **2011**, *4* (0), 554-561; (b) Vogt, M.; Pasel, C.; Bathen, D., Characterisation of CO₂ absorption in various solvents for PCC applications by Raman spectroscopy. *Energy Procedia* **2011**, *4* (0), 1520-1525.

13. (a) You Jeong, K.; Jong Kyun, Y.; Won Hi, H.; Kwang Bok, Y.; Chang Hyun, K.; Jong-Nam, K., Characteristics of CO₂ Absorption into Aqueous Ammonia. *Sep. Sci. Technol.* **2008**, *43* (4), 766-777; (b) Zhao, Q.; Wang, S.; Qin, F.; Chen, C., Composition Analysis of CO₂-NH₃-H₂O System Based on Raman Spectra. *Ind. Eng. Chem. Res.* **2011**, *50* (9), 5316-5325; (c) Jilvero, H.; Jens, K.-J.; Normann, F.; Andersson, K.; Halstensen, M.; Eimer, D.; Johnsson, F., Equilibrium measurements of the NH₃-CO₂-H₂O system – measurement and evaluation of vapor-liquid equilibrium data at low temperatures. *Fluid Phase Equilib.* **2015**, *385* (0), 237-247.

14. Wen, N.; Brooker, M. H., Ammonium Carbonate, Ammonium Bicarbonate, and Ammonium Carbamate Equilibria: A Raman Study. *The Journal of Physical Chemistry* **1995**, *99* (1), 359-368.

15. Davis, A. R.; Oliver, B. G., A vibrational-spectroscopic study of the species present in the CO₂-H₂O system. *J. Solution Chem.* **1972**, *1* (4), 329-339.

16. Ohno, K.; Matsuura, H.; Iwaki, T.; Suda, T., Remarkable Changes in the (N)CH₃ Stretching Wavenumbers of Amines on Protonation. *Chem. Lett.* **1998**, *27* (6), 531-532.

Part III

Molecular structure-activity relationships

1. Overview

Insight into fundamental chemistry associated with CO₂ and aqueous amine, supports the rational development of novel solvents and speciation based predictive models. Important chemical reactions relevant to CO₂ absorption for sterically unhindered primary amines are carbamate formation (1.1-a) and hydrolysis reactions (1.1-c). The equilibrium constants of these two reactions (K_{CBM} and K_{HYD}) can influence the CO₂ capture performance of amines. Further, they can be used as input values for speciation based predictive model. Typically, determination of such values requires time and resource consuming laboratory work. A readily accessible method for prediction of carbamate related equilibrium constants is therefore beneficial. Thus, correlations to predict the carbamate related equilibrium constant based on the molecular structure feature of amine, was established. Such relationships can enable understanding of the effect of the molecular structure of amine towards its reactivity with CO₂.

This part of the dissertation examines the substituent effects of amine on its reactivity towards carbamate formation and carbamate hydrolysis. The molecular structure of a reactant can influence the equilibrium constant of a specific reaction through polar, steric, or resonance effects.¹ R.W. Taft introduced a basis for separating these individual effects to assess the relative molecular reactivity.² His work involved use of free energy relationships to analyse the rate constant of alkaline and acid-catalysed hydrolysis of esters. The free energy of activation or free energy of reaction change can be induced by a substituent in the reactant. At constant temperature the logarithm of a rate constant is proportional to the standard free energy of activation. Thus, change in the rate constant of a specific reaction relative to a reference substituent can introduce a parameter that describe the electron donating or electron withdrawing characteristic of a substituent. Mostly individual substituents influence reactions in a consistent manner. No matter which reaction they involve, their polar effects are same. Only the magnitude of their influences varies depending on the sensitivity in the reaction involved.

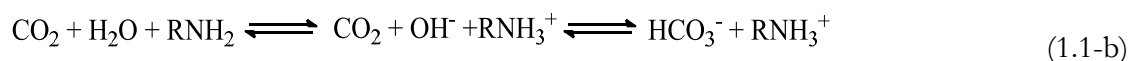
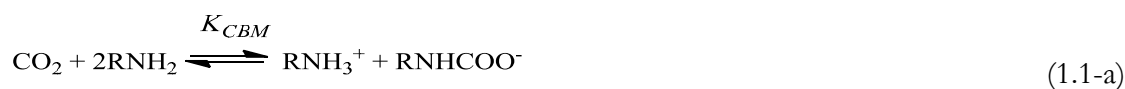
The approach of this dissertation is inspired by an earlier study by Hall³ in which Taft's polar parameter was applied to study the base strength of amines. Quantitative structure-reactivity relationships (Taft's polar parameter vs pK_a) have been built for primary (1°), secondary (2°) and tertiary (3°) non-aromatic amines.³ These correlations could permit the prediction of the unknown pK_a values of amines. Here, the objective is to build a similar kind of quantitative structure-activity

relationship to predict the equilibrium constants of the carbamate formation (1.1-a) and hydrolysis (1.1-c) reactions (K_{CBM} and K_{HYD}). This study is limited to the primary alkyl amines.

The relative electron density present on the N nucleus, which depends on molecular structure and medium effects, influences the chemical reactions between amine and CO_2 . The ^{15}N NMR chemical shift value is a measure to determine the relative electron density available on the N nucleus. Therefore, ^{15}N NMR experiment data was also used to qualitatively analyse the structure-activity relationship of 1° alkylamines.

1.1. Carbamate related equilibrium constants

The reaction of aqueous amines with CO_2 generally follows two path-ways. One, typically of primary (RNH_2) and secondary amines (R_2NH), except for sterically hindered amines, consists in the direct reaction of amines with CO_2 to form carbamate as shown in reaction(1.1-a). The second path is CO_2 hydration to form bicarbonate, as shown in reaction (1.1-b), where amines act as a base catalyst.⁴ Mainly, tertiary amines (R_3N) follow reaction (1.1-b) that gives higher capacity since it consumes only one mole of amine to react with one mole of CO_2 . However, the low rate of this reaction (1.1-b) may limit their use.



R = organic radical, substituent

Formation of carbamate features faster kinetics. The reaction of CO_2 and OH (1.1-b) obviously depends on the pH of the solution which is defined by the basicity of the amine, however, for primary and secondary amines absorption will mainly depend on carbamate formation. The sensitivity of carbamate formation depends on carbamate stability, which varies from amine to amine. The instability of carbamate ions that are formed in an aqueous system of sterically hindered amines has been claimed to be responsible for the high absorption capacity of

such a solution⁵ over the other unhindered primary and secondary amines. However, at high CO₂ partial pressure, carbamates may hydrolyze to generate free amines which can further react with additional CO₂ to give loading over the stoichiometric ratio of reaction (1.1-a). From an equilibrium point of view, carbamate stability reaction (1.1-c) is very important and strongly influences the speciation.⁵ This makes studies on equilibrium constants of reactions (1.1-a) and (1.1-c) vital to elucidate chemical behavior of amines at equilibria. Formation of carbamate leads to higher reaction rates while instability of carbamate leads to higher loading and less energy demand for desorption.

2. Previous studies on molecular structure–activity relationships

Structure and activity relationships for amine based CO₂ capture absorbents has been studied in a previous work as first screening of various absorbents based on the initial rate of absorption for CO₂ and the capacity of various solvent for CO₂ absorption.⁶ The carbon dioxide absorption was measured volumetrically. Among the several molecular structure effects investigated in the study, the chain length and side chain at α -carbon position are preferably highlighted in the context of current study. The effect of an increase in the chain length between the amino group and hydroxyl substituent on absorption capacity of an alkanolamine based absorbent (from monoethanolamine to 5-amino-1-pentanol) has been experimented.^{6a} A slight increase in CO₂ absorption capacity from monoethanolamine to 3-amino-1-propanol was reported and further increase did not increase absorption as it remained approximately the same. The experiment on absorption capacities of alkylamines with chain length varying from two carbon chain (ethylamine) up to five (pentylamine) have shown that increases in chain length have a general trend of decreasing absorption capacity. However, butylamine had slightly higher capacity than propylamine and pentylamine. The effect of a methyl (CH₃) group substitution at the α and β carbon to the amino functional group in alkylamines was also investigated in the same study.^{6b} It reported that substitution of the CH₃ group at the α -carbon (sec-butylamine) increased the absorption capacity up to 0.84 mole CO₂/moles amine when compared with a CH₃ group substitution on the β carbon (iso-butylamine 0.78 moles CO₂/moles amine). The reason for such performance was a steric hindrance effect due to the substitution at the α -carbon. The steric hindrance lowers the stability of carbamate and enhances its hydrolysis. This can drive the equilibrium to the bicarbonate giving higher CO₂ absorption capacity.

Another study on the influence of amine structure on amine capacity in CO₂ absorption and desorption reported that the chemical structure of an amine has a strong impact on the amine's capacity to capture CO₂.⁷ The speciation during the absorption and desorption of CO₂ using ¹³C NMR techniques has been used to examine the influence. An experiment with primary alkanolamines of 4 M concentration with different chain lengths between amino and hydroxyl groups, H₂N(CH₂)_nOH, where n was from 2, to 6, showed little difference on carbamate and bicarbonate formation in absorption. The total CO₂ absorbed was similar for all the amines. Both

studies^{7, 6a} illustrated that the chain length alone does not have an obvious impact on the CO₂ absorption capacity in this group of amines.

Further, N-methylalkanolamines of 4 M concentration with different chain lengths (CH₃NH(CH₂)_nOH, where n is 2 to 6) showed similar behavior, except N-methylhexanol (n=6) which had the lowest total CO₂ loading. In the same study, replacement of a methyl group on N by hydroxyethyl group decreased CO₂ loading capacity of both the secondary amines (N-Methylethanolamine and Diethanolamine) and tertiary amines (N,N-dimethylethanol-amine, N-methyl-diethanolamine, triethanolamine).⁷

A series of nonvolatile amino acid salts with sterically hindered amine groups were investigated to determine their potential as direct replacements for MEA.⁸ The study found that methyl groups substituted adjacent to the amine function (α carbon) increased solution absorption capacities. A similar behavior was reported with alkylamine with CH₃ at an α carbon.^{6b} One methyl substituted to an α carbon was reported to be sufficient to produce total carbamate hydrolysis.⁸

A screening study of the carbon dioxide absorption performance of 76 amines reported that primary and secondary amines, with some form of steric hindrance and hydroxyl functionality with 2 or 3 carbon from nitrogen, exhibited higher CO₂ absorption capacities.⁹ One possible reason for this is that a hydroxyl group, the appropriate distance from the amine functionality, and with the appropriate structural features surrounding it, enables formation of a stable intramolecular hydrogen bond with the nitrogen to form a five or six member ring structure. While this may decrease the amine pK_a, for primary and secondary amines it may also destabilize carbamate formation. It results in higher absorption capacity via carbamate hydrolysis path way (1.1-c).

All of the studies mentioned above have investigated the effect of the amine molecular structure on CO₂ absorption capacity or rate. Rational development of the absorbent requires looking into equilibrium constants of important reactions and their rate. A systematic investigation of carbamate stability constants has been carried out in some studies.¹⁰ Supporting the statement that carbamate stability decreases with increasing steric hindrance⁵, a systematic experimental investigation into carbamate stability constants^{10a} revealed that the carbon α to the amine group would be expected to increase steric hindrance rather than the β carbon. Another study on carbamate formation and molecular structure has pointed to the same.^{10b} This study observed that MEA forms more stable carbamate, than AP (2-amino-1-propanol), which has a -CH₃ group on the α carbon to the amine nitrogen. However, 2-amino-1,3-propanediol which has a -CH₂OH group on the carbon α to the amine nitrogen does not form a carbamate. The effect of -CH₂OH is apparently greater than that of the -CH₃. According to this study, the reduced stability of a carbamate with one or more -CH₃ groups on the α carbon is caused by the close approach of the oxygen atoms of the -COO⁻ group

to the hydrogen atoms of one or more close $-\text{CH}_3$ groups. This introduces a significant stereochemical strain in the molecule. With one or more $-\text{CH}_3$ groups on the α carbon, the $\text{N}-\text{C}-\text{C}(\text{OH})$ angle decreases. This indicates that the nitrogen atom, along with the carbamate functionality, is forced away from a $-\text{CH}_3$ on the α carbon. A consequence of a smaller $\text{N}-\text{C}-\text{C}(\text{OH})$ angle is that the intramolecular $(\text{OC})\text{O} \dots \text{H}(\text{O})$ bond becomes shorter, but also that the $(\text{O}2)\text{C}-\text{N}-\text{C}$ angle increases. This results in a more unstable carbamate.^{10b} Interestingly, *t*-butylamine forms a carbamate¹¹, yet it has three $-\text{CH}_3$ groups on the α carbon to the NH_2 group. On the contrary AMP (2-amino-2-methyl-1-propanol) forms very unstable carbamate at undetectable levels. However, a study by Conway et al. reported that no carbamate was observed in both a CO_2 – *t*-butylamine reaction system and a CO_2 -AMP reaction system.¹²

The effects of methyl substitutions on α carbon to the amino group is also described based on molecular orbital approach.¹³ Methyl groups have two pairs of degenerate orbitals of π type symmetry (occupied and unoccupied) that are symmetry compatible with the lone-pair orbital of the amino group. Interaction of the amine group lone-pair orbital with the unoccupied π orbital of the CH_3 group leads to the amino group having a lower charge at the N donor site and hence becoming a “softer base”.¹⁴ The softer the base RNH_2 the weaker the N-C bond formed in the adduct ($\text{CO}_2:\text{RNH}_2$), which in turn results in formation of a less stable carbamate species enhancing the formation of the bicarbonate species.¹³

All of the above studies pointed qualitatively to a structure effect to explain the reactivity of amines with different structures. If we want to predict the reactivity of an amine or estimate the equilibrium data related to it, based on the molecular structure, we need a parameter which describes structural effects. A Brønsted correlation relating the kinetic and equilibrium constants for formation of carbamic/carbamates with the protonation constant (pK_a) of amine is reported in an attempt to elucidate a fundamental chemical understanding of the relationship between the amine structure and chemical properties.¹² The electronic effect of the amine structure was approximated by the protonation constant (pK_a). Such correlations were found to work fairly well for sterically unhindered amines, deviation from this relation has been proposed to be due to steric effects.

Another method to estimate the reaction equilibrium constants is to use molecular modeling. Computational chemistry has been used as a tool to calculate reaction energies of reactions involved in CO_2 with aqueous solutions of amines and amino acids for screening purposes.¹⁵ The free energies of reactions have been calculated in the gas phase. The free energy in solution was obtained as a summation of the free energy in gaseous phase with the respective solvation energies of the

different species. The uncertainty of the calculations lie in the solvation model used, since several different models exist.¹⁵

As presented above many approaches have been used by different teams to elucidate structure and reactivity relationships in CO₂-amine reaction systems. However, more rational approaches still need to be examined. This dissertation work is expected to give a contribution to fulfill this gap. As background for our own study, the structure-activity relationship for aq. Amine base strength is reviewed in the next section.

2.1. Quantitative structure-activity relationships for the base strength of amines

The molecular structural effect on the ionisation of the conjugate acids of nitrogen bases was studied to establish the structure-reactivity relationship on base strength of amine.^{3, 16} Taft's polar parameter has been used as a parameter to characterize the substituents.

Taft's polar parameter ($\sum \sigma^*$) has been plotted against pK_a of non-aromatic 1°, 2° and 3° amines³(Figure 2.1-1). Three liner relationships were found for the three different classes of amines. Tertiary amines conformed well to its liner relationship. Certain secondary and primary amines showed deviations as bulkiness of the alkyl group increased. This was attributed to steric effects since the electronic effects are accounted for in the Taft polar parameter.

Separation of three lines indicated that the importance of solvation of the alkylammonium ion through the N-H bonds with water molecule. The more N⁺-H bonds, the more such hydrogen-bonding can occur. The intense of bonding follows; ammonia > primary > secondary > tertiary amines. Further, the deviations in bulky primary and secondary amines indicated the possible importance of the steric inhibition of the solvation. Folkers and Runquist reported a single relationship for all classes of amines which was reported by Hall.³ This single relationship between polar effects and base strength has included extra parameters to account for the numbers of hydrated groups (N⁺-H) in the ammonium ion and measuring base-strengthening effects of each hydrated N⁺-H group.¹⁷

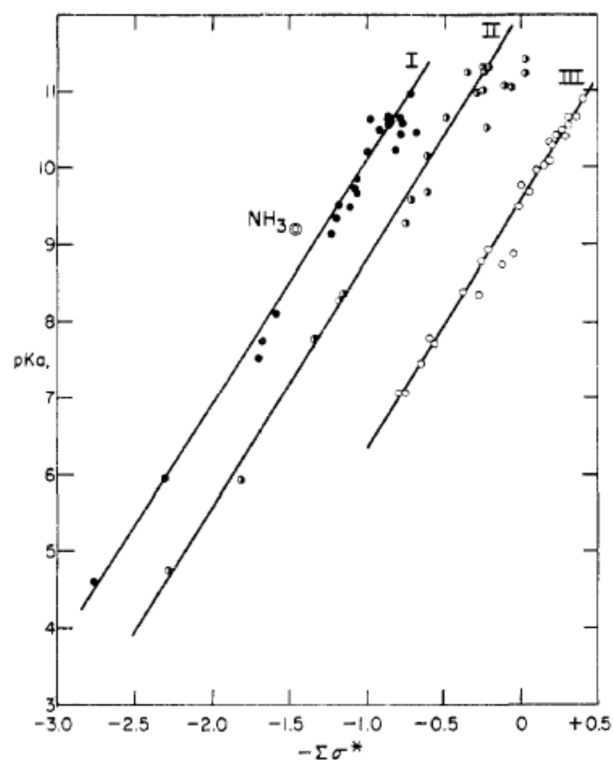


Figure 2.1-1 : Taft's polar parameter ($\Sigma \sigma^*$) has been plotted against pK_a of non-aromatic I (primary) II (secondary) and III (tertiary) amines.³

These relationships could be used to predict unknown pK_a values of amines. The study by Hall inspired the present dissertation work which attempts to find out molecular structure effects on CO_2 -amine reactions in aqueous medium.

3. Molecular structure and activity

Currently there two mechanisms have been introduced for the reaction between CO₂ and primary/secondary amine. The Zwitterion mechanism (by Caplow 1968¹⁸), which is the currently accepted mechanism (Figure 3-1)¹⁹ and, the termolecular mechanism (by Crooks and Donnellan 1989²⁰). According to the Zwitterion mechanism, CO₂ and amine react directly to form zwitterion, and this zwitterion reacts with a base (H₂O or amine) to transfer its proton.

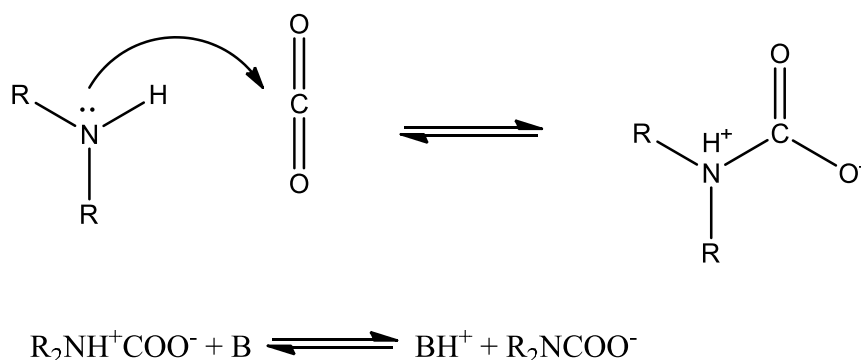


Figure 3-1: Amine- CO₂ interaction to form carbamate (R₂-NH can be any primary/secondary amine component. B represents the base).

Absorption of CO₂ in aqueous primary and secondary amine is driven by the Lewis acid-base reaction as shown in Figure 3-1. An amine molecule which is a Lewis base donates its electron pair while Lewis acid CO₂ accepts the electron pair. Thus, changes in the electronic environment around nitrogen (N) will determine the donor properties of the amino species and hence its interactions with Lewis acids. Several factors could affect the electron density of the functional group N and, hence, the reaction with CO₂ and the stability of the N- C bond. Among them, the polar effect of substituents plays a role. Atoms or groups of atoms bonded to the functional group (i.e. N) in the amine molecule have the ability to withdraw or donate electrons through the bonds. It can distort the electron density distribution of the structure.²¹ Such distortion affects the electron density on the N atom and is referred to as “inductive” or “polar” effect.

Taft introduced an empirical parameter which describes the polar effect of substituents. The parameter is based on evaluating the polar effects of substituents R in the rate of hydrolysis of ester (ROOR')² as given in reaction (3-a). The formula of the empirical parameter is given in the equation (3-1).

$$\sigma^* \equiv \frac{1}{2.48} [\log (k/k_0)_B - \log (k/k_0)_A] \quad (3-1)$$

σ^* is the numerical value obtained to quantify the polar substituent effect (called polar substituent constants or Taft polar parameter). The reaction rate constant k refers to the hydrolysis of a substituted (in acyl ($\mathbf{RC(O)O-}$) part of the ester) ester (3-a). k_0 is related to the hydrolysis of the reference ester in which R is CH_3 . \mathbf{B} and \mathbf{A} refer to base-catalyzed hydrolyses and acid-catalyzed hydrolyses respectively, for the same ester, solvent and temperature.



The ratio of rate constants (k/k_0) is taken as a measure of how the rate is deviated when substituent in acyl part changes from CH_3 to another substituent R. The mechanisms for the acid and base-catalyzed hydrolyses are very similar. The transition for acid-catalyzed differs from that of base-catalyzed by the presence of two protons.² Thus, it makes the steric interactions of the substituent R cancelled out in the ratio of the corresponding rate constants.

σ^* for different substituents is tabulated in the literature.^{2, 22} σ^* for selected substituents, taken from the literature, are presented in Table 3-1.²

Table 3-1: σ^* for selected substituents are presented

Substituent	H	CH_3	C_2H_5	n- C_3H_7	i- C_3H_7	n- C_4H_9	i- C_4H_9	s- C_4H_9	t- C_4H_9
σ^*	+0.49	0	-0.1	-0.115	-0.19	-0.13	-0.125	-0.21	-0.3

A positive σ^* value is attributed to an electron withdrawing effect on the functional group (e.g N in amine) while a negative σ^* value is attributed to electron donating ability towards the functional group. For molecular structures consisting of many substituents, their effects at the reaction center are additive ($\sum \sigma^*$). Electron withdrawing substituents are consistently electron withdrawing, no matter what reaction they are involved in and are so electron donating substituents.²¹

The current study focuses on molecular structure effects of primary alkylamines reaction with CO₂. The collective Taft polar substituents effects of alkyl on amino functional group have to be determined first. Estimation of such values²³ for ethylamine (simple example) and 2-Amino-2-methyl-1-propanol (rather complex example) are illustrated in Figure 3-2, employing the additivity of contribution from fragments attached to functional group. Collective polar substituent effects ($\sum \sigma^*$) of systematically selected primary alkylamines and alkanolamines estimated in similar way, are presented in Table 3-2.

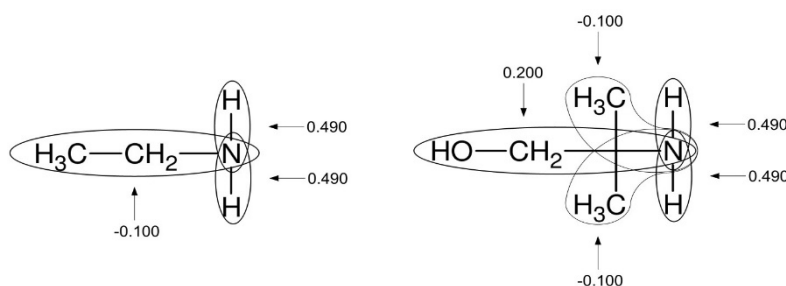


Figure 3-2: Illustration for estimating cumulative polar substituents constant ($\sum \sigma^*$) of an amine molecule. (right: ethylamine, left: 2-Amino-2-methyl-1-propanol)

Determination of the $\sum \sigma^*$ value of ethylamine: Two hydrogen atoms and one ethyl fragment are attached to N. The calculation is followed as shown below in equation (3-2) polar substituent effects (σ^*) of -H is 0.490 and that of $-\text{C}_2\text{H}_5$ is -0.100 (values as given in Table 3-1). Since there are two H s, σ^* of H is multiplied by two. This means that substituting a H atom with a C_2H_5 group on a NH_3 molecule draws less electron density off the N atom as compared to NH_3 .

$$\sum \sigma^* (\text{CH}_3\text{CH}_2\text{NH}_2) = (-0.100) + 0.490 * 2 = 0.880 \quad (3-2)$$

Determination of the $\sum \sigma^*$ value of 2-Amino-2-methyl-1-propanol: Two hydrogen atoms, an ethanol fragment and two ethyl fragments are attached to N. The calculation is followed as

below (3-3), polar substituent effects (σ^*) of -H is 0.490 and that of $-\text{C}_2\text{H}_5$ is -0.100 (values as given in Table 3-1); contribution from $-\text{CH}_2\text{CH}_2\text{OH}$ is 0.2. Since there are two H s and two ethyl fragments corresponding σ^* are multiplied by two.

$$\sum \sigma^* (\text{HOCH}_2\text{C}(\text{CH}_3)_2\text{NH}_2) = 0.200 + (-0.100) * 2 + 0.490 * 2 = 0.980 \quad (3-3)$$

Table 3-2: Collective polar substituent effects ($\sum \sigma^*$) of systematically selected primary alkylamines and alkanolamines.

Amine	Structure	$\sum \sigma^*$
Methyl		0.980
Ethyl		0.880
n-Propyl		0.865
iso-Propyl		0.790
n-Butyl		0.850
sec-Butyl		0.770
iso-Butyl		0.855
tert-Butyl		0.680
Ethanol		1.180 ³
2-Amino-2-methyl-1-propanol (AMP)		0.980
3-Amino-1-propanol (MPA)		1.062

4. ¹⁵N NMR spectroscopy

¹⁵N NMR experimental data was used to get information on the relative electron density on the nitrogen atom in various amines. This section will explain briefly the experimental procedure together with the background of ¹⁵N NMR.

As mentioned in the NMR spectroscopy section (1.1 of Part II : Raman Spectroscopy), the NMR spectrometer detects RF energy absorbed by the nuclei at lower spin energy states to align against the external magnetic field. The field strengths required for resonance of a specific nuclei in a molecule varies depending on the electron shielding around it. The electron shielding is distinguishing character defined by chemical environment of the specific nucleus. This variation in the absorption frequency of NMR gives the information on subtle changes in the distribution of electron density around a specific nucleus.

In the context of the current study with ¹⁵N NMR, the substituents attached to a nitrogen containing molecule can influence the electron shielding of atomic nuclei depending on their electron donating or withdrawing ability. Additionally, the lone-pair of electrons which N atoms of molecules have, can interact with the molecules surrounding the amine or the amine molecule itself. This results in changes of the electron density.²⁴ This feature makes the ¹⁵N nucleus more sensitive to medium effects (e.g. solvent, concentration and temperature) than ¹H and ¹³C nuclei.

Applied to amines, the nitrogen lone pair of the amine can make hydrogen bonds with the hydrogen of polar protic solvents, such as water. Consequently, it leads to reduced electron density over N and so reduced nucleus shielding.²⁵ The chemical shift measured by NMR increases as deshielding increases. However, protonated amine and molecular amine give a single signal due to the fast proton exchange in NMR time scale. Therefore, the chemical shift value by the single signal depends on the ratio between protonated and molecular base.²⁵⁻²⁶

Further, hyperconjugation with lone pairs in aliphatic amines may have a strong influence on electron density over N.^{13,27} With aromatic amines, the lone pair electrons of N can be involved in resonance which leads to electron delocalization.

Therefore, one should account all of these possible effects which influence the electron density over N, when interpreting ¹⁵N NMR data. This is very applicable to the present study of amine reactivity towards carbon dioxide. The nitrogen is the nucleus acting as a nucleophile and, other things being equal, the tendency of the reacting depends on the availability of the lone pair electrons on N, which may be monitored through the measured ¹⁵N NMR chemical shift values.²⁵

4.1. ^{15}N NMR experimental method

The ^{15}N NMR experimental work was carried out in cooperation with B. Arstad, A. Bouzga and C. Perinu at the SINTEF NMR facility in Oslo employing a Bruker Avance III spectrometer.



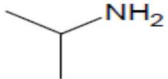
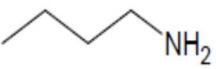
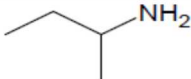
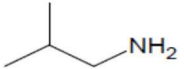
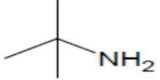
Samples of *n*-Propylamine Iso-Propylamine *n*-Butylamine iso-Butylamine Sec-Butylamine and tert-Butylamine were analyzed with ^{15}N NMR (details of the chemicals presented in Appendix A). In a typical sample preparation, a weighed amount of amine and water (deionised and degassed) were mixed and the concentrations (2.00 ± 0.04 M) were calculated by measuring the density with a pycnometer. The samples were then transferred to a NMR tube for ^{15}N NMR measurements.

The samples of amine solutions were kept at the same concentration (2 M) and at the same temperature (298.15 K) to avoid corresponding effects on the chemical shift values. The ^{15}N NMR spectra were acquired at 9.4 T on a Bruker Avance III 400 MHz spectrometer using a BBFO Plus double resonance probe head at 298.15 K. The spectra were processed using MestreNova software v 7.1.1. For all amines, the experiments were run with the inverse gated decoupling method, pulse angle of 90° (14 μs pulse width), a pre-scan delay of 250 μs , a recycle delay of 10 s and scans from 624 up to 3834 (except for 2 M propylamine solution which required a recycle delay of 100 s and 48 scans). The uncertainty in the chemical shift values was estimated to be in the range of ± 0.01 -0.03 ppm. The method used has been fully described previously.²⁵

5. Correlations for carbamate related equilibrium constants

In the period 1925-1957, C. Faurholt and coworkers studied the hydrolysis reaction (1.1-c) at 18 °C for systematically selected amines.^{11, 28} Logarithmic values of the equilibrium constants (K_{CBM} and K_{HYD}) of both reactions (1.1- a and c) for primary alkyamines, studied here, are assembled in Table 5-1, with their protonation constants values and polar substituent constants ($\sum \sigma^*$).

Table 5-1: chemical structure, polar substituent constants ($\sum \sigma^*$), equilibrium constants for carbamate formation and hydrolysis (K_{CBM} and K_{HYD}) at 18 °C and protonation constants at 25 °C. ¹⁵N chemical shift values at 25 °C (expressed in ppm).

Amine	Structure	$\sum \sigma^*$	$\text{p}K_{\text{a}}^{29}$	Log $K_{\text{CBM}}^{\text{I}}$	Log $K_{\text{HYD}}^{\text{II}}$	Ref ⁱⁱ	ppm ¹⁵ N NMR
Methylamine (NH ₂ Me)		0.98	10.641	6.60	-2.22	^{28a}	n.a
Ethylamine (NH ₂ Et)		0.88	10.630	6.30	-1.74	^{28b}	n.a.
n-Propylamine(NH ₂ Pr)		0.865	10.568	6.18	-1.89	^{28c}	25.23
Iso-Propylamine (NH ₂ Pr)		0.79	10.670	5.56	-1.20	^{28c}	46.81
n-Butylamine (NH ₂ Bu)		0.85	10.640	6.04	-1.80	¹¹	25.40
Sec-Butylamine NH ₂ Bu		0.77	10.560	5.58	-1.31	¹¹	42.44
iso-Butylamine NH ₂ Bu		0.855	10.480	6.11	-2.00	¹¹	22.15
tert-Butylamine NH ₂ Bu		0.68	10.685	5.04	-0.85	¹¹	60.87

ⁱ values taken from Dell'Amico et al.³⁰. ⁱⁱreference for K_{HYD} values

Relationships for carbamate related equilibrium constants and polar substituent constant was built as show in Figure 5-1. This could contribute to finding out whether carbamate formation and hydrolysis are influenced by inductive effects of substituents in the amine molecule.

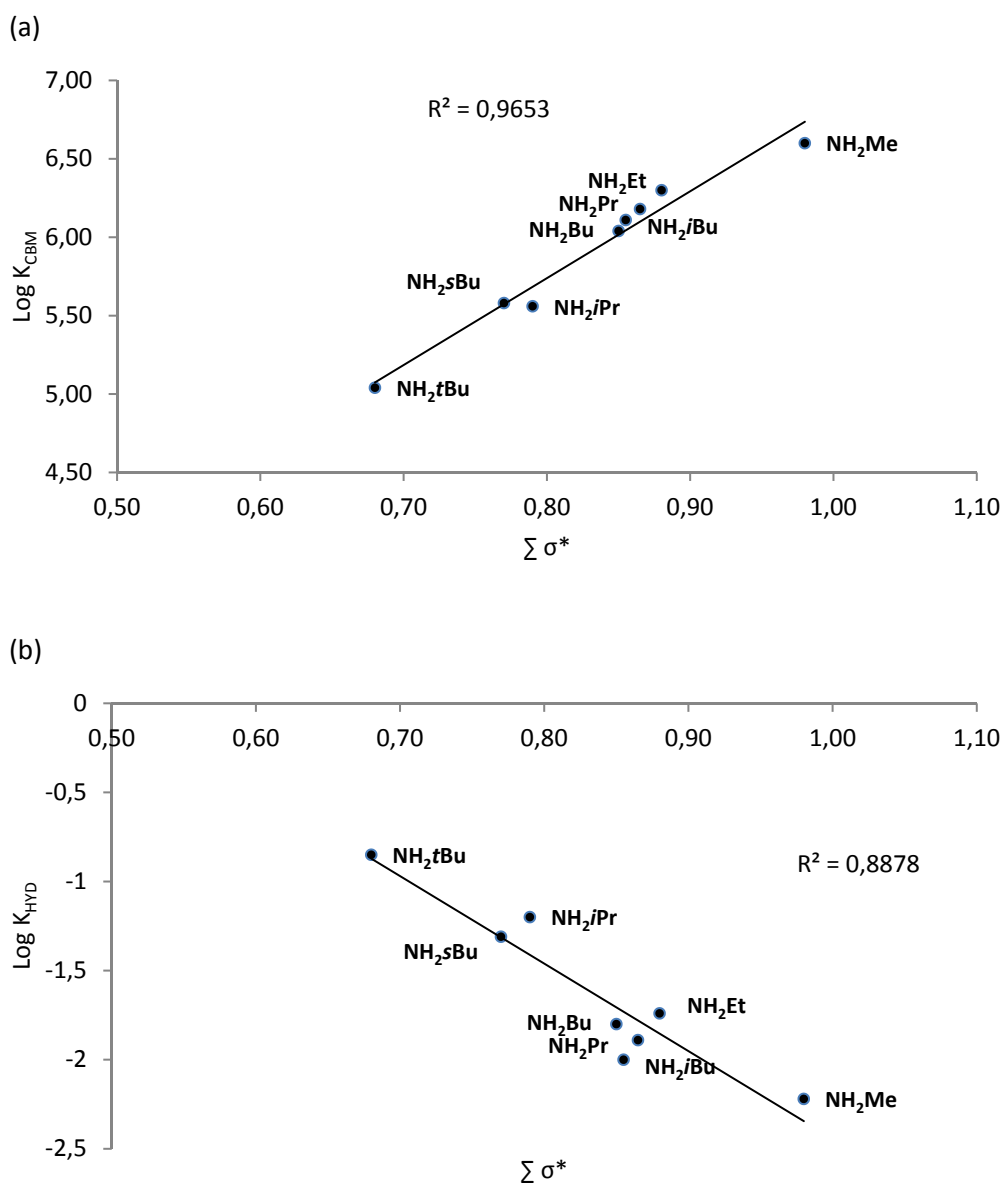


Figure 5-1: Polar substituent constants versus (a) carbamate forming equilibrium constants ($\text{Log } K_{CBM}$) and (b). carbamate hydrolyzing equilibrium constants ($\text{Log } K_{HYD}$).

According to Figure 5-1, the linear relationships between $\Sigma \sigma^*$ and both K_{CBM} and K_{HYD} are observed even for “steric hindered” amines. The carbamate formation constant increases as $\Sigma \sigma^*$ increases (Figure 5-1a), whereas the carbamate hydrolysis increases as $\Sigma \sigma^*$ decreases (Figure 5 1-

b). Since these relationships are linear, they could have the potential to predict the unknown K_{CBM} and K_{HYD} of amines. However, as positive $\sum\sigma^*$ value increases, the electron withdrawing ability increases. It turns out that the carbamate formation and its stability increase as the electron withdrawing from N increases (i.e. less electron density over N), though high electron density favours Lewis acid-base reaction.

This behavior is quite similar to the relation between pK_a values and carbamate formation, reported in Perinu et al., where the linear primary alkanolamines with higher pK_a (higher basicity) resulted in less carbamate at equilibrium.²⁵ A computational study on carbamate stability reported that a clear trend could be seen with a reverse correlation between carbamate stability and the base strength of a series of cyclic amine (morpholine, piperazine and piperidine).³¹ To get a better understanding on this aspect, the equilibrium constants for carbamate formation and hydrolysis are plotted against the protonation constants (pK_a) of the amines investigated in this study (Figure 5-2)

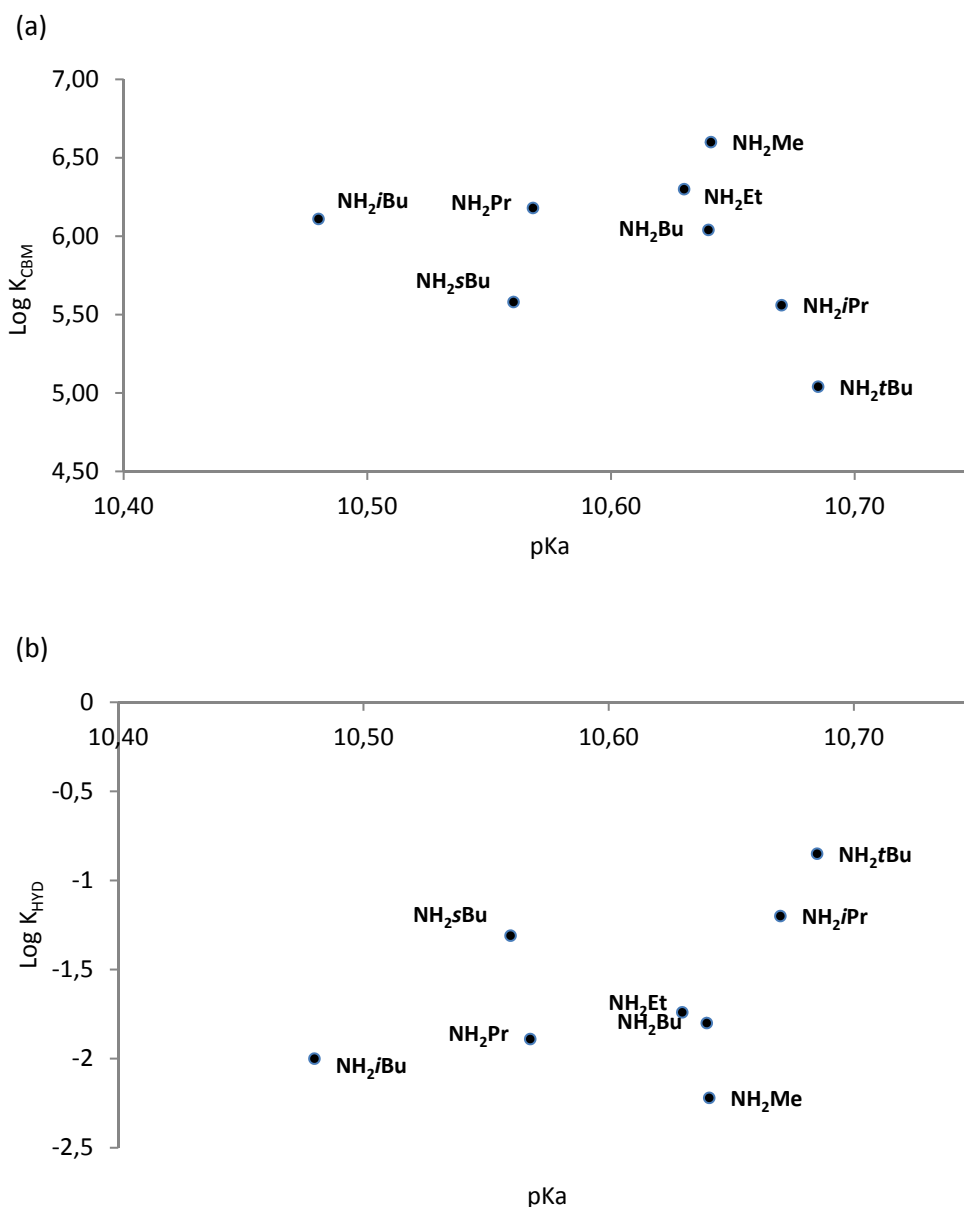


Figure 5-2: Dependence of basicity pK_a (at 25 °C) on the equilibrium constants (at 18 °C) of (a) carbamate forming equilibrium constants ($\text{Log } K_{\text{CBM}}$) and (b). carbamate hydrolyzing equilibrium constants ($\text{Log } K_{\text{HYD}}$).

It appears there are no clear relationships between these equilibrium constants and pK_a . However, the general trends seem to be less carbamate formation (Figure 5-2a) and higher carbamate hydrolysis (Figure 5-2b) as basicity increases. Moreover, these trends are not linear as observed for the correlation of K vs. $\sum\sigma^*$ (Figure 5-1 a & b).

Therefore, the above situations (Figure 5-1 and Figure 5-2) indicate that all underlying factors influencing amine reactivity to form carbamate may not be reflected by the pK_a . pK_a consists, in

our case, of two additive terms; i) the proton accepting power of a Brønsted base (e.g., the amine) and ii) the hydration stabilization of the ammonium ion (e.g. amine H⁺ solvation) through the N-H protons.³² $\sum\sigma^*$ on the other hand, is a measure of the electron withdrawing or releasing ability of substituents collectively, from or towards a functional group (in this case, N) only. Since all amines (including steric hindered amines) show a linear relationship in Figure 5-2, but not in Figure 5-2, it may be assumed that amine reactivity (aqueous amine with CO₂) can be described by the polar effect which is an electronic effect.

¹⁵N NMR chemical shift values, expressed in ppm, have been measured for selected amines (without CO₂ loading) to gain more insight into the reactivity of the amine N nucleus (Table 5-1). Lower ppm values correspond to more shielded nuclei, meaning that the nucleus is surrounded by higher electron density. Figure 5-3a shows that the carbamate formation equilibrium constant increases at increased electron density on the N nucleus (lower ppm values). On the contrary, Figure 5 3-b shows that the carbamate hydrolysis constant increases for those amines which have the tendency to form less carbamate and are characterized by a lower relative electron density on the N (high ppm values). Therefore, the ¹⁵N NMR data is in line with the concept that Lewis acid-base reactions are favored by an increased availability of lone pair electrons on the amine base (higher electron density).

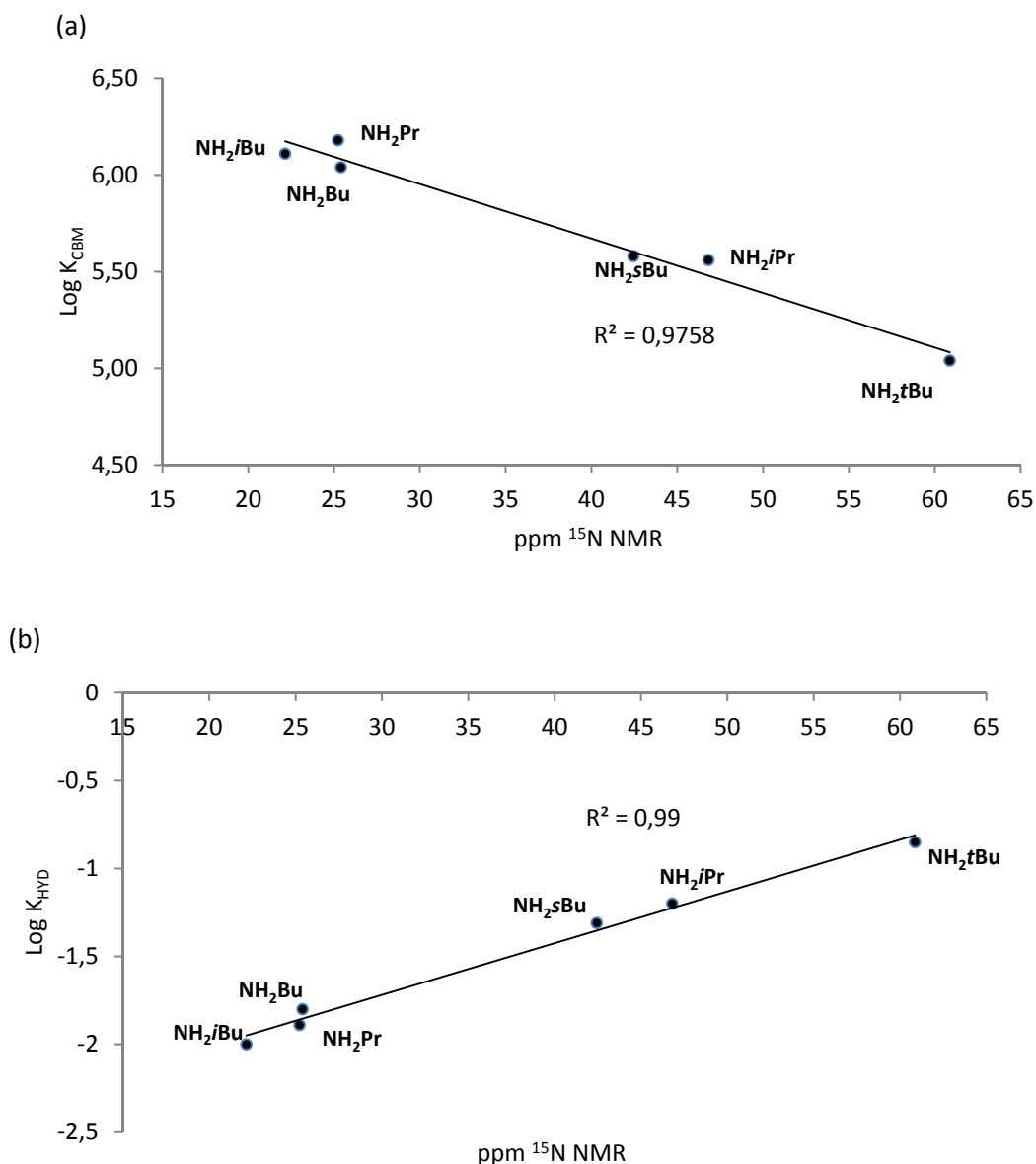


Figure 5-3: ^{15}N NMR chemical shift values of aqueous primary alkylamines (2 M, before CO_2 loading) versus a). carbamate forming equilibrium constants ($\text{Log } K_{\text{CBM}}$) and b). carbamate hydrolyzing equilibrium constants ($\text{Log } K_{\text{HYD}}$).

The $\sum\sigma^*$ parameter is assigned only to the inductive (polar) effect of substituents. However, the inductive effect of substituents also influences the ^{15}N ppm values. Other effects that influence the ^{15}N ppm values and, consequently, the electron density on nitrogen and carbamate formation, are the chemical environment defined by inter- and intra-molecular interactions (e.g. solvent effects). Note, however, that the ^{15}N NMR experiments have been performed at the same

concentration and temperature to avoid any influence by them on the N chemical shift values. As a general trend, the ¹⁵N ppm increases as the pK_a increases (Figure 5-4). Water can form hydrogen bonds with the unshared electron pair on nitrogen or the N-H protons of ammonium ions. The stronger the base, the more interactions occur of the free amine with water. Such interaction results in reduced electron density over N leading to increased ¹⁵N ppm value. However, the ¹⁵N ppm value corresponds to a common signal from the protonated amine and the free amine. Therefore, ¹⁵N ppm values also include the effect of solvation of the ammonium ion.

Scatters of the plot (Figure 5-3) are apparently grouped as sterically hindered (NH₂tBu), less hindered (NH₂iPr, NH₂sBu) and unhindered amines (NH₂iBu, NH₂Bu, NH₂Pr). It is worth noting that the chemical shift values increase (lower electron density) at increasing steric hindrance in the carbon to amino. This can be explained, as proposed by Chakraborty et al., as the electronic effect of methyl substitution on the carbon atom adjacent to the amino group (α carbon).¹³ Similar finding has been reported in a ¹⁵N NMR study by Yoon and Lee.³³

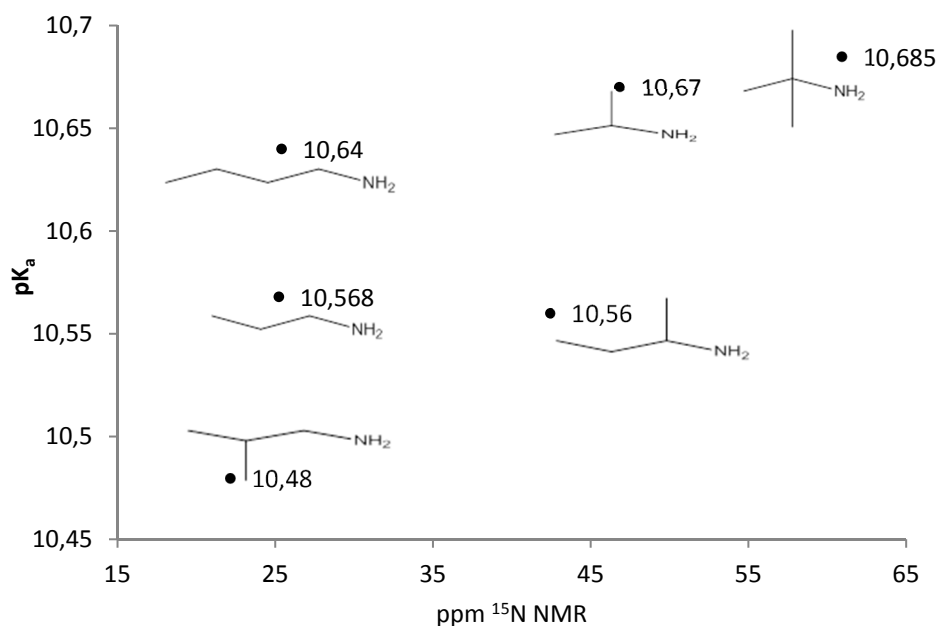


Figure 5-4: Protonation constants of alkylamines at 25 °C against ¹⁵N NMR chemical shift values at 25 °C

(Figure 5-5) shows a plot of the inductive (polar) effect of amine substituents vs pK_a values. It can be observed for steric hindered amines (NH₂iBu, NH₂s Bu, NH₂tBu) that pK_a increases (basicity increases) as the steric hindrance in the α -C increases. According to Figure 5-5, such

amines also have relatively low $\sum\sigma^*$ values (i.e. less “electron withdrawing”). Therefore, a possible explanation for higher basicity could be that more electrons are donating substituents in α carbon, which raises up the electron density on nitrogen by an inductive effect.

Figure 5-5 shows that inside one group of compounds (e.g. non-hindered amines NH_2Et , NH_2Pr , NH_2Bu , NH_2iBu) larger and more branched substituents lead to a lower pK_a value. This means that the substituents may interfere with hydration stabilization of the ammonium ion. This observation is in accordance with (Figure 5-4) where these respective amines show a lower ^{15}N NMR shift value indicating less ammonium ions present.

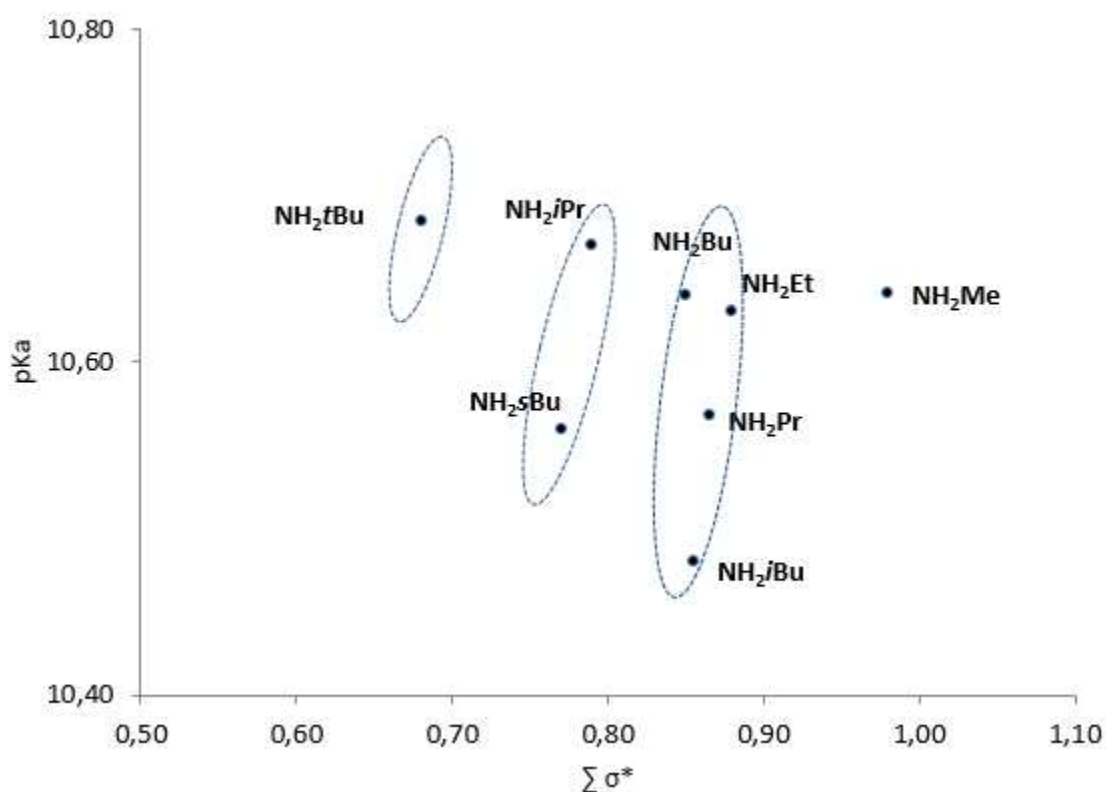


Figure 5-5: protonation constants at 25 °C against Polar substituent constants ($\sum\sigma^*$)

The current study provides evidence that in addition to polar effects from substituents, water solvents and steric hindrance (in terms of electron delocalization) influence the reaction of the current primary alkylamines toward CO_2 . The result shows that higher basicity and higher α -C substituent effect (steric hindrance) reduces carbamate formation.

Yet, the correlations between equilibrium constants and polar substituents constants ($\sum\sigma^*$) highlights the potential of using $\sum\sigma^*$ to estimate the equilibrium constants for amines. Further investigations are needed to see if this approach is valid for other classes of amine absorbents for

CO₂ capture, and if it would be possible to predict $\sum\sigma^*$ and/or carbamate related equilibrium constants from ¹⁵N NMR chemical shift values.

Further, the equilibrium constants (K) cannot be correlated to only a single effect because electron density on N depends on several factors. K could be a function of inductive (σ^*), steric (E_s) and/or solvation (S) effects.

$$K_{\text{CBM} / \text{HYD}} = f(\sum\sigma^*, E_s, S) \quad (5-1)$$

¹⁵N ppm is a promising tool providing information on electron density over N, but it should be noted that the value is taken from the common signal given from the neutral and protonated amine.

6. Conclusions and further work

Conclusions

- Correlations between equilibrium constants of carbamate formation or hydrolysis (K_{CBM} and K_{HYD}) and Taft polar substituent constants ($\sum\sigma^*$) was established. The significance of this result is that these relationships are linear and could have the potential to estimate the equilibrium constants of new amines and to get an idea of the equilibrium behavior for such amines.
- Our results show that steric hindrance is, as proposed by Chakraborty et al.,¹³ an electronic effect rather than a steric effect as proposed by Sartori and Savage⁵ and Conway et al. Our results are in accordance with another NMR study³³ which also supported the proposal by Chakraborty et al.

Further work

- These relations have to be validated with known equilibrium constants. Further investigations are also needed to see if this approach is valid for other classes of amine absorbents for CO₂ capture. The main issue is that the equilibrium constants are not available. Therefore, K_{eq} of several amines with changing substituents have to be determined with a reliable analytical method.
- It is possible to make such relationship for the reaction rates as well. Future work for this study could be to build correlations of polar effects on reaction rate.

Reference

1. Shorter, J., The separation of polar, steric, and resonance effects in organic reactions by the use of linear free energy relationships. *Quarterly Reviews, Chemical Society* **1970**, *24* (3), 433-453.
2. Taft, R., Separation of Polar, Steric, and Resonance Effects in Reactivity. In *Steric Effects in Organic Chemistry*, Newman, M., Ed. John Wiley: New York 1956
3. Hall, H. K., Correlation of the Base Strengths of Amines. *J. Am. Chem. Soc.* **1957**, *79* (20), 5441-5444.
4. Bishnoi, S. Carbon Dioxide Absorption and Solution Equilibrium in Piperazine Activated Methyl-diethanolamine. Ph.D. Dissertation, The University of Texas, 2000.
5. Sartori, G.; Savage, D. W., Sterically hindered amines for carbon dioxide removal from gases. *Industrial & Engineering Chemistry Fundamentals* **1983**, *22* (2), 239-249.
6. (a) Singh, P.; Niederer, J. P. M.; Versteeg, G. F., Structure and activity relationships for amine based CO₂ absorbents—I. *International Journal of Greenhouse Gas Control* **2007**, *1* (1), 5-10; (b) Singh, P.; Niederer, J. P. M.; Versteeg, G. F., Structure and activity relationships for amine-based CO₂ absorbents-II. *Chem. Eng. Res. Des.* **2009**, *87* (2), 135-144.
7. Qi, Y.; Susan, J.; Mathew, B.; Mark, B., Influence of Amine Chemical Structures to Amine Capacities in CO₂ Capture. In *Recent Advances in Post-Combustion CO₂ Capture Chemistry*, American Chemical Society: 2012; Vol. 1097, pp 29-42.
8. Hook, R. J., An Investigation of Some Sterically Hindered Amines as Potential Carbon Dioxide Scrubbing Compounds. *Ind. Eng. Chem. Res.* **1997**, *36* (5), 1779-1790.
9. Puxty, G.; Rowland, R.; Allport, A.; Yang, Q.; Bown, M.; Burns, R.; Maeder, M.; Attalla, M., Carbon Dioxide Postcombustion Capture: A Novel Screening Study of the Carbon Dioxide Absorption Performance of 76 Amines. *Environ. Sci. Technol.* **2009**, *43* (16), 6427-6433.
10. (a) McCann, N.; Phan, D.; Fernandes, D.; Maeder, M., A systematic investigation of carbamate stability constants by ¹H NMR. *International Journal of Greenhouse Gas Control* **2011**, *5* (3), 396-400; (b) Fernandes, D.; Conway, W.; Burns, R.; Lawrance, G.; Maeder, M.; Puxty, G., Investigations of primary and secondary amine carbamate stability by ¹H NMR spectroscopy for post combustion capture of carbon dioxide. *The Journal of Chemical Thermodynamics* **2012**, *54* (0), 183-191.
11. Jensen, M. B., Studies on Carbamates, XII. The Carbamates of the Butylamines. *Acta Chem. Scand.* **1957**, *11*, 499 - 505.
12. Conway, W.; Wang, X.; Fernandes, D.; Burns, R.; Lawrance, G.; Puxty, G.; Maeder, M., Toward the Understanding of Chemical Absorption Processes for Post-Combustion Capture of

Carbon Dioxide: Electronic and Steric Considerations from the Kinetics of Reactions of CO₂(aq) with Sterically hindered Amines. *Environ. Sci. Technol.* **2012**, *47* (2), 1163-1169.

13. Chakraborty, A. K.; Bischoff, K. B.; Astarita, G.; Damewood, J. R., Molecular orbital approach to substituent effects in amine-CO₂ interactions. *Journal of the American Chemical Society* **1988**, *110* (21), 6947-6954.

14. Pearson, R. G.; Songstad, J., Application of the Principle of Hard and Soft Acids and Bases to Organic Chemistry. *J. Am. Chem. Soc.* **1967**, *89* (8), 1827-1836.

15. Gupta, M.; da Silva, E. F.; Svendsen, H. F., Computational Study of Equilibrium Constants for Amines and Amino Acids for CO₂ Capture Solvents. *Energy Procedia* **2013**, *37* (0), 1720-1727.

16. Hall, H. K., Field and Inductive Effects on the Base Strengths of Amines. *J. Am. Chem. Soc.* **1956**, *78* (11), 2570-2572.

17. Folkers, E.; Runquist, O., Correlation of Base Strengths of Aliphatic and N-Substituted Anilines. *The Journal of Organic Chemistry* **1964**, *29* (4), 830-832.

18. Caplow, M., Kinetics of carbamate formation and breakdown. *J. Am. Chem. Soc.* **1968**, *90* (24), 6795-6803.

19. (a) Donaldson, T. L.; Nguyen, Y. N., Carbon Dioxide Reaction Kinetics and Transport in Aqueous Amine Membranes. *Industrial & Engineering Chemistry Fundamentals* **1980**, *19* (3), 260-266;

(b) Danckwerts, P. V., The reaction of CO₂ with ethanolamines. *Chem. Eng. Sci.* **1979**, *34* (4), 443-446.

20. Crooks, J. E.; Donnellan, J. P., Kinetics and mechanism of the reaction between carbon dioxide and amines in aqueous solution. *Journal of the Chemical Society, Perkin Transactions 2* **1989**, (4), 331-333.

21. Anslyn, E. V.; Dougherty, D. A., *Modern physical organic chemistry*. University Science Books: 2006.

22. Perrin, D. D.; Dempsey, B.; Serjeant, E. P., *pKa prediction for organic acids and bases*. Chapman and Hall London; New York: 1981; Vol. 1.

23. Williams, A., *Free energy relationships in organic and bio-organic chemistry*. Royal Society of Chemistry: 2003.

24. (a) Marek, R., ¹⁵N NMR Applications. In *Encyclopedia of Spectroscopy and Spectrometry (Second Edition)*, Lindon, J. C., Ed. Academic Press: Oxford, 2010; (b) Michel, D.; Germanus, A.; Pfeifer, H., Nitrogen-15 nuclear magnetic resonance spectroscopy of adsorbed molecules. *Journal of the Chemical Society, Faraday Transactions 1: Physical Chemistry in Condensed Phases* **1982**, *78* (1), 237-254.

25. Perinu, C.; Arstad, B.; Bouzga, A. M.; Jens, K.-J., ¹³C and ¹⁵N NMR Characterization of Amine Reactivity and Solvent Effects in CO₂ Capture. *The Journal of Physical Chemistry B* **2014**, *118* (34), 10167-10174.
26. Burrell, G. L.; Burgar, I. M.; Separovic, F.; Dunlop, N. F., Preparation of protic ionic liquids with minimal water content and ¹⁵N NMR study of proton transfer. *Physical Chemistry Chemical Physics* **2010**, *12* (7), 1571-1577.
27. De M. Carneiro, J. W.; Dias, J. F.; Tostes, J. G. R.; Seidl, P. R.; Taft, C. A., Hyperconjugation effects of hydroxyl and amine groups on chemical shifts of neighboring carbon nuclei. *International Journal of Quantum Chemistry* **2003**, *95* (3), 322-328.
28. (a) Faurholt, C., Etudes sur les solutions aqueuses de carbamates et de carbonates. *J. Chim. Phys.* **1925**, *22*, 1; (b) Lund, V.; Faurholt, C., Carbamates. III. The carbamates of ethylamine and diethylamine. . *Dansk Tidsskrift for Farmaci* **1948**, *22*, 109-23; (c) Olsen, J.; Vejlbj, K.; Faurholt, C., Studies on Carbamates, VII. The Carbamates of *n*-Propylamine and *iso*-Propylamine. *Acta Chem. Scand.* **1952**, *6*, 398-403.
29. Christensen, J. J.; Izatt, R. M.; Wrathhall, D. P.; Hansen, L. D., Thermodynamics of Proton Ionization in Dilute Aqueous Solution. Part XI. ¹pK, ΔH°, and ΔS° Values for Proton Ionization from Protonated Amines at 25°. *Journal of the Chemical Society (A)* **1969**, 1212-23.
30. Dell'Amico, D. B.; Calderazzo, F.; Labella, L.; Marchetti, F.; Pampaloni, G., Converting Carbon Dioxide into Carbamate Derivatives†. *Chem. Rev. (Washington, DC, U. S.)* **2003**, *103* (10), 3857-3898.
31. da Silva, E. F., Theoretical study of the equilibrium constants for solvents for CO₂ capture. *Energy Procedia* **2011**, *4* (0), 164-170.
32. Trotman-Dickenson, A. F., 280. The basic strength of amines. *Journal of the Chemical Society (Resumed)* **1949**, (0), 1293-1297.
33. Yoon, S. J.; Lee, H., Substituent Effect in Amine-CO₂ Interaction Investigated by NMR and IR Spectroscopies. *Chem. Lett.* **2003**, *32* (4), 344-345.

Appendix A: List of Chemicals

All chemicals used for experiments were of laboratory grade or better quality, and used as received. Table A1 presents the details of the chemicals.

Table A1: Details of Chemicals Used

*synonym

Chemical Reagent	Abbreviation	Chemical formula	CAS#	M.W.	Purity (%)	Supplier
2-Amino-2-methyl-1-propanol	AMP	$(\text{CH}_3)_2\text{C}(\text{NH}_2)\text{CH}_2\text{OH}$	124-68-5	89.14	99	Acros Organics
Acetonitrile		CH_3CN				
Barium chloride dihydrate		$\text{BaCl}_2 \cdot \text{H}_2\text{O}$	10326-27-9	244.28	99	MERCK
Diethanolamine	DEA	$\text{HN}(\text{CH}_2\text{CH}_2\text{OH})_2$	111-42-2	105.14		MERCK
Hydrochloric acid (Titrisol)		HCl	7647-01-0	36.46	1 mol/L	MERCK
Hydrochloric acid (Titrisol)					0.1 mol/L	MERCK
Isobutylamine *1-Amino-2-methylpropane	NH_2iBu	$(\text{CH}_3)_2\text{CHCH}_2\text{NH}_2$	78-81-9	73.14	≥ 99.5	FLUKA
Isopropilamine *2-Aminopropane	NH_2iPr	$(\text{CH}_3)_2\text{CHNH}_2$	75-31-0	59.11	≥ 99.5	ALDRICH
Monoethanolamine *Ethanolamine *2-aminoethnaol *2-Aminoethyl alcohol	MEA	$\text{NH}_2\text{CH}_2\text{CH}_2\text{OH}$	141-43-5	61.08	≥ 99.5	ALDRICH
Monoethanolamine	MEA	$\text{NH}_2\text{CH}_2\text{CH}_2\text{OH}$	141-43-5	61.08	99.5	MERCK
n-butylamine *1-Aminobutane	NH_2Bu	$\text{CH}_3(\text{CH}_2)_3\text{NH}_2$	109-73-9	73.14	99.5	Sigma-Aldrich

Chemical Regent	Abbreviation	Chemical formula	CAS#	M.W.	Purity (%)	Supplier
N-Methyldiethanolamine	MDEA	$\text{CH}_3\text{N}(\text{CH}_2\text{CH}_2\text{OH})_2$	105-59-9	119.16		MERCK
n-pentylamine *1-Aminopentane *n-Amylamine		$\text{CH}_3(\text{CH}_2)_4\text{NH}_2$	110-58-7	87.16	99	ALDRICH
n-Propylamine *1-Aminopropane	NH_2Pr	$\text{CH}_3\text{CH}_2\text{CH}_2\text{NH}_2$	107-10-8	59.11	≥ 99.5	ALDRICH
secbutylamine	NH_2sBu	$\text{CH}_3\text{CH}_2\text{CH}(\text{NH}_2)\text{CH}_3$	13952-84-6	73.14	99	ALDRICH
Sodium bicarbonate		NaHCO_3	144-55-8	84.01	99	MERCK
Sodium carbonate		Na_2CO_3	497-19-8	105.99	99	MERCK
Sodium hydroxide (Titrisol)		NaOH	1310-73-2	40	1 mol/L	MERCK
Sodium hydroxide (Titrapur)					1 mol/L	MERCK
Sodium hydroxide (Titrapur)					0.1 mol/L	MERCK
Sodium perchlorate *Hyperchloric acid sodium salt		NaClO_4	7601-89-0	122.44	$\geq 98.0\%$	SIGMA-ALDRICH
Tertbutylamine *2-Amino-2-methylpropane	NH_2tBu	$(\text{CH}_3)_3\text{CNH}_2$	75-64-9	73.14	≥ 99.5	Aldrich

Appendix B: List of Publications

- I. Samarakoon, P. A. G. L.; Andersen, N. H.; Perinu, C.; Jens, K.-J., Equilibria of MEA, DEA and AMP with Bicarbonate and Carbamate: A Raman Study. *Energy Procedia* **2013**, *37* (0), 2002-2010.
- II. Perinu, C.; Samarakoon, G.; Arstad, B.; Jens, K.-J., Application of ^{15}N -NMR Spectroscopy to Analysis of Amine Based CO_2 Capture Solvents. *Energy Procedia* **2014**, *63* (0), 1144-1150.
- III. Samarakoon, G.; Svendsen J. A.; Perinu, C.; Jens, K.-J, Speciation of carbonated aqueous amine solutions for CO_2 capture. *to be submitted*
- IV. Samarakoon, G.; Perinu, C.; Jens, K.-J, Correlations of carbamate related equilibrium constants: structure-reactivity relationships. *In preparation*
(This manuscript is not attached in this dissertation.)

Paper I

GHGT-11

Equilibria of MEA, DEA and AMP with Bicarbonate and Carbamate: A Raman Study

Gamunu L. Samarakoon P.A.^a, Niels H. Andersen^b, Cristina Perinu^a,

Klaus-J.Jens^{a*}

^aFaculty of Technology, Telemark University College, P.O. Box 203, Porsgrunn N-3901, Norway

^bDepartment of Chemistry, University of Oslo, P.O. Box 1033, Blindern, Oslo N-0372, Norway

Abstract

Species distribution analysis in carbonated alkanolamine solution is important in order to estimate accurate thermodynamic properties. The applicability of Raman spectroscopy as an analytical tool for speciation of carbonated aqueous alkanolamine systems was studied. Alkanolamine solutions loaded with HCO_3^- were measured using ClO_4^- as internal standard. The same solutions were measured with ^{13}C -NMR spectroscopy. The molar scattering intensity factors for HCO_3^- , CO_3^{2-} and MEA- and DEA-carbamate were found to be 0.1973, 0.2901, 0.0632 and 0.0400 respectively. Characteristic bands of these species were identified at 1017, 1067, and 1162 cm^{-1} . A lower detection limit for HCO_3^- anions in MEA and DEA solution was observed. Bands for potential quantification of free- and protonated alkanolamine are identified in the region of 2800 - 3800 cm^{-1} .

© 2013 The Authors. Published by Elsevier Ltd.
Selection and/or peer-review under responsibility of GHGT

Keywords : CCS; CO_2 ; Raman spectroscopy; alkanolamine solution; carbamate

1. Introduction

Aqueous alkanolamine solutions are the current state-of-the-art sorbents in post-combustion CO_2 capture (PCC) technology[1]. Chemical absorption of CO_2 into an aqueous alkanolamine solution typically comprises several parallel reaction pathways leading to formation of many different species. It is important for prediction purposes to determine reliable thermodynamic vapour-liquid equilibrium models. Hence, analysis of the liquid phase species distribution is mandatory for thermodynamic model optimization. Furthermore, such species analysis provides structure-property information on the

* Corresponding author. Tel.: +47 35 57 51 93; fax: +47 35 57 50 01.
E-mail address: Klaus.J.Jens@hit.no.

alkanolamine - CO₂ reaction. Despite the importance, detailed liquid phase speciation is difficult due to the lack of easily available analytical methods

Speciation based on spectroscopic methods is receiving increased attention. ¹H- and ¹³C-NMR spectroscopy is being used for this purpose [2-4]. ¹³C-NMR spectroscopy can be considered to be a successful technique because non-invasive, direct measurements can be performed allowing estimation of all species formed in aqueous alkanolamine solvents with the exception of H₂O and its ions. However, because of low natural isotopic abundance and slow relaxation time of the ¹³C nuclei, long measurement times are required for determination of accurate quantitative data [4].

FT-IR spectroscopy combined with an attenuated total reflectance (ATR) probe head is a recent method for alkanolamine-CO₂-H₂O system speciation [5-7]. However, high absorption of water still remains an obstacle in certain spectral ranges. In this regard, Raman spectroscopy is more promising for disclosing speciation in carbonated alkanolamine solution, both because special sample preparation is not necessary and that it shows less sensitivity to water content in the sample as compared to IR spectroscopy. Hence Raman spectroscopy is also a tempting method because of reasonable acquisition times which are considerably shorter than for ¹³C-NMR based techniques.

The focus of this work is on the applicability of Raman spectroscopy as an analytical tool to determine the speciation of carbonated aqueous alkanolamine systems. Previously, two such Raman studies [8,9] have been reported, both utilizing a multivariate linear regression analysis approach for spectrum calibration. While such methods work well in practice, a drawback is the large number of calibration samples that have to be prepared and measured. This work constitutes a simple 'short-cut' type approach to semi-quantitative speciation information employing measurement of selected Raman bands in conjunction with an internal standard (ClO₄⁻), assisted by ¹³C-NMR.

2. Experimental Methods

2.1. Sample preparation

All chemicals were of analytical grade or better quality and used as received. AMP was purchased from Acros Organic, NaClO₄ from Sigma Aladrich while the others were purchased from Merck. Carbonated alkanolamine samples were prepared according to literature [10,11]. Deionised (Milli-Q) water was used to prepare the aqueous alkanolamine solution (20 % w/w: 3.28 mol/l of MEA, 1.97 mol/l of DEA 1.78 mol/l of MDEA and 2.22 mol/l of AMP) which was degassed before use. In a typical sample preparation run, the carbonated aqueous alkanolamine solution was prepared by dissolution of a predetermined NaHCO₃ amount into an aqueous alkanolamine (MEA, DEA, MDEA or AMP) solution. The system was allowed to react and equilibrate for 24 hours in a thermostated closed cell (Grant LTD 6G) at 23 ± 2 °C. After equilibration, the samples were transferred to a NMR tube (Wilma LabGlas, 500MHz quality) after addition of a known amount of the internal standard NaClO₄.

2.2. Raman measurement

The Raman scans were performed with a Jobyn Yvon Horiba T64000 instrument working in backscattering single grating mode. The light was collected through a confocal microscope with an Olympus 10x objective while the samples were kept in rotating ¹³C-NMR -tubes. The 400mW 532nm illumination was generated by a frequency doubled Millennia Pro 12sJS Nd:YVO₄ laser. To keep the signal to noise level low, 3 scans of 120 seconds were collected for each Raman spectral range. An extended range protocol was employed to cover the ranges from 700 to 1700 cm⁻¹ (three overlapping spectra) and from 2600 to 3700 cm⁻¹ (five overlapping spectra). A grating with 1800 rules pr. mm and a

slit width of 100 microns ensured a spectral resolution ranging from 2 cm^{-1} at 1000 cm^{-1} to 1.6 cm^{-1} in the neighborhood of 3000 cm^{-1} . After removal of spikes and spectrograph artifacts, the overlapping spectra were merged. Fluorescence effects were subtracted by fitting with moderate degree polynomial functions. The wavenumber scale was calibrated against the Raman spectrum of a 50/50% (v/v) mixture of toluene and acetonitrile. No attempts were made to control polarization. However, the optical setup between each experiment was kept unchanged, to prevent such effects to interfere. All the scans were done at room temperature ($20 \pm 1\text{ }^\circ\text{C}$).

For a given Raman band j , of a given species i , the relative scattering intensity I_{ij} is directly related to the concentration of the determined substance through the formula.

$$I_{ij} = J_{ij}c_i \quad (1)$$

I_{ij} is the relative scattering intensity. J_{ij} is the Molar scattering intensity factor for each Raman band of each substance and is characteristic of the designated band at given measurement conditions and medium. c_i is the concentration of the species. According to the formula (1), once the relative scattering intensity is known, the concentration of the substance can be calculated. Since many instrument and sample factors influence this linear relationship an internal standard is added to each sample assuming its Raman band to be independent of the other molecules in the solution.

Raman active bands for the carbonated aqueous alkanolamine solutions (alkanolamine/ HCO_3^-) were identified based on previous work [8,9,12] in addition to this work. ClO_4^- has a Raman shift at 935 cm^{-1} . Having identified the relevant Raman active band, the spectral envelopes was fitted to an area-normalized Gauss-Lorentzian peak function along with a polynomial baseline. Numeric evaluation of the corresponding parameters was performed using the Gnuplot program. The accuracy of this method is dependent on sufficient resolution to clearly distinguish the bands to be analyzed.

The molar scattering intensity factors (J) were calculated relative to the internal ClO_4^- standard according to equation 2. The integrated area (A) under the relevant band was calculated since it is proportional to the band intensity. The concentration c is given in mol/l.

$$\frac{A_i}{A_{\text{ClO}_4^-}} = J \frac{c_i}{c_{\text{ClO}_4^-}} \quad (2)$$

For determination of the molar scattering intensity factor of HCO_3^- , CO_3^{2-} and the alkanolamines, pure solutions of each substance in different concentration were prepared containing NaClO_4 as internal standard. Since HCO_3^- is in equilibrium with CO_3^{2-} , the CO_3^{2-} concentration was calculated first according to equation 2 followed by the HCO_3^- concentration calculation taking into account carbon mass conservation. The solutions of MEA and DEA were standardized by titration.

2.3. ^{13}C -NMR measurement

The ^{13}C -NMR experiments were performed at 9.4 T on a Bruker Avance III 400 MHz spectrometer using a BBFO Plus double resonance probehead at room temperature and the spectra were using MestreNova software v 7.1.1. A capillary containing a solution of $\text{CH}_3\text{CN} / \text{D}_2\text{O}$ was inserted in the ^{13}C -NMR tube as a reference standard and 'lock' solvent respectively. After the measurements of the longitudinal relaxation time T_1 of the ^{13}C nuclei of all the species in solution, including the standard in the

capillary, the following ^{13}C -NMR parameters were adjusted: recycle delay was 120 s, pulse angle=90° and number of scans was 480.

To obtain quantitative results, the area under the spectral peaks were integrated and scaled to the area of the reference standard peak. The effective concentration of the reference standard in the capillary was calibrated as a function of the solutions under study. Since the fast exchanging protons species are represented by a common signal in the ^{13}C -NMR spectra, calibration experiments to distinguish between HCO_3^- and CO_3^{2-} and between alkanolamine and its protonated form were performed. Solutions of HCO_3^- and CO_3^{2-} and of alkanolamine and its protonated form were prepared and mixed in appropriate ratios. The pH of each sample was measured (using a 718 STAT Tritino produced by Metrohm) and ^{13}C -NMR spectra were acquired. Since the chemical shift of the common peak depends on the relative amount of the two species, the variations of chemical shift were recorded and reported as a function of the species ratios and pH [3].

3. Results and discussion

After identification of the relevant characteristic Raman active bands for each substance by use of reference spectra, the molar scattering intensity factors (J) were calculated. Finally spectra of aqueous alkanolamine solutions loaded with HCO_3^- were acquired and analyzed.

3.1. Band identification

The most characteristic Raman active band of CO_3^{2-} suitable for quantitative measurement [13] is reported [8,12] to be 1065 cm^{-1} while the most characteristic bands of HCO_3^- are reported [13] at 1017 , 1302 , 1360 and 1630 cm^{-1} . Figure 1 shows our reference spectra for CO_3^{2-} and HCO_3^- including the internal ClO_4^- standard (935 cm^{-1}). We observed the characteristic CO_3^{2-} band at 1067 cm^{-1} and the characteristic HCO_3^- bands at 1017 and 1360 cm^{-1} .

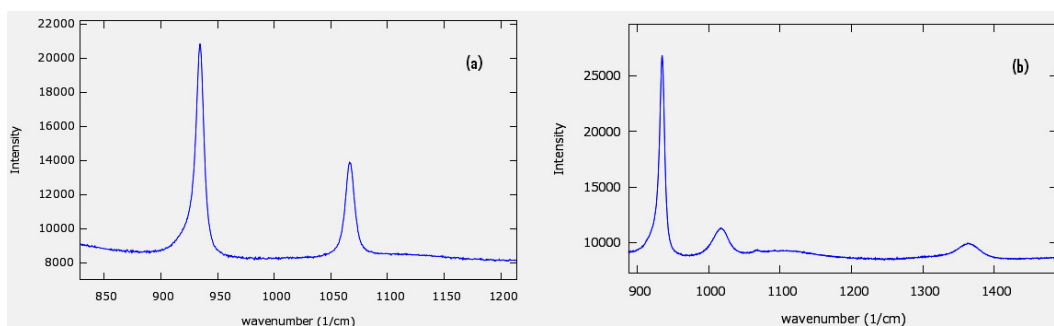


Figure 1: Reference Raman spectra for CO_3^{2-} (a) and HCO_3^- (b). CO_3^{2-} concentration is 0.185 mol/l and HCO_3^- concentration is 0.216 mol/l

Ammonium carbamate shows 5 characteristic Raman active bands[13]. Only the band at 1034 cm^{-1} is suitable for quantitative measurement. For MEA and DEA solutions loaded with CO_2 , the carbamate band was clearly identified at 1162 cm^{-1} [8].

In a previous study[9] characteristic Raman bands for free alkanolamine have been observed at 400 , 1200 , 1350 and 1600 cm^{-1} . Two of these were detected at 1350 and 1600 cm^{-1} in our spectra for MEA (Figure 2). Figure 5 shows corresponding bands in the DEA Raman spectrum at 1200 cm^{-1} . These two bands have the potential for quantification of free MEA (1350 cm^{-1}) and DEA (1200 cm^{-1}). However, these bands become weak at lower concentration leading to an under estimation of the quantification. As

similarly for ammonia (3310 cm^{-1}) [13], we can observe a band at 3313 cm^{-1} in the MEA spectrum (figure 2) which is not visible in the spectrum of the protonated form (figure 3). Therefore the 3313 cm^{-1} band is characteristic for the free alkanolamine, however the band is overlapping somewhat with a water band. A proper curve model in this spectral range is expected to enable quantification of free alkanolamine. In addition to the band at 3313 cm^{-1} , further bands be observed at 2890 , 2930 - 2960 and 3381 cm^{-1} . Previous work[14] on protonated alkanolamines has reported that characteristic bands at 2952 , 2940 and 2884 cm^{-1} for MEA were shifted to 3005 , 2971 and 2898 cm^{-1} on protonation. A similar result is demonstrated in Figure 3 showing that protonated MEA leads to a Raman shift at 2900 and 2980 cm^{-1} with a shoulder.

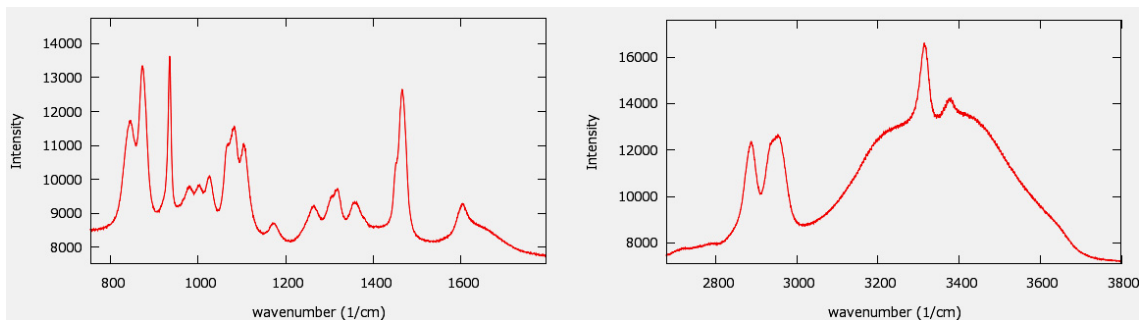


Figure 2: Reference Raman spectra for MEA

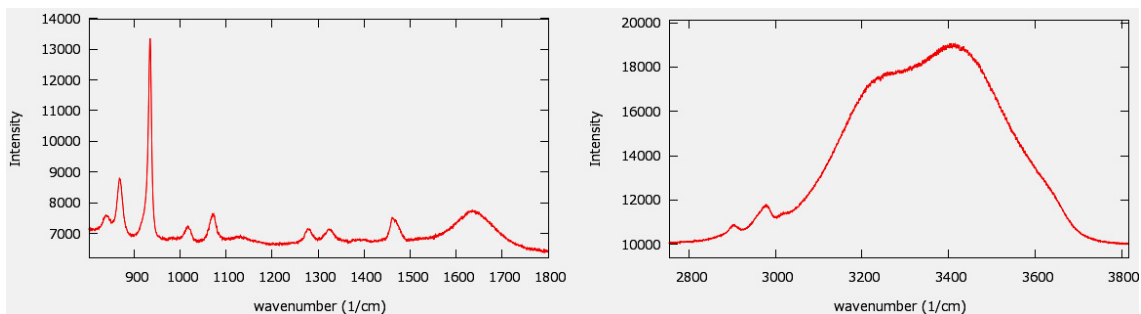


Figure 3: Reference Raman spectra for protonated MEA

3.2. Molar scattering intensity factor

The determined molar scattering intensity factors are presented in Table 1. The value for HCO_3^- and CO_3^{2-} were calculated to be 0.1973 and 0.2901 respectively. These values are consistent with a previous study [12] which reported 0.188 and 0.302 respectively. Our calculations are based on the 1350 and 1200 cm^{-1} band for MEA and DEA respectively. However these bands were weak in the scattering envelop which increases the error margin; it was found that the bands were not visible in samples with low alkanolamine concentration. More work is needed to reduce the error margin.

Figure 4 and 5 show a clearly distinguishable band at 1160 cm^{-1} . The band was not visible in the MDEA Raman spectrum with 0.5 loading. Since MDEA is a tertiary alkanolamine, no carbamate can be formed. Our molar scattering intensity factors for carbamate are relevant for this band. The reference

concentrations for the calculations were taken from ^{13}C -NMR measurements on the carbonated solutions analyzed by Raman at different concentration levels. The calculated value for the MEA- and DEA-carbamate is 0.0632 and 0.04 respectively.

Table 1: Molar scattering intensity factors.

Component	J	Standard deviation
CO_3^{2-}	0.2901	0.0062
HCO_3^{2-}	0.1973	0.0250
$\text{OHC}_2\text{H}_4\text{NHCOO}^-$	0.0632	0.0070
$(\text{HOC}_2\text{H}_4)_2\text{NHCOO}^-$	0.0400	0.0060
$\text{HOC}_2\text{H}_4\text{NH}_2$ at 1350 cm^{-1}	0.0040	0.0012
$(\text{HOC}_2\text{H}_4)_2\text{NH}$ at 1200 cm^{-1}	0.0130	0.0014

3.3. HCO_3^- loaded alkanolamine solutions

Three different concentration levels (HCO_3^- to alkanolamine loading ratio: 0.5, 0.75, 1) of carbonated aqueous systems were analyzed for MEA and DEA. MDEA and AMP were analyzed only at 0.5 loading. The spectra of MEA solution with/without 0.5 loading are given in Figure 5. The characteristic bands of CO_3^{2-} and MEA-carbamate are clearly visible at 1067 cm^{-1} and 1162 cm^{-1} respectively. A similar result was observed for the other two loadings.

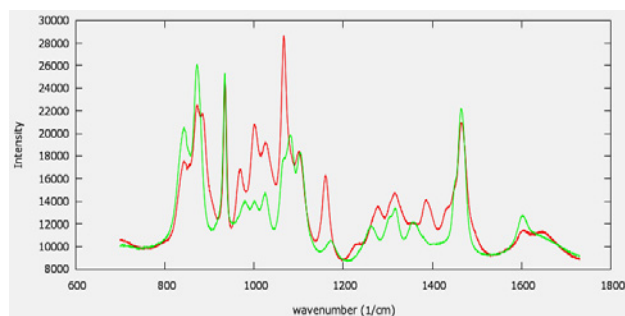


Figure 4: Raman spectra of MEA 20 % w/w aqueous solution without loading (green) and with 0.5 loading (red).

The CO_3^{2-} concentration was calculated using equation 2 and the bicarbonate loaded MEA Raman spectra. The calculated concentrations were 0.285, 0.382 and 0.536 mol/l at 0.5, 0.75 and 1.00 loadings respectively. ^{13}C -NMR measurements were run for each of the prepared samples. The results are summarized in Table 2. The CO_3^{2-} quantification based on Raman measurements are in the same order of magnitude as the ^{13}C -NMR quantification. The CO_3^{2-} Raman band is particularly strong. It might be a reason for over estimated values. We speculate that this effect may be due to molecular species interaction effect as concentration increases. However, the correspondence between Raman and ^{13}C -NMR

determined concentration varies. This could be due to overlapping bands in combination with our method of data deconvolution.

Furthermore, neither the characteristic HCO_3^- band (1017 cm^{-1}) nor the 1350 cm^{-1} alkanolamine band was truly visible at all three loadings. The reason may be that the HCO_3^- band is masked by the alkanolamine spectrum due to low concentration of the former. According to ^{13}C -NMR results, the HCO_3^- concentration is rather low. However, even though the alkanolamine concentration is quite high, the band at 1350 cm^{-1} is very weak and below the detection level. Thus the 1.521 mole/l of free MEA was under estimated by more than 50 %. Hence, we suggest use of the stronger bands in the high frequency range ($2800\text{-}4000\text{ cm}^{-1}$) for quantification of free- and protonated alkanolamine.

Table 2: Concentration determined by ^{13}C -NMR measurement for MEA/ HCO_3^- and DEA/ HCO_3^- systems

HCO_3^- loading	Alkanolamine	CO_3^{2-} mole/l	HCO_3^{2-} mole/l	RNHCOO^- mole/l	Free alkanolamine mole/l
0.50	MEA	0.243	0.018	1.340	1.521
	DEA	0.219	0.108	0.595	0.953
0.75	MEA	0.360	0.044	1.880	0.793
	DEA	0.312	0.208	0.787	0.602
1.00	MEA	0.520	0.234	2.475	0.187
	DEA	0.396	0.412	0.911	0.344

Similar results as for MEA were observed for the DEA solutions at the three different loadings. Again, clearly visible characteristic bands for CO_3^{2-} and carbamate were noticed. The Raman and ^{13}C -NMR results are quite compatible in respect to CO_3^{2-} concentration. The calculated ‘Raman’ concentrations were 0.273 , 0.372 and 0.306 mol/l for the respective loadings at 0.5 , 0.75 and 1.00 . Figure 5 shows the Raman spectra of the DEA sample with/without 0.5 loading. The characteristic HCO_3^- Raman band at 1017 cm^{-1} is probably masked by other bands near 1017 cm^{-1} which is seen in the unloaded DEA solution spectra. Interestingly, a 0.412 mol/l of HCO_3^- concentration was not detected in loaded DEA solution, while a 0.216 mol/l of HCO_3^- was clearly visible in the pure solution (Figure 1). This demonstrates clearly the masking of the 1017 cm^{-1} band.

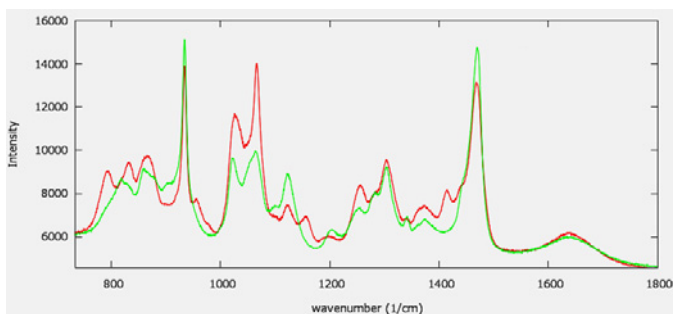


Figure 5: Raman spectra of DEA 20 % w/w aqueous solution without loading (green) and with 0.5 loading (red).

In comparison with MEA, a quite distinct band at 1200 cm^{-1} is visible for free DEA. However, it is barely visible at 0.75 and 1.00 loading and gave 0.584 mol/l of DEA concentration at 0.5 loading.

Figure 6 shows the AMP Raman spectra with/without 0.5 loading. AMP is a sterically hindered alkanolamine which is believed not to form carbamate. Hence no corresponding band at 1067 cm^{-1} is detected. The characteristic bands for CO_3^{2-} and free alkanolamine are visible. However the band of ClO_4^- internal standard is overlapping with the AMP spectrum precluding use of the internal standard for quantification.

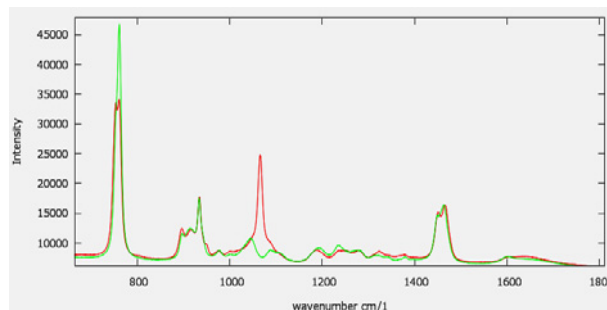


Figure 6: Raman spectra of AMP 20 % w/w aqueous solution without loading (green) and with 0.5 loading (red).

4. Conclusion

This demonstrated Raman spectroscopic method is able to pick out selected characteristic Raman bands which can be used as part of a simple model allowing quick, semi-quantitative insight into carbonated alkanolamine solutions.

The molar scattering intensity factors for HCO_3^- , CO_3^{2-} and MEA- and DEA-carbamate were found to be 0.1973, 0.2901, 0.0632 and 0.0400 respectively.

Potential bands for quantification of free- and protonated alkanolamine are identified in the spectral region of $2800 - 3800\text{ cm}^{-1}$

However, still there are some challenges to be attained, such as the lower detection limit observed for the HCO_3^- concentration in loaded samples. In addition, the use of an alternative standard is recommended where the well known internal ClO_4^- standard (935 cm^{-1}) is fail for AMP.

Acknowledgements

The financial assistance and a scholarship (G.S., C.P.) provided by the Research Council of Norway (CLIMIT grant nr. 199890) and the support by the SINTEF NMR lab, incl. staff is gratefully acknowledged.

References

- [1] Rochelle, G. T. *Science* **2009**, *325*, 1652-1654.
- [2] Barth, D.; Rubini, P.; Delpuech, J.-J. *Bull. Soc. Chim. Fr.* **1984**, *1*, 227-230.
- [3] Jakobsen, J. P.; Krane, J.; Svendsen, H. F. *Industrial & Engineering Chemistry Research* **2005**, *44*, 9894-9903.
- [4] Böttinger, W.; Maiwald, M.; Hasse, H. *Fluid Phase Equilib.* **2008**, *263*, 131-143.
- [5] Diab, F.; Provost, E.; Laloué, N.; Alix, P.; Souchon, V.; Delpoux, O.; Fürst, W. *Fluid Phase Equilib.* **2012**, *325*, 90-99.
- [6] Archane, A.; Fürst, W.; Provost, E. *J. Chem. Eng. Data* **2011**, *56*, 1852-1856.

- [7] Jackson, P.; Robinson, K.; Puxty, G.; Attalla, M. *Energy Procedia* **2009**, *1*, 985-994.
- [8] Souchon, V.; Aleixo, M. d. O.; Delpoux, O.; Sagnard, C.; Mougin, P.; Wender, A.; Raynal, L. *Energy Procedia* **2011**, *4*, 554-561.
- [9] Vogt, M.; Pasel, C.; Bathen, D. *Energy Procedia* **2011**, *4*, 1520-1525.
- [10] Chen, H. M.; Danckwerts, P. V. *Chem. Eng. Sci.* **1981**, *36*, 229-230.
- [11] Aroua, M. K.; Amor, A. B.; Haji-Sulaiman, M. Z. *J. Chem. Eng. Data* **1997**, *42*, 692-696.
- [12] Zhao, Q.; Wang, S.; Qin, F.; Chen, C. *Industrial & Engineering Chemistry Research* **2011**, *50*, 5316-5325.
- [13] Wen, N.; Brooker, M. H. *The Journal of Physical Chemistry* **1995**, *99*, 359-368.
- [14] Ohno, K.; Matsuura, H.; Iwaki, T.; Suda, T. *Chem. Lett.* **1998**, *27*, 531-532.

Paper II



GHGT-12

Application of ^{15}N -NMR spectroscopy to analysis of amine based CO_2 capture solvents

Cristina Perinu^a, Gamunu Saramakoon^a, Bjørnar Arstad^b, Klaus-J. Jens^{a*}

^aFaculty of Technology, Telemark University College, Kjølnes Ring 56, Porsgrunn 3918, Norway

^bSINTEF, Materials and Chemistry, Forskningsveien 1, 0314 Oslo, Norway

Abstract

^{15}N NMR spectroscopy is a useful tool for amine reactivity characterization since it can provide information about the availability of the lone pair of electrons on nitrogen through the measured chemical shift values, which depend on molecular structure and medium effects. Although the amino nitrogen is the focal nucleus of the carbon dioxide-amine reaction, ^{15}N NMR measurements have so far received little attention in the field of amine-based chemical absorption of carbon dioxide. In this study, from one hand, through ^{15}N NMR chemical shifts measurements, the effect of solvent on the electron density of the nitrogen of 2-methyl-2-amino-1-propanol (AMP) in solvent blends was investigated; from the other hand, ^{15}N NMR chemical shifts of aqueous primary non-hindered and hindered alkyl amines were related to the corresponding carbamate forming and carbamate stability equilibrium constants as well as carbamate forming kinetic constants, showing linear relationships. Such correlations could be useful for predictive estimation of carbamate-related equilibrium and kinetic constants.

© 2014 The Authors. Published by Elsevier Ltd. This is an open access article under the CC BY-NC-ND license (<http://creativecommons.org/licenses/by-nc-nd/3.0/>).

Peer-review under responsibility of the Organizing Committee of GHGT-12

Keywords: ^{15}N NMR; amines; carbon dioxide; reactivity; carbamate-related constants.

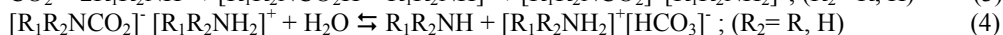
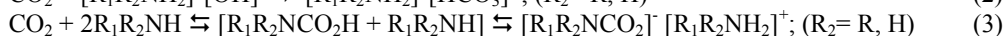
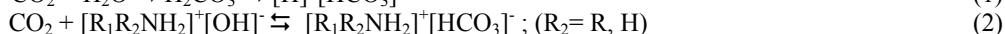
1. Introduction

In spite of intensive global carbon dioxide (CO_2) capture research and development initiatives, the well known CO_2 gas-liquid absorption process is expected to be the technology of choice for early large scale deployment of post combustion carbon capture (PCC) [1, 2]. The main current challenge is to develop more cost effective and

* Corresponding author. Tel.: +47-35575193; fax: +47-35575001.

E-mail address: Klaus.J.Jens@hit.no

superior performing amine solvents. Molecular structure property understanding of solvents is crucial in this respect. Reaction of CO₂ with primary or secondary aqueous amine solutions can be described by equations (1) to (4) [3].



In general, carbamate formation reaction (3) is the fast reaction, defining the CO₂ capacity of the aqueous amine solvent to be 0.5 mol CO₂ per mol of amine. Reactions (1), (2) and (4) are less important under these circumstances. However, carbamate hydrolysis reaction (4) is important for steric hindered amines for which CO₂ capacities larger than 0.5 can be achieved [4]. Understanding reactions (3) and (4) is important background for identification of improved aqueous amine solvents.

The equilibrium constant and the kinetic constant for carbamic acid formation (first step in reaction (3)) have been rationalized for some amines to be a function of amine protonation constant. Deviation from this Brønsted relationship has been proposed to be due to steric effects (e.g. steric hindered amines); for ammonia (NH₃), solvation effects have been thought to be the reason for deviation from this relationship [5].

NMR spectroscopy is a non-invasive analytical technique which allows direct measurement of specific nuclei of the species in solution and it is hence a good method for gaining chemical insight into PCC solvent systems [6]. In spite of numerous valuable results obtained by use of ¹H- and ¹³C-NMR spectroscopic experiments on PCC solvents, direct measurement of the amino atom, the focal nucleus of the CO₂-amine reaction, has so far received little attention [7, 8]. ¹⁵N-NMR, a well known spectroscopic method, is a powerful tool for assessment of nitrogen (N) containing molecular reactivity [9, 10], including insight into the solvent effects on the carbamate formation reaction [7]. Indeed, due to the presence of a lone pair of electrons on the nitrogen, the relative electron density on the N atom depends not only on the electronic environment as defined by the molecular structure but, as compared to ¹H and ¹³C, it is also more sensitive to medium effects (e.g. solvent, concentration and temperature) and, in general, to inter- and intra-molecular effects. The changes in electron density are reflected through the chemical shifts variations [11, 12].

The carbamate formation reaction is a nucleophilic addition reaction: the N atom is acting as nucleophile (Lewis base) which donates the lone pair electrons to the electrophilic centre (carbon, C) of the CO₂ (Lewis acid), forming a new bond and, consequently, a new species (i.e. amine carbamic acid/carbamate). Estimation of the relative electron density on the nitrogen atom by means of ¹⁵N NMR spectroscopy appears to be a useful method to characterize the reactivity of the amines, both in terms of reaction equilibrium [7] and of reaction kinetics [13].

We here report application examples of ¹⁵N-NMR spectroscopy for PCC solvent understanding.

Qualitative ¹⁵N-NMR experiments have been performed at 298.15 K on primary amines (2 M). From one hand, the effect of solvents, other than water, on the ¹⁵N chemical environment of a primary steric hindered amine, 2-amino-2-methyl-1-propanol (AMP), has been investigated in order to achieve insights into the relative availability of the lone pair of electrons on the nitrogen to react with CO₂. On the other hand, the ¹⁵N chemical shift values of aqueous primary alkylamines (before CO₂ loading) have been related to corresponding carbamate-related constants available in literature [14]. It can be shown that there is a linear relationship between the ¹⁵N chemical shift values, the equilibrium constants, i.e. log K_c for reaction (3) and log K_{hyd} for reaction (4), and the kinetic constants, i.e. log k for reaction (3), of the amines under study.

2. Experimental Section

All the amines were purchased from Sigma Aldrich (assay: ≥ 99%) and used as received. In a typical sample preparation, weighed amount of amine and water (deionised and degassed) were mixed and the concentrations (2.00 ± 0.04 M) were calculated by measuring the density with a pycnometer. The same procedure was used for preparation of AMP solutions in solvent blends. The samples were then transferred to a NMR tube for ¹⁵N NMR measurements.

¹⁵N NMR experiments were performed at 9.4 T on a Bruker Avance III 400 MHz spectrometer using a BBFO Plus double resonance probe head at 298.15 K; the spectra were processed using MestreNova software v 7.1.1. The

experiments were carried out on amine solutions at the same concentration (2M) and at the same temperature (298.15 K) to avoid corresponding effects on the chemical shift values. The uncertainty in the chemical shift values was estimated to be in the range of ± 0.01 -0.03 ppm. The used method is fully described in the ^{15}N NMR study by Perinu et al.[7].

3. Results and Discussion

The ^{15}N NMR chemical shift is a measure for the relative electron density present on the N nucleus which is depending on molecular structure and medium effects. Increased electron density on the nitrogen corresponds to an increased energy of the lone pair electrons, making the amino function more reactive.

Recently, ^{15}N NMR spectroscopy has been applied to investigation of the carbamate formation reactions of selected aqueous amine absorbents belonging to different classes (primary, secondary and steric hindered amines). In that study, the ^{15}N NMR chemical shifts fairly reflected the observed amount of carbamate formed at equilibrium, resulting in a linear relationship. Moreover, analysis of ^{15}N NMR data for non-hindered primary amines clearly provided evidence of the effect of solvent on the carbamate formation reaction [7]. It was demonstrated that at equilibrium the amount of carbamate formed from non-hindered primary amines decreased at increasing basicity due to the higher tendency of the stronger bases to interact with water which reduced the availability of the lone pair electrons on the nitrogen for the carbamate formation reaction [7].

In Figure 1, ^{15}N chemical shifts (expressed in part per million, ppm) observed for AMP in different solvent blends are reported. Considering that the ^{15}N chemical shift reflects the availability of lone pair electrons of the nitrogen atom to react [7], it would be expected that the equilibrium for carbamate formation could be influenced by changing the type of solvent.

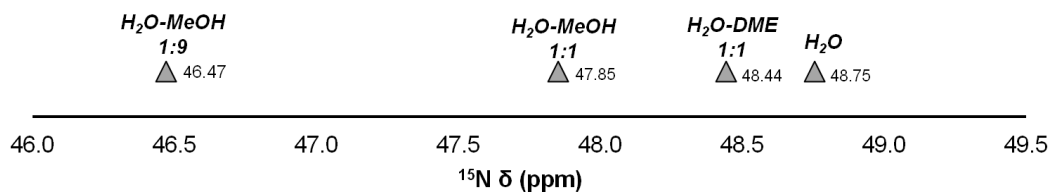


Figure 1. ^{15}N NMR chemical shifts measured at 298.15 K on AMP (2 M) in solvent blends (DME: 1,2-Dimethoxyethane; H_2O : Water; MeOH: Methanol).

Table 1 shows the carbamate-related constants of sterically hindered and non-hindered primary alkyl amines for reaction (3) and (4), the pK_b values and the ^{15}N NMR chemical shift values of the respective aqueous amine solutions (2 M, before CO_2 loading).

Since both reactions (3) and (4) are Lewis acid-base reactions, as expected, reaction equilibrium constants can be related to the relative electron density on the nitrogen nucleus of the respective amine, similar to our above mentioned study [7].

In Figure 2, the ^{15}N NMR chemical shifts of the primary alkyl amines (before CO_2 loading) are plotted versus the equilibrium constants for a) the carbamate formation reaction (K_c , reaction 3) and b) the carbamate stability or hydrolysis reaction (K_{hyd} , reaction 4), taken from literature [14] (Table 1). Linear relationships are observed.

Decreasing ppm value of the ^{15}N NMR chemical shift corresponds to increased relative electron density on the N nucleus. Figure 2a shows that the carbamate formation equilibrium constant increases at increased electron density on the N nucleus (lower ppm values). On the contrary, Figure 2b shows that carbamate hydrolysis constant increases for those amines which have the tendency to form less carbamate and are characterized by a lower relative electron density on the N (high ppm values). It is worth noting that both non-hindered and hindered amines lie on the same line in both correlations plotted in Figure 2.

Table 1. Names, structures, carbamate-related equilibrium constants (Log K_c and Log K_{hyd}), kinetic constants of carbamate formation (Log k), base dissociation constants (pK_b) and measured ^{15}N chemical shift (δ , expressed in ppm) values of aqueous primary alkyl amines (2 M, before CO_2 loading).

Amine name and abbreviation	Structure	Log K_c (291.15 K) [14]	Log K_{hyd} (291.15 K) [14]	Log k (291.15 K) [14]	pK_b^* (298.15K) [5, 15, 16]	^{15}N δ (ppm) (298.15 K)
Propylamine (NH ₂ Pr)		6.18	-1.89	5.20	3.43	25.23
Butylamine (NH ₂ Bu)		6.04	-1.80	5.30	3.36	25.40
Isobutylamine (NH ₂ <i>i</i> Bu)		6.11	-2.00	5.20	3.52	22.15
Sec-Butylamine (NH ₂ <i>s</i> Bu)		5.58	-1.31	4.85	3.44	42.44
Isopropylamine (NH ₂ <i>i</i> Pr)		5.56	-1.20	4.83	3.33	46.81
Tert-Butylamine (NH ₂ <i>t</i> Bu)		5.04	-0.85	4.28	3.32	60.87

* $pK_b = pK_w(298.15\text{ K}) - pK_a$ that is $pK_b = 14.00 - pK_a$

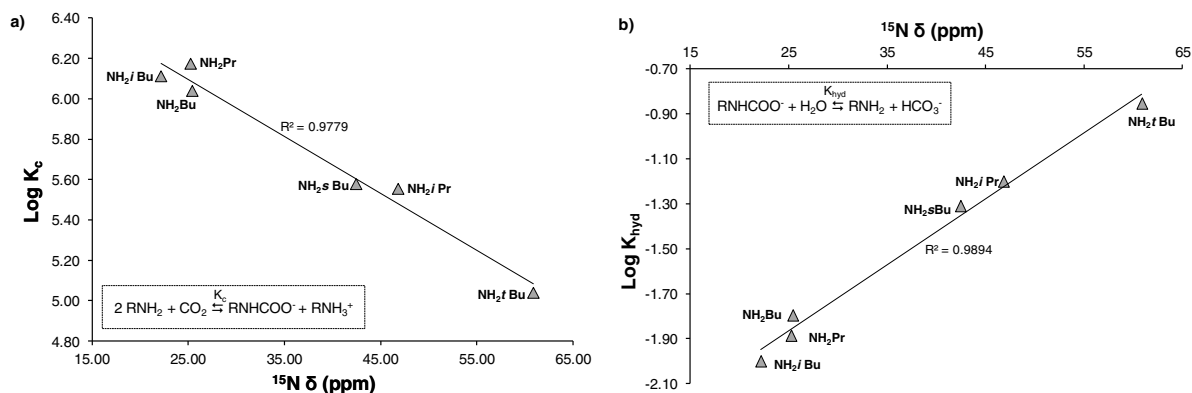


Figure 2. ^{15}N NMR chemical shifts (δ) values of aqueous primary non-hindered and hindered alkyl amines (2 M, before CO_2 loading) as a function of the corresponding a) carbamate forming equilibrium constants (Log K_c) and b) carbamate stability equilibrium constants (Log K_{hyd}).

However, when plotting the carbamate formation and hydrolysis constants as a function of pK_b , the above linear relationships are not observed anymore (Figure 3).

Figure 3 shows that at increasing steric hindrance on the alpha carbon to the N atom, there is a deviation from the trend line observable for non-hindered primary alkylamines. A similar result, as shown in Figure 3, has been observed for several other related alkyl and alkanol amines [5, 7, 17].

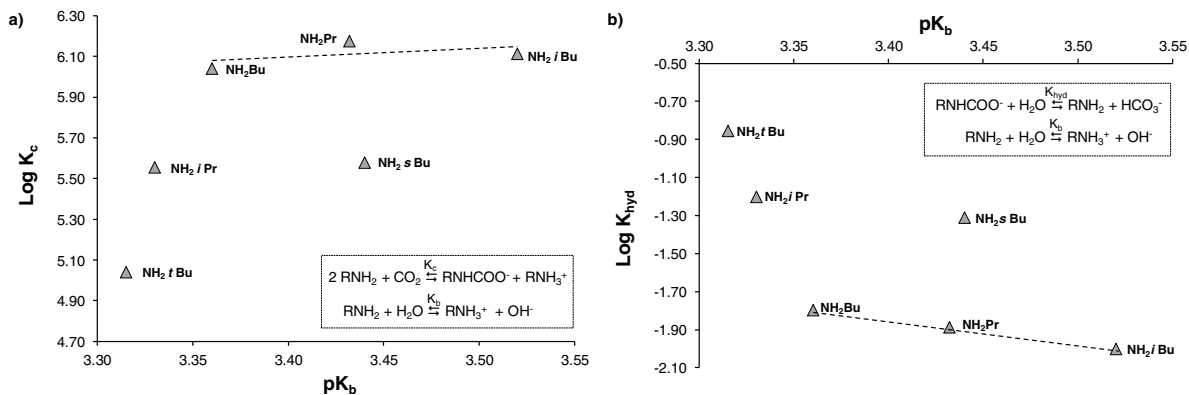


Figure 3. pK_b values as a function of a) carbamate forming equilibrium constants ($\text{Log } K_c$) and b) carbamate stability equilibrium constants ($\text{Log } K_{\text{hyd}}$) of aqueous primary non-hindered and hindered alkyl amines.

The discrepancy between the ^{15}N NMR chemical shift and the pK_b relationships may rely on the fact that the ^{15}N NMR chemical shift is a measure of the relative electron density on the N atom in respect to molecular structure and medium effects, whereas the pK_b is a measure of the proton accepting strength of a Brønsted base in water [7].

The Brønsted basicity scale is indeed built on the base-dissociation constant of Brønsted bases in water (reaction 5).



For amines, the ammonium ion solvation term is considered to give an important contribution to the position of the reaction equilibrium and is thought to be the main reason for the “anomalous order” of substituent effects in amines [16]. Apparently this basicity scale contains some contributing components which do not directly reflect factors affecting the carbamate forming reaction. So far, only in a closely related series of non-hindered primary or secondary amines, a linear Brønsted relationship has been found [5, 7, 17, 18].

On the other hand, with respect to the ^{15}N NMR data, it is interesting to note that even sterically hindered amines, like e.g. tert-butylamine, are part of the linear relationships. The origin of the steric hindered amine effect on the carbamate formation reaction has been proposed to be due to electron charge transfer from the nitrogen nucleus to the substituting methyl group bonded to the carbon in alpha position to the N atom [19]. Recently, however, the effect of the methyl group has been suggested to be rather stereochemical than electronic [20]. Our ^{15}N NMR chemical shift data obtained so far on sterically hindered amines are consistent with the theory indicating steric hindrance in amines to be an electronic effect.

The ^{15}N NMR chemical shift is a useful parameter to investigate amine reactivity also in terms of reaction kinetics [13]. Figure 4 shows a linear relationship between the kinetic constants for carbamate formation (reaction 3) and the ^{15}N chemical shift values of aqueous primary alkyl amines, including steric hindered alkyl amines.

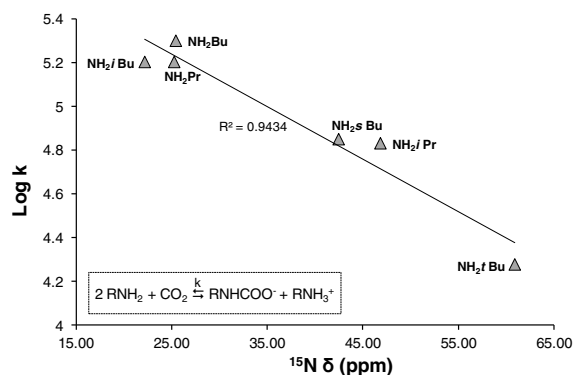


Figure 4. ^{15}N NMR chemical shifts (δ) values of aqueous primary non-hindered and hindered alkyl amines (2 M, before CO_2 loading) as a function of carbamate forming kinetic constants (Log k, $\text{M}^{-1}\text{min}^{-1}$).

So far, the results shown in Figure 2 and 4 suggest that a correlation between K_c , K_{hyd} , k and the ^{15}N NMR chemical shifts of amines can be found. Such correlation could be useful for predictive estimation of carbamate-related reaction constants, in both thermodynamic and kinetic terms.

4. Conclusions

^{15}N NMR spectroscopy is a useful tool for amine reactivity characterization since it can provide information about the lone electron pair availability on the nitrogen nucleus through the measured chemical shift values, which depend on molecular structure and medium effects. In this study, through ^{15}N NMR measurements, it was confirmed that, as expected, the electron density on the nitrogen atom changes as a function of the type of solvent used, which may lead to a change of amine reactivity.

Moreover, a linear correlation between $\log K_c$, $\log K_{\text{hyd}}$, $\log k$ and the ^{15}N NMR chemical shifts of aqueous primary non-hindered and hindered alkyl amines was found. Such correlations could be useful for predictive estimation of carbamate forming and carbamate stability (hydrolysis) equilibrium constants as well as carbamate forming kinetic constants of amine absorbents for CO_2 capture.

Acknowledgements

The financial assistance and a scholarship (C.P.) provided by the Research Council of Norway (CLIMIT grant nr. 199890) and the support by the SINTEF NMR lab, incl. staff is gratefully acknowledged.

References

- [1] Rochelle GT. *Amine Scrubbing for CO_2 Capture*. Science, 2009. **325**(5948): p. 1652-1654.
- [2] Eimer D. *Gas Treating: Absorption Theory and Practice*. 2014: John Wiley and Sons.
- [3] McCann N, et al. *Kinetics and Mechanism of Carbamate Formation from $\text{CO}_2(\text{aq})$, Carbonate Species, and Monoethanolamine in Aqueous Solution*. The Journal of Physical Chemistry A, 2009. **113**(17): p. 5022-5029.
- [4] Sartori G, Savage D. *Sterically Hindered Amines for CO_2 Removal from Gases*. Ind. Eng. Chem. Fundam., 1983. **22**: p. 239-249.
- [5] Conway W, et al. *Toward the Understanding of Chemical Absorption Processes for Post-Combustion Capture of Carbon Dioxide: Electronic and Steric Considerations from the Kinetics of Reactions of $\text{CO}_2(\text{aq})$ with Sterically hindered Amines*. Environmental Science & Technology, 2013. **47**(2): p. 1163-1169.

- [6] Perinu C, et al. *NMR spectroscopy applied to amine-CO₂-H₂O systems relevant for post-combustion CO₂ capture: A review*. International Journal of Greenhouse Gas Control, 2014. **20**: p. 230-243.
- [7] Perinu C, et al. *¹³C and ¹⁵N NMR Characterization of Amine Reactivity and Solvent Effects in CO₂ Capture*. The Journal of Physical Chemistry B, 2014. **118**(34): p. 10167-10174.
- [8] Yoon SJ, Lee H. *Substituents Effect in Amine-CO₂ Interaction Investigated by NMR and IR Spectroscopies*. Chem. Lett., 2003. **32**(4): p. 344-5.
- [9] von Philipsborn W, Müller R. *¹⁵N-NMR Spectroscopy—New Methods and Applications [New Analytical Methods (28)]*. Angewandte Chemie International Edition in English, 1986. **25**(5): p. 383-413.
- [10] Duthaler RO, Roberts JD. *Nitrogen-15 nuclear magnetic resonance spectroscopy. Solvent effects on the ¹⁵N chemical shifts of saturated amines and their hydrochlorides*. Journal of Magnetic Resonance (1969), 1979. **34**(1): p. 129-139.
- [11] Burrell GL, et al. *Preparation of protic ionic liquids with minimal water content and ¹⁵N NMR study of proton transfer*. Physical Chemistry Chemical Physics, 2010. **12**(7): p. 1571-1577.
- [12] Martin GT, et al. *¹⁵N NMR Spectroscopy*. Springer-Verlag Berlin Heidelberg New York, 1981. **18**: p. 54-74
- [13] Ando S, et al. *¹⁵N-, ¹H-, and ¹³C-NMR chemical shifts and electronic properties of aromatic diamines and dianhydrides*. Journal of Polymer Science Part A: Polymer Chemistry, 1992. **30**(11): p. 2285-2293.
- [14] Dell'Amico DB, et al. *Converting Carbon Dioxide into Carbamate Derivatives†*. Chemical Reviews, 2003. **103**(10): p. 3857-3898.
- [15] Christensen JJ, et al. *Thermodynamics of proton ionization in dilute aqueous solution. Part XI. pK, ΔH°, and ΔS° values for proton ionization from protonated amines at 25°*. Journal of the Chemical Society A: Inorganic, Physical, Theoretical, 1969(0): p. 1212-1223.
- [16] Jones FM, Arnett EM. *Thermodynamics of Ionization and Solution of Aliphatic Amines in Water*. Progress in Physical Organic Chemistry. Vol. 11. 1974: John Wiley & Sons, Inc. 263
- [17] Conway W, et al. *Toward Rational Design of Amine Solutions for PCC Applications: The Kinetics of the Reaction of CO₂(aq) with Cyclic and Secondary Amines in Aqueous Solution*. Environmental Science & Technology, 2012. **46**(13): p. 7422-7429.
- [18] Versteeg GF, van Swaaij WPM. *On the kinetics between CO₂ and alkanolamines both in aqueous and non-aqueous solutions—I. Primary and secondary amines*. Chemical Engineering Science, 1988. **43**(3): p. 573-585.
- [19] Chakraborty A., et al., *Molecular orbital approach to substituent effects in amine-CO₂ interactions*. Journal of the American Chemical Society, 1988. **110**(21): p. 6947-6954.
- [20] Fernandes D, et al. *Investigations of primary and secondary amine carbamate stability by ¹H NMR spectroscopy for post combustion capture of carbon dioxide*. The Journal of Chemical Thermodynamics, 2012. **54**(0): p. 183-191.



ISBN 978-82-7206-395-4
ISSN 1893-3068

www.hit.no
2015